Development of Kinesin Spindle Protein Inhibitors with Fused-indole and Diaryl Amine Scaffolds

Thesis Presented for

the Degree of Doctor of Kyoto University

(Pharmaceutical Sciences)

2013

Tomoki Takeuchi

Contents

Preface

Many studies have been carried out on the development of mitotic inhibitors. Most antimitotic agents inhibit the function of the β-tubulin protein (a component of the microtubule).[1] For example, vinca alkaloids such as vincristine, vinblastine, vindesine and vinorelbine interfere with the polymerization process of microtubules, thereby leading to cell cycle arrest in mitosis and subsequent anticancer activity (Figure 1). Taxanes such as paclitaxel and docetaxel, and epothilones such as ixabepilone are also the anticancer agents which prevent the depolymerization process of microtubules. However, the inhibition of microtubule dynamics leads to severe peripheral neuropathy because microtubules are also present in other nondividing cells (e.g., postmitotic neurons) and possess other critical physiological functions in cellular processes.[2] Acquired drug resistance is another obstacle after the long-term use of antimitotic agents in the treatment of cancer.[3] To overcome these limitations, novel anticancer agents with fewer adverse effects against the other molecular targets which are directly involved in cell division are being developed.[4]
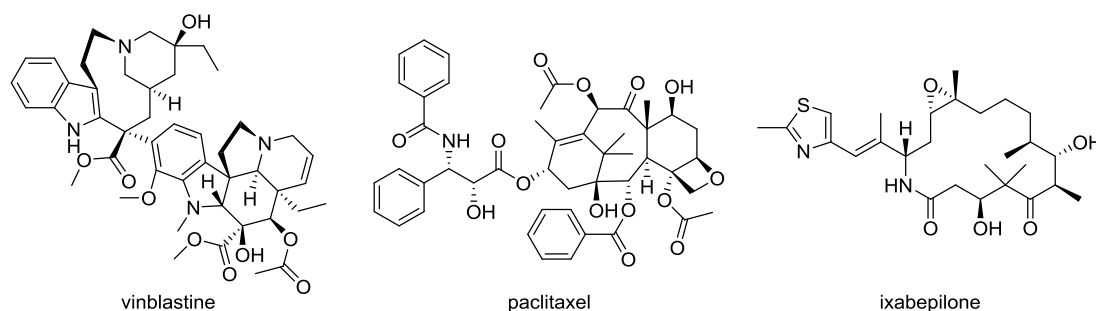

Figure 1. Structures of known antimitotic agents for cancer chemotherapy.

Kinesins constitute a superfamily of molecular motor proteins to move along microtubules.[5] Kinesins are categorized into 14 subfamilies based on sequence homology. Mitotic kinesins are involved in cell division. Non-mitotic kinesins are principally involved in intracellular transport of organelles and vesicles. The globular motor domain of ~360 amino acid residues which contains both a catalytic site for ATP hydrolysis and microtubule binding region is a hallmark of kinesins.[6] A possible mechanism to convert the chemical energy obtained from ATP hydrolysis into the motility of kinesin motors was proposed using the crystal structures of monomeric kinesin KIF1A.[7] The region composed of helix α4 and loops L11 and L12 is considered to be the main microtubule-binding element of KIF1A. Before the hydrolysis of ATP, KIF1A is tightly fixed to microtubule at the loop L11. ATP hydrolysis then generates an
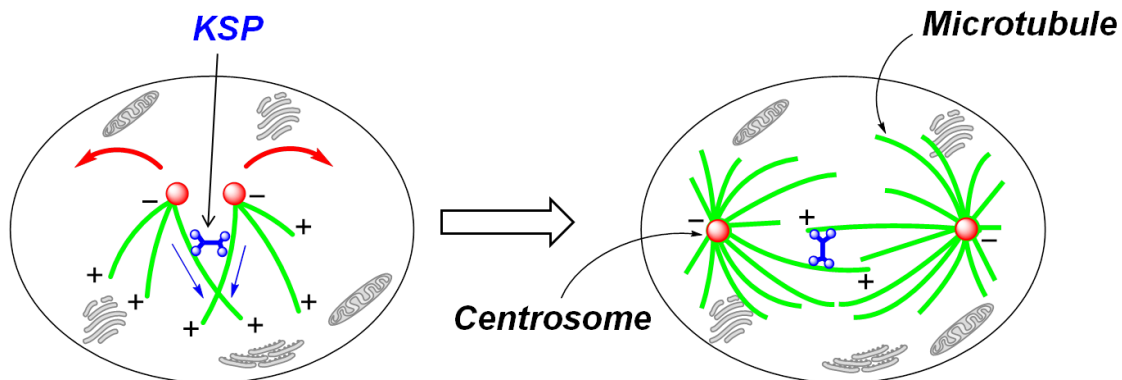
Figure 2. Simplified model of the roles of KSP during mitosis.

actively detaching state by raising loops L11 and L12. After phosphate release, the flexible loop L12 extends down onto the microtubule. When ADP is released, the kinesin steps forward in the direction of movement and binds strongly to microtubule again. Kinesins with an N-terminal motor domain move along antiparallel microtubules toward the plus end (or growing end), whereas those with a C-terminal motor domain direct the minus end.

The kinesin spindle protein (KSP; also known as Eg5) is the mitotic kinesin that belongs to the kinesin-5 family. The structure of KSP is comprised of three parts: an N-terminal motor domain, an α-helical coiled coil stalk domain in the middle, and a C-terminal tail domain. The N-terminal motor domain contains a catalytic site for ATP hydrolysis and microtubule binding region just like other kinesins. Therefore, KSP moves toward the plus end, using the energy generated from the hydrolysis of ATP (Figure 2).[8] The KSP movement produces the outward force that pushes the centrosomes apart during cell division and provides the following formation and maintenance of the bipolar spindle. Inhibition of KSP leads to mitotic arrest in prometaphase with irregular formation of the monopolar spindle and subsequent apoptotic cell death.[9] Unlike tubulin and microtubules, KSP expression is abundant only in dividing cells but not in post-mitotic neurons in the human peripheral and central nervous system.[10] Therefore, KSP inhibitors are expected to be more favorable agents for cancer chemotherapy without the neurotoxic side effects.

The first small-molecule KSP inhibitor was discovered in 1999 by Mitchison and colleagues.[11] Initially, a whole-cell immunodetection assay was carried out to identify the compounds that increase the phosphorylation of nucleolin. Compounds that cause mitotic arrest were expected to increase the amount of phosphonucleolin because nucleolin is specifically phosphorylated in mitotic cells. Using this assay, 139

compounds were selected from a library of 16,320 small molecules. After the exclusion of the compounds that affected tubulin polymerization, the remaining 86 compounds were examined for the distribution of microtubule and chromatin in mammalian epithelial kidney cells (BS-C-1) by fluorescence microscopy. One of the compounds induced an interesting mitotic phenotype, in which the monoastral microtubule array is surrounded by a ring of chromosomes. The compound, named monastrol, was proven to target KSP by inhibiting KSP with KSP-specific antibodies and inducing a similar phenotype to monastrol (Figure 3). Monastrol inhibited KSP-driven microtubule motility (IC_{50} = 14 μM), whereas it did not affect the motility of other motor proteins.

Since the discovery of monastrol, researchers recognized the vital importance of developing the novel agents targeting KSP for cancer chemotherapy. To date, a number of KSP inhibitors with various scaffolds have been reported.[12] Dihydropyrimidin-2-thione derivatives were investigated as monastrol-like KSP inhibitors. Structure–activity relationship studies of the substituents on the phenyl group in the upper part of monastrol and the ester moiety at the 5-position of the dihydropyrimidine ring were mainly performed. These studies revealed that the thiocarbonyl group at the 2-position and the 3′-hydroxyphenyl group at the 4-position of the dihydropyrimidine core were essential for potent KSP inhibitory activity. Replacing the ester group at the 5-position with a benzoyl group resulted in dramatic improvement of KSP inhibitory activity [(R)-Mon-97; IC_{50} = 0.15 μM] compared with monastrol (Figure 3). Furthermore, dimethylenastron with a 6–6 fused structure was identified as a potent KSP inhibitor (IC_{50} = 0.20 μM) from the investigation of bicyclic compounds fused at the 5- and 6-positions of the dihydropyrimidine ring.[13]
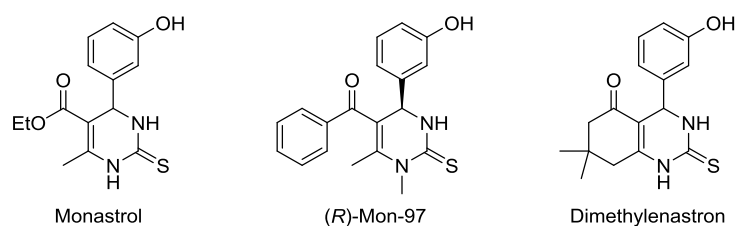

Figure 3. Structures of the first KSP inhibitor (monastrol) and the related inhibitors.

Ispinesib is a representative of quinazoline-based inhibitors that possess highly potent KSP inhibitory activity (IC_{50} = 0.6 nM; Figure 4). After the identification of ispinesib, studies replacing the quinazolin-4-one scaffold with other heterocycles were performed. From these studies, SB-743921 with a chromen-4-one scaffold was identified as a more potent KSP inhibitor (IC_{50} = 0.1 nM) than ispinesib.[14] In addition, AZD4877, which has a fused-isothiazole scaffold, has recently been identified as a

potent KSP inhibitor (IC_{50} = 2 nM) with a favorable pharmacokinetic profile and notable in vivo efficacy.[15]
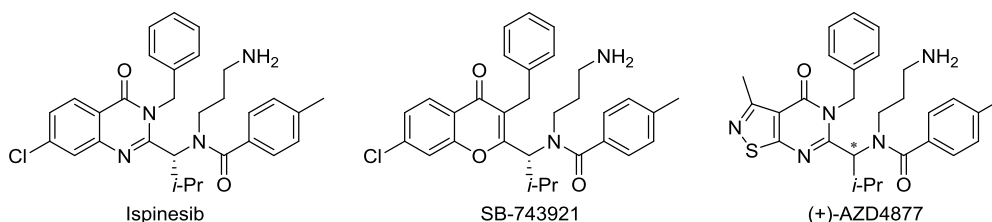

Figure 4. Structures of quinazoline-type KSP inhibitor and the related inhibitors.

KSP inhibitory activity of dihydropyrazole derivative **1** was identified by high-throughput screening (IC_{50} = 3.6 μM; Figure 5).[16] Replacing the core, along with optimization of each part of dihydropyrazole **1**, provided highly potent dihydropyrrole-type KSP inhibitor **2** (IC_{50} = 4 nM).[17] The introduction of a hydroxymethyl group at the dihydropyrrole 2-position of **2** resulted in a decreased binding affinity to the hERG channel and an increase of in vivo potency. Problematic P-glycoprotein-mediated efflux and generation of a toxic metabolite in vivo were resolved by modulating the pK_a of the piperidine nitrogen by the appropriate incorporation of a fluorine atom. The optimized compound (MK-0731) exhibited acceptable overall safety and pharmacokinetic profiles (IC_{50} = 2.2 nM).[18] In addition, ARRY-520, with a dihydrothiadiazole core, is a highly promising KSP inhibitor that looks set to enter a global phase 3 clinical trial.[19]
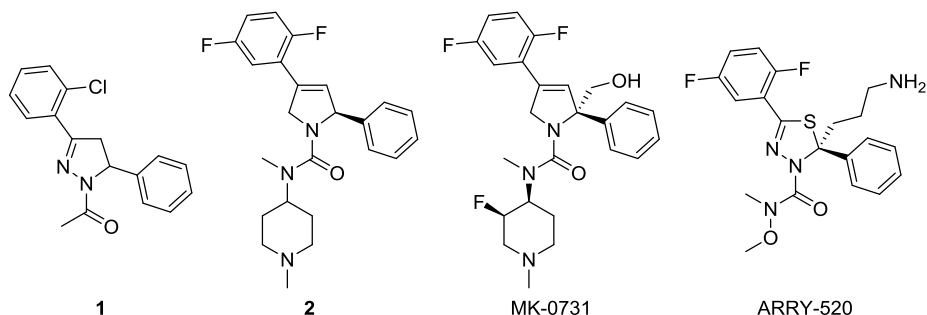
Figure 5. Structures of dihydropyrazole-type KSP inhibitor and the related inhibitors.

Tetrahydroquinoline derivative **3**, with a 2-phenyl group and a 3,4-fused tetrahydropyran ring, was also identified by high-throughput screening (IC_{50} = 0.30 μM; Figure 6).[20] Functionalizations on the tetrahydropyran ring provided the highly potent KSP inhibitor EMD-534085 (IC_{50} = 8 nM).[20] HR22C16 is a tetrahydrocarboline-type inhibitor (IC_{50} = 0.80 μM), which was proven to induce mitotic arrest and cell death in taxol-resistant cancer cells.[21] Replacing the *n*-butyl group with a benzyl group provided

the most active KSP inhibitor **4** in this series (IC$_{50}$ = 0.65 μM).[22]
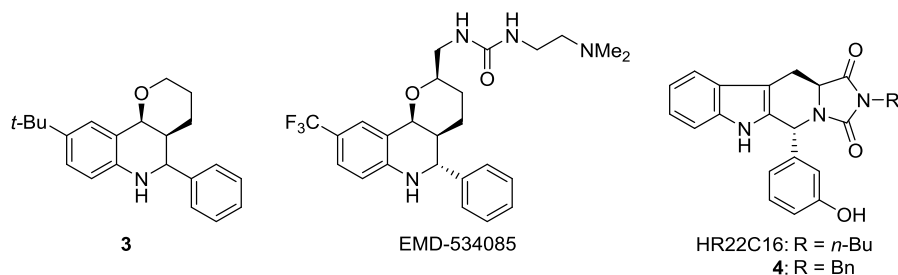

Figure 6. Structures of tetrahydroquinoline-type and tetrahydrocarboline-type KSP inhibitors.

S-Trityl-L-cysteine (STLC) was identified as a KSP inhibitor without azaheterocyclic scaffolds from in vitro screening in 2004 (IC$_{50}$ = 1.0 μM; Figure 7).[23] Structure–activity relationship studies of STLC derivatives revealed that a triarylmethyl group and free terminal amino and carboxylic groups were crucial for a high level of inhibition of KSP ATPase. Introduction of a 4-methoxy or 4-methyl group into one of the phenyl groups produced KSP inhibitor **5** [IC$_{50}$(**5a**) = 0.15 μM; IC$_{50}$(**5b**) = 0.10 μM], approximately ten times more potent compared with STLC.[24]
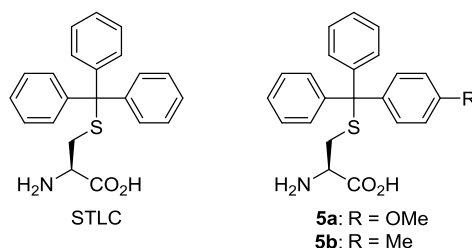
Figure 7. Structures of *S*-trityl-L-cysteine and the related inhibitors.

Biaryl derivatives are novel chemotypes of KSP inhibitors (Figure 8). The hydrogen bond acceptors such as a pyridine nitrogen atom (**6**) and donors such as a urea group (**7**) significantly contribute to KSP inhibitory activity.[25] The bulky substituents such as a trifluoromethyl group and a *t*-butyl group on the opposite phenyl group were also essential components for high level of KSP inhibition. Thiazole-containing inhibitor **8** was identified by high-throughput screening (IC$_{50}$ = 11 μM).[26] Replacing the methyl group on the benzylic methylene with a 1,1-substituted cyclopropane and 4-chloro modification of the phenyl ring led to a large increase (**9**) in KSP inhibitory activity (IC$_{50}$ = 0.29 μM).

Figure 8. Structures of biaryl-type KSP inhibitors **6–9**.

Figure 9. Three possible binding sites of KSP inhibitors.
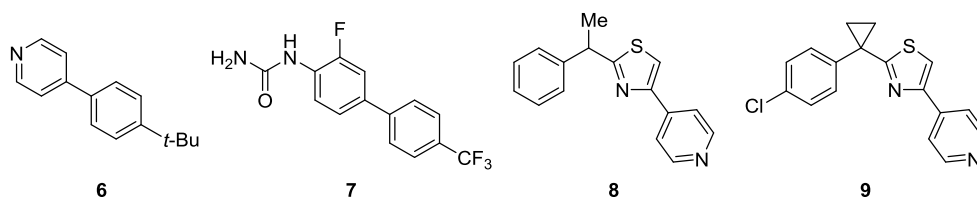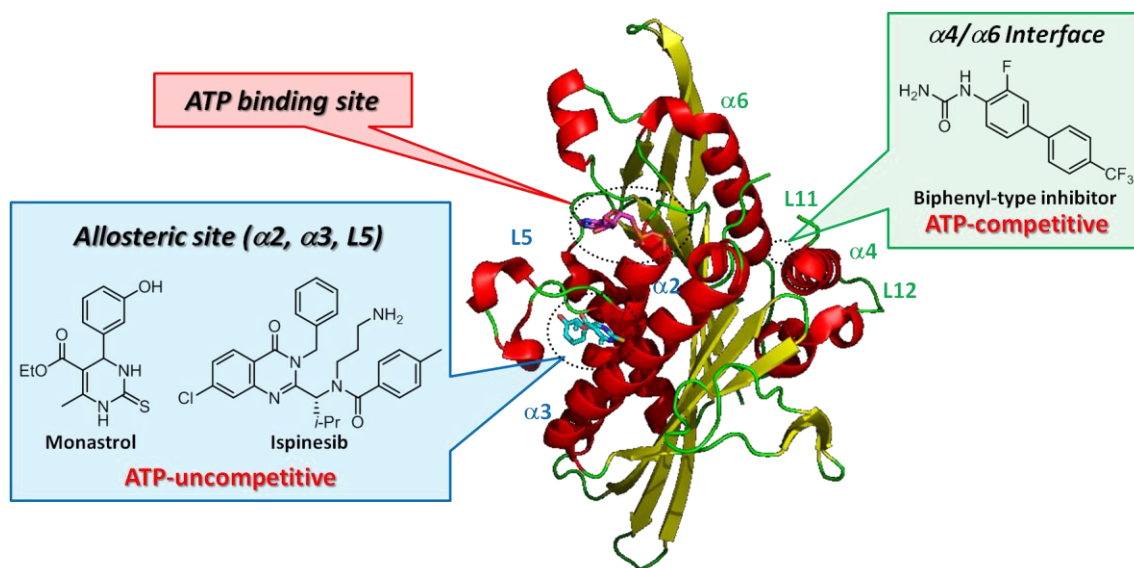
Three pockets in KSP motor domain were reported to be possible binding sites of KSP inhibitors (Figure 9). No inhibitors that bind to the ATP binding site have been reported so far. The majority of KSP inhibitors bind to the allosteric pocket formed by helices α2, α3 and loop L5 to show ATP-uncompetitive behavior.[16,18,20,27] This allosteric site includes two characteristic hydrophobic pockets that are highly involved in the binding of inhibitors. For example, the phenyl and difluorophenyl groups in MK-0731, the phenyl and trifluoromethyl groups in EMD-534085, and two phenyl groups in STLC fill up the hydrophobic pockets. Although there is no hydrophilic cavity in the allosteric site, characteristic functional group(s) of inhibitors could form hydrogen bond(s) to participate in favorable interactions. For example, the hydroxymethyl group in MK-0731 and the amino group in STLC form hydrogen bonds with the carbonyl oxygen of Gly117 at this site of KSP. The secondary amino group of the tetrahydroquinoline core in EMD-534085 also makes a hydrogen bond with the backbone carbonyl oxygen of Glu116. Long-term exposure of SB-743921 (targeting to this allosteric pocket) induced point mutations in loop L5, leading to drug resistance.[28]

6

Biaryl derivatives **7** and **9** showed KSP inhibitory activity in an ATP-competitive manner.[25a,b,26] In recent years, the inhibitory mechanism and binding modes of biaryl-type ATP-competitive KSP inhibitors was revealed by several approaches. The binding site of biphenyl-type inhibitor **7** was considered to be distinct from that of the existing KSP inhibitors because it also inhibited KSP ATPase with ispinesib-resistant mutations.[25a,b] Photoaffinity labeling analysis and molecular modeling indicated that the biphenyl derivative **7** binds to the secondary allosteric site formed by helices α4 and α6 (remote from ATP binding site and the allosteric site formed by α2, α3 and L5). Separately, it was suggested by photoaffinity labeling analysis that biaryl derivative **9** binds to the α2/α3/L5 allosteric pocket just like traditional KSP inhibitors.[29] In a recent report, the unique binding mode of benzimidazole-type inhibitor **10** to KSP was demonstrated by X-ray crystallography, in which two molecules of **10** bind to the well-characterized α2/α3/L5 allosteric pocket and the secondary α4/α6 allosteric pocket (Figure 10).[30]
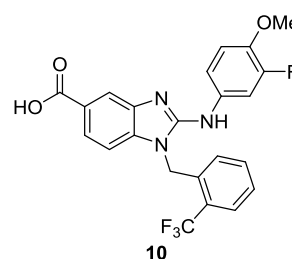
Figure 10. Structure of benz-imidazole-type KSP inhibitor **10**.

The development of KSP inhibitors by the author's group began with the comparative scaffold analysis of the reported KSP inhibitors. Terpendole E is the first KSP inhibitor of natural product origin, that was discovered in 2003 by Osada and colleagues (IC$_{50}$ = 23.0 μM; Figure 11).[31] HR22C16 is a tetrahydrocarboline-type KSP inhibitor, as mentioned above. From the common structure of these compounds, it was assumed that a 2,3-fused indole would be the minimal scaffold for KSP inhibition (Figure 11). Substituted carbazoles were obtained via palladium-catalyzed one-pot continuous reactions including *N*-arylation of anilines and the oxidative biaryl coupling, which was established by the author's group (Scheme 1).[32] The carbazole derivatives previously obtained in studies of this one-pot reaction were screened for KSP inhibitors. Among 54 compounds evaluated, carbazoles **11a–c** with a 2-CF$_3$, 2-*t*-Bu or 3-CF$_3$ group

terpendole E   HR22C16

11a: R^1 = H, R^2 = CF$_3$
11b: R^1 = H, R^2 = *t*-Bu
11c: R^1 = CF$_3$, R^2 = H

Figure 11. Identification of carbazole-type KSP inhibitors **11a–c** based on the reported KSP inhibitors.

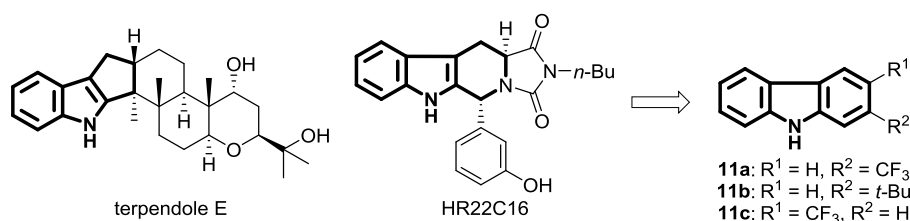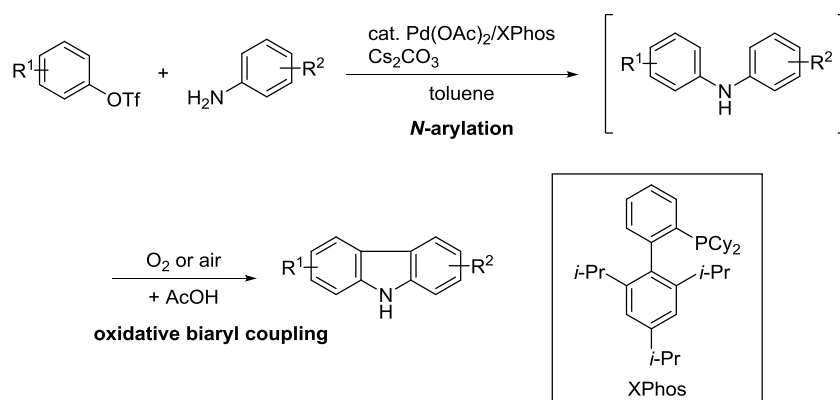**Scheme 1.** One-pot synthesis of carbazoles by *N*-arylation and oxidative biaryl coupling.

exhibited potent KSP inhibitory activity [IC_{50}(**11a**) = 0.21 μM; IC_{50}(**11b**) = 0.25 μM; IC_{50}(**11c**) = 0.99 μM].[33] HeLa cells treated with compounds **11a–c** were arrested in M-phase and had monopolar spindles, the typical phenotype of KSP suppression. Compound **11a** had the most potent activity in this series, and was therefore employed as the lead compound for the subsequent experiments in this study.

In this study, the author describes development of novel classes of KSP inhibitors with fused-indole and diaryl amine scaffolds.

In Chapter 1, the author describes the structure–activity relationship studies of fused indole-type KSP inhibitors with carboline and carbazole scaffolds.

In Chapter 2, Section 1, the author describes the development of diaryl amine-type KSP inhibitors to improve aqueous solubility. Structural investigation of the factors contributing to the enhanced solubility by X-ray analysis and free energy calculation is also presented.

In Chapter 2, Section 2, the author describes the optimization studies of diaryl amine-type KSP inhibitors to identify novel inhibitors with a favorable balance of potency and solubility. The inhibitory mechanism and potential binding mode to KSP of these inhibitors are also presented.

References

(1)   (a) Dutcher, J. P.; Novik, Y.; O'Boyle, K.; Marcoullis, G.; Secco, C.; Wiernik, P. H. *J. Clin. Pharmacol.* **2000**, *40*, 1079–1092. (b) Jordan, M. A.; Wilson, L. *Nat. Rev. Cancer* **2004**, *4*, 253–265.

(2)   (a) Rowinsky, E. K.; Chaudhry, V.; Cornblath, D. R.; Donehower, R. C. *J. Natl. Cancer Inst. Monogr.* **1993**, *15*, 107–115. (b) Quasthoff, S.; Hartung, H. P. *J. Neurol.* **2002**, *249*, 9–17.

(3)   Kavallaris, M. *Nat. Rev. Cancer* **2010**, *10*, 194–204.

(4)   Wood, K. W.; Cornwell, W. D.; Jackson, J. R. *Curr. Opin. Pharmacol.* **2001**, *1*, 370–377.

(5)   Miki, H.; Okada, Y.; Hirokawa, N. *Trends Cell Biol.* **2005**, *15*, 467–476.

(6)   Woehlke, G.; Ruby, A. K.; Hart, C. L.; Ly, B.; Hom-Booher, N.; Vale, R. D. *Cell* **1997**, *90*, 207–216.

(7)   Nitta, R.; Kikkawa, M.; Okada, Y.; Hirokawa, N. *Science* **2004**, *305*, 678–683.

(8)   Sawin, K. E.; LeGuellec, K.; Philippe, M.; Mitchison, T. J. *Nature* **1992**, *359*, 540–543.

(9)   (a) Blangy, A.; Lane, H. A.; d'Herin, P.; Harper, M.; Kress, M.; Nigg, E. A. *Cell* **1995**, *83*, 1159–1169. (b) Walczak, C. E.; Vernos, I.; Mitchison, T. J.; Karsenti, E.; Heald, R. *Curr. Biol.* **1998**, *8*, 903–913. (c) Tao, W.; South, V. J.; Zhang, Y.; Davide, J. P.; Farrell, L.; Kohl, N. E.; Sepp-Lorenzino, L.; Lobell, R. B. *Cancer Cell* **2005**, *8*, 49–59.

(10)   Sakowicz, R.; Finer, J. T.; Beraud, C.; Crompton, A.; Lewis, E.; Fritsch, A.; Lee, Y.; Mak, J.; Moody, R.; Turincio, R.; Chabala, J. C.; Gonzales, P.; Roth, S.; Weitman, S.; Wood, K. W. *Cancer Res.* **2004**, *64*, 3276–3280.

(11)   Mayer, T. U.; Kapoor, T. M.; Haggarty, S. J.; King, R. W.; Schreiber, S. L.; Mitchison, T. J. *Science* **1999**, *286*, 971–974.

(12)   For recent reviews, see: (a) Jackson, J. R.; Patrick, D. R.; Dar, M. M.; Huang, P. S. *Nat. Rev. Cancer* **2007**, *7*, 107–117. (b) Matsuno, K.; Sawada, J.; Asai, A. *Expert Opin. Ther. Patent* **2008**, *18*, 1–22. (c) Sarli, V.; Giannis, A. *Clin. Cancer Res.* **2008**, *14*, 7583–7587. (d) Rath, O.; Kozielski, F. *Nat. Rev. Cancer* **2012**, *12*, 527–539.

(13)   (a) Gartner, M.; Sunder-Plassmann, N.; Seiler, J.; Utz, M.; Vernos, I.; Surrey, T.; Giannis, A. *ChemBioChem* **2005**, *6*, 1173–1177. (b) Sarli, V.; Huemmer, S.; Sunder-Plassmann, N.; Mayer, T. U.; Giannis, A. *ChemBioChem* **2005**, *6*, 2005–2013.

(14) Talapatra, S. K.; Anthony, N. G.; Mackay, S. P.; Kozielski, F. *J. Med. Chem.* **2013**, *56*, 6317–6329.

(15) Theoclitou, M.; Aquila, B.; Block, M. H.; Brassil, P. J.; Castriotta, L.; Code, E.; Collins, M. P.; Davies, A. M.; Deegan, T.; Ezhuthachan, J.; Filla, S.; Freed, E.; Hu, H.; Huszar, D.; Jayaraman, M.; Lawson, D.; Lewis, P. M.; Nadella, M. V. P.; Oza, V.; Padmanilayam, M.; Pontz, T.; Ronco, L.; Russell, D.; Whitston, D.; Zheng, X. *J. Med. Chem.* **2011**, *54*, 6734–6750.

(16) Cox, C. D.; Breslin, M. J.; Mariano, B. J.; Coleman, P. J.; Buser, C. A.; Walsh, E. S.; Hamilton, K.; Huber, H. E.; Kohl, N. E.; Torrent, M.; Yan, Y.; Kuo, L. C.; Hartman, G. D. *Bioorg. Med. Chem. Lett.* **2005**, *15*, 2041–2045.

(17) Fraley, M. E.; Garbaccio, R. M.; Arrington, K. L.; Hoffman, W. F.; Tasber, E. S.; Coleman, P. J.; Buser, C. A.; Walsh, E. S.; Hamilton, K.; Fernandes, C.; Schaber, M. D.; Lobell, R. B.; Tao, W.; South, V. J.; Yan, Y.; Kuo, L. C.; Prueksaritanont, T.; Shu, C.; Torrent, M.; Heimbrook, D. C.; Kohl, N. E.; Huber, H. E.; Hartman, G. D. *Bioorg. Med. Chem. Lett.* **2006**, *16*, 1775–1779.

(18) Cox, C. D.; Coleman, P. J.; Breslin, M. J.; Whitman, D. B.; Garbaccio, R. M.; Fraley, M. E.; Buser, C. A.; Walsh, E. S.; Hamilton, K.; Schaber, M. D.; Lobell. R. B.; Tao, W.; Davide, J. P.; Diehl, R. E.; Abrams, M. T.; South, V. J.; Huber, H. E.; Torrent, M.; Prueksaritanont, T.; Li, C.; Slaughter, D. E.; Mahan, E.; Fernandez-Metzler, C.; Yan, Y.; Kuo, L. C.; Kohl, N. E.; Hartman, G. D. *J. Med. Chem.* **2008**, *51*, 4239–4252.

(19) Owens, B. *Nat. Med.* **2013**, *19*, 1550.

(20) Schiemann, K.; Finsinger, D.; Zenke, F.; Amendt, C.; Knöchel, T.; Bruge, D.; Buchstaller, H.; Emde, U.; Stähle, W.; Anzali, S. *Bioorg. Med. Chem. Lett.* **2010**, *20*, 1491–1495.

(21) (a) Hotha, S.; Yarrow, J. C.; Yang, J. G.; Garrett, S.; Renduchintala, K. V.; Mayer, T. U.; Kapoor, T. M. *Angew. Chem., Int. Ed.* **2003**, *42*, 2379–2382. (b) Marcus, A. I.; Peters, U.; Thomas, S. L.; Garrett, S.; Zelnak, A.; Kapoor, T. M.; Giannakakou, P. *J. Biol. Chem.* **2005**, *280*, 11569–11577.

(22) Sunder-Plassmann, N.; Sarli, V.; Gartner, M.; Utz, M.; Seiler, J.; Huemmer, S.; Mayer, T. U.; Surrey, T.; Giannis, A. *Bioorg. Med. Chem.* **2005**, *13*, 6094–6111.

(23) (a) DeBonis, S.; Skoufias, D. A.; Lebeau, L.; Lopez, R.; Robin, G.; Margolis, R. L.; Wade, R. H.; Kozielski, F. *Mol. Cancer Ther.* **2004**, *3*, 1079–1090. (b) Skoufias, D. A.; DeBonis, S.; Saoudi, Y.; Lebeau, L.; Crevel, I.; Cross, R.; Wade, R. H.; Hackney, D.; Kozielski, F. *J. Biol. Chem.* **2006**, *281*, 17559–17569.

(24) (a) Ogo, N.; Oishi, S.; Matsuno, K.; Sawada, J.; Fujii, N.; Asai, A. *Bioorg. Med.*

Chem. Lett. **2007**, *17*, 3921–3924. (b) DeBonis, S.; Skoufias, D. A.; Indorato, R.; Liger, F.; Marquet, B.; Laggner, C.; Joseph, B.; Kozielski, F. *J. Med. Chem*. **2008**, *51*, 1115–1125.

(25) (a) Parrish, C. A.; Adams, N. D.; Auger, K. R.; Burgess, J. L.; Carson, J. D.; Chaudhari, A. M.; Copeland, R. A.; Diamond, M. A.; Donatelli, C. A.; Duffy, K. J.; Faucette, L. F.; Finer, J. T.; Huffman, W. F.; Hugger, E. D.; Jackson, J. R.; Knight, S. D.; Luo, L.; Moore, M. L.; Newlander, K. A.; Ridgers, L. H.; Sakowicz, R.; Shaw, A. N.; Sung, C. M. M.; Sutton, D.; Wood, K. W.; Zhang, S. Y.; Zimmerman, M. N.; Dhanak, D. *J. Med. Chem*. **2007**, *50*, 4939–4952. (b) Luo, L.; Parrish, C. A.; Nevins, N.; McNulty, D. E.; Chaudhari, A. M.; Carson, J. D.; Sudakin, V.; Shaw, A. N.; Lehr, R.; Zhao, H.; Sweitzer, S.; Lad, L.; Wood, K. W.; Sakowicz, R.; Annan, R. S.; Huang, P. S.; Jackson, J. R.; Dhanak, D.; Copeland, R. A.; Auger, K. R. *Nat. Chem. Biol*. **2007**, *33*, 722–726. (c) Matsuno, K.; Sawada, J.; Sugimoto, M.; Ogo, N.; Asai, A. *Bioorg. Med. Chem. Lett*. **2009**, *19*, 1058–1061.

(26) Rickert, K. W.; Schaber, M.; Torrent, M.; Neilson, L. A.; Tasber, E. S.; Garbaccio, R.; Coleman, P. J.; Harvey, D.; Zhang, Y.; Yang, Y.; Marshall, G.; Lee, L.; Walsh, E. S.; Hamilton, K.; Buser, C. A. *Arch. Biochem. Biophys*. **2008**, *469*, 220–231.

(27) (a) Yan, Y.; Sardana, V.; Xu, B.; Homnick, C.; Halczenko, W.; Buser, C. A.; Schaber, M.; Hartman, G. D.; Huber, H. E.; Kuo, L. C. *J. Mol. Biol*. **2004**, *335*, 547–554. (b) Brier, S.; Lemaire, D.; DeBonis, S.; Forest, E. Kozielski, F. *J. Mol. Biol*. **2006**, *360*, 360–376. (c) Garcia-Saez, I.; DeBonis, S.; Lopez, R.; Trucco, F.; Rousseau, B.; Thuery, P.; Kozielski, F. *J. Biol. Chem*. **2007**, *282*, 9740–9747. (d) Roecker, A. J.; Coleman, P. J.; Mercer, S. P.; Schreier, J. D.; Buser, C. A.; Walsh, E. S.; Hamilton, K.; Lobell, R. B.; Tao, W.; Diehl, R. E.; South, V. J.; Davide, J. P.; Kohl, N. E.; Yan, Y.; Kuo, L. C.; Li, C.; Fernandez-Metzler, C.; Mahan, E. A.; Prueksaritanont, T.; Hartman, G. D. *Bioorg. Med. Chem. Lett*. **2007**, *17*, 5677–5682. (e) Kaan, H. Y. K.; Ulaganathan, V.; Hackney, D. D.; Kozielski, F. *Biochem. J*. **2010**, *425*, 55–60. (f) Kaan, H. Y. K.; Ulaganathan, V.; Rath, O.; Prokopcova, H.; Dallinger, D.; Kappe, C. O.; Kozielski, F. *J. Med. Chem*. **2010**, *33*, 5676–5683. (g) Barsanti, P. A.; Ni, W. W. Z.; Duhl, D.; Brammeier, N.; Martin, E.; Bussiere, D.; Walter, A. O. *Bioorg. Med. Chem. Lett*. **2010**, *20*, 157–160.

(28) Talapatra, S. K.; Anthony, N. G.; Mackay, S. P.; Kozielski, F. *J. Med. Chem*. **2013**, *56*, 6317–6329.

(29) Wacker, S. A.; Kashyap, S.; Li, X.; Kapoor, T. M. *J. Am. Chem. Soc*. **2011**, *133*,

12386–12389.

(30) Ulaganathan, V.; Talapatra, S. K.; Rath, O.; Pannifer, A.; Hackney, D. D.; Kozielski, F. *J. Am. Chem. Soc*. **2013**, *135*, 2263–2272.

(31) Nakazawa, J.; Yajima, J.; Usui, T.; Ueki, M.; Takatsuki, A.; Imoto, M.; Toyoshima, Y.; Osada, H. *Chem. Biol.* **2003**, *10*, 131–137.

(32) (a) Watanabe, T.; Ueda, S.; Inuki, S.; Oishi, S.; Fujii, N.; Ohno, H. *Chem. Commun.* **2007**, 4516–4518. (b) Watanabe, T.; Oishi, S.; Fujii, N.; Ohno, H. *J. Org. Chem.* **2009**, *74*, 4720–4726.

(33) Oishi, S.; Watanabe, T.; Sawada, J.; Asai, A.; Ohno, H.; Fujii, N. *J. Med. Chem.* **2010**, *53*, 5054–5058.

Chapter 1. Development of Novel Kinesin Spindle Protein Inhibitors with Fused-indole Scaffolds

A variety of carboline and carbazole derivatives were designed for novel KSP inhibitors based on the natural product scaffold-derived KSP inhibitors and reported biphenyl-type inhibitors. β-Carboline and lactam-fused carbazole derivatives exhibited remarkably potent KSP inhibitory activity and mitotic arrest in prometaphase with formation of a monopolar spindle. The planar tri- and tetracyclic analogs inhibited KSP ATPase in an ATP-competitive manner like biphenyl-type inhibitors.

As described in preface, carbazoles **3a–c** (= **11a–c** in preface) with a hydrophobic alkyl group at the 2- or 3-position exhibited potent KSP inhibitory activity.[1] Based on the common substructure of the known KSP inhibitory terpendole E (**1**) and HR22C16 (**2**) (Figure 1),[2,3] the ring-fused indoles were identified to be minimal scaffolds for KSP inhibition. During the course of the study, it was also demonstrated that the cytotoxic activity of β-carboline alkaloids harman and harmine was in part caused by KSP inhibitory activity.[1] The use of the core substructures of these natural products and natural product-related compounds could facilitate further structure–activity relationship studies.
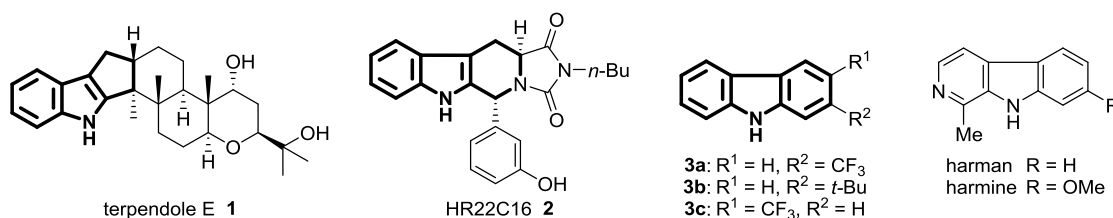

Figure 1. Structures of the reported KSP inhibitors **1** and **2** and the potent KSP inhibitors with a 2,3-fused indole substructure.

Alternatively, KSP inhibitors with biaryl scaffolds such as **4–6** have been reported (Figure 2).[4-6] Biphenyls **5** and **6** bind to the interface of helices α4 and α6 (which is remote from the ATP binding site) to inhibit KSP activity in an ATP-competitive manner.[4a] The author assumed that carbazole derivative **3a** with KSP inhibitory activity could be regarded as compounds with a nitrogen atom bridged between the 2- and 2′-carbons of biphenyl. The introduction of the accessory groups of biphenyls **4–6** into carbazole derivative **3a** would lead to the increase of KSP inhibitory activity. Accordingly, the structure–activity relationship studies of planar carbazole and carboline derivatives from the lead compound **3a** were carried out. The enzymatic analysis of the potent derivatives is also described to investigate the potential binding and functional modes of action.
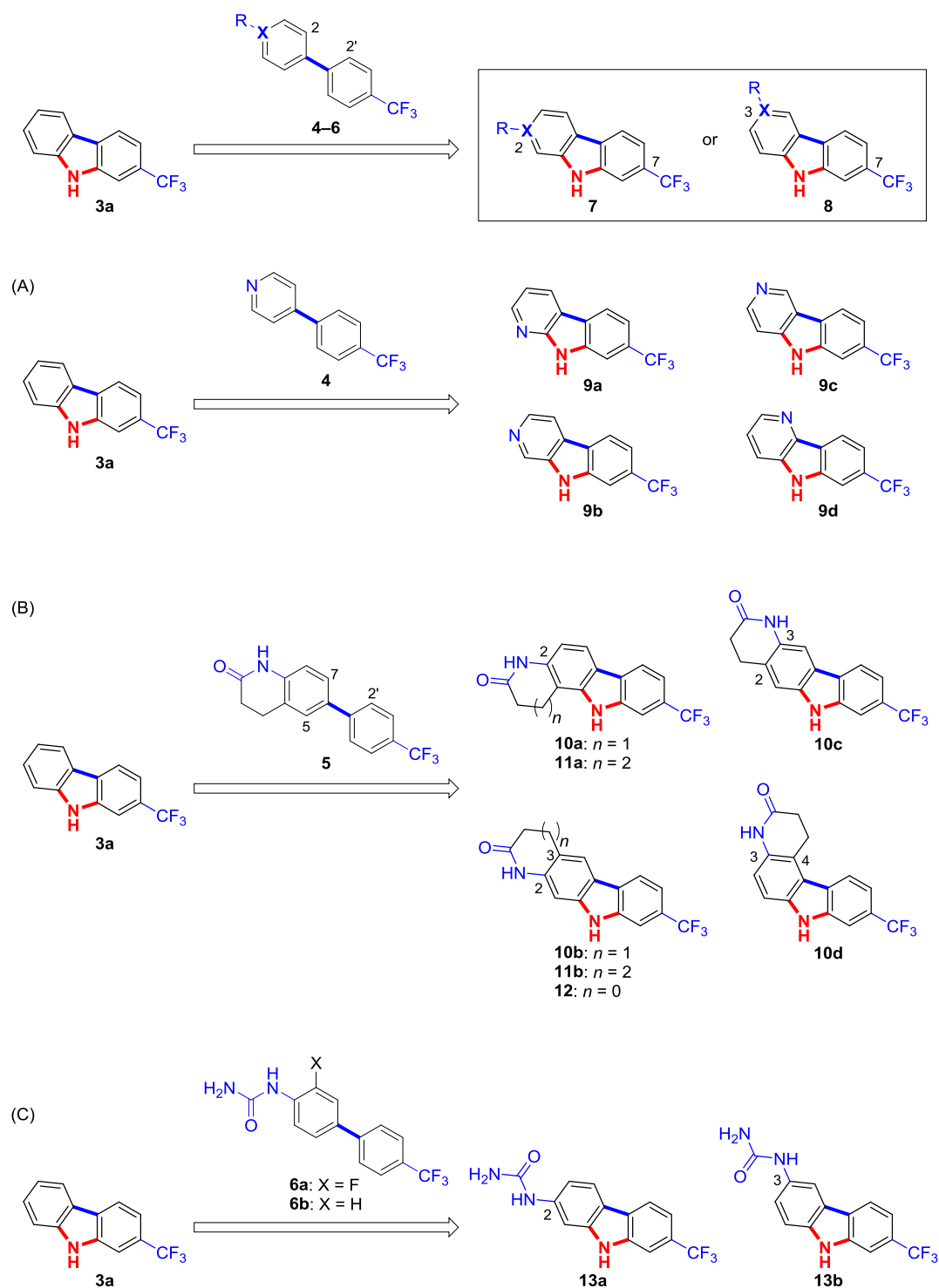
Figure 2. Design of novel KSP inhibitors **9–13** with carboline (A) and carbazole (B, C) scaffolds.

Two possible orientations of the accessory groups on the carbazole core were deliberated to reoptimize the position of the functional group, considering the orientation change of two aryl groups owing to the nitrogen bridge. Bidirectional

14

orientation of **7** at the carbazole 2- and 7-positions was designed from ring-closing via one-nitrogen linkage between biphenyl 2- and 2′-positions. Reproduction of the outward-facing orientations of two accessory groups in biaryl compounds **4–6** could provide the 3,7-disubstituted carbazoles **8**.

Carboline derivatives **9a–d** with a 7-trifluoromethyl group were designed by the introduction of a pyridine nitrogen atom of 4-[4-(trifluoromethyl)phenyl]pyridine (**4**)[6] into carbazole **3a** (Figure 2A). β-Carboline **9b** was designed to examine the ring-closing effect via nitrogen linkage of compound **4**, in which the 4-phenylpyridine framework was included in the 6-5-6 tricyclic structure of β-carboline. The arrangement of a pyridine nitrogen and a CF$_3$ group of γ-carboline **9c** was presumably mimicked by the relative orientation of the pyridine nitrogen and the CF$_3$ group of **4**. Additional α- and δ-carbolines **9a,d** were the alternative regioisomers, which were incompatible with the conformations of 4-phenylpyridine derivative **4**.

Dihydroquinolinone **5** is also a potent KSP inhibitor with a 4-trifluoromethyl-biphenyl scaffold (Figure 2B), which presumably binds in a twisted conformation of the biphenyl at the interface of the α4 and α6 helices of KSP.[4a] The author designed four lactam-fused carbazole derivatives **10a–d** based on carbazole **3a** and biphenyl **5**. Carbazole **10a** or **10b** was designed by bridging via an NH group between dihydro-quinolinone 5- or 7-positions and the 2′-position of **5**. In carbazoles **10c,d** with 2,3- and 3,4-fused lactams, the orientation of the trifluoromethyl and lactam amide moieties in **5** were reproduced. To optimize the appropriate ring systems of **10a,b** for KSP inhibition, carbazoles **11a,b** and **12** with different ring-sized lactams were also evaluated. Carbazoles **13a,b** with a urea group at the 2- or 3-positions were similarly designed based on carbazole **3a** and biphenyls **6a,b** (Figure 2C).[4b]

A series of carboline derivatives **9a–d** were prepared by *N*-arylation using iodopyridine (**14**, **16** and **17**) / 2-bromo-5-(trifluoromethyl)aniline **15** or 3-amino-2-chloropyridine **18** / substituted iodobenzene **19** and the subsequent palladium-catalyzed intramolecular C–H arylation of *N*-aryl-2-haloaniline derivatives (Scheme 1).[7]

For carbazoles **10a,b** with a six-membered lactam, aryl bromide **20a** was initially converted to pinacolboronate **21a**[8] by a palladium-catalyzed coupling reaction with bis(pinacolato)diboron.[9] The subsequent Suzuki–Miyaura cross-coupling of **21a** led to the 2-nitrobiphenyl derivative **22a** (Scheme 2A). The carbazoles **10a,b** were obtained by triphenylphosphine-mediated reductive cyclization of **22a**.[10] Carbazoles **11a,b** with a seven-membered lactam were also synthesized in a similar procedure. The other lactam-fused carbazoles **10c** was obtained by palladium-catalyzed *N*-arylation of
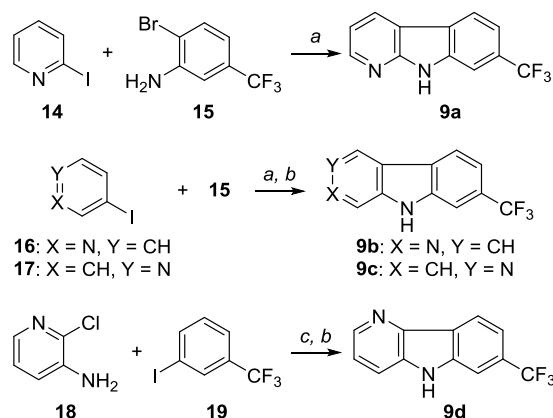
Scheme 1. Synthesis of carboline derivatives. *Reagents and conditions*: (a) Pd(OAc)$_2$, Xantphos, NaO*t*-Bu, toluene, reflux; (b) Pd(OAc)$_2$, PCy$_3$·HBF$_4$, K$_2$CO$_3$, *t*-BuCO$_2$H, DMA, 130 °C; (c) CuI, 1,10-phenanthroline, K$_2$CO$_3$, DMF, 110 °C.
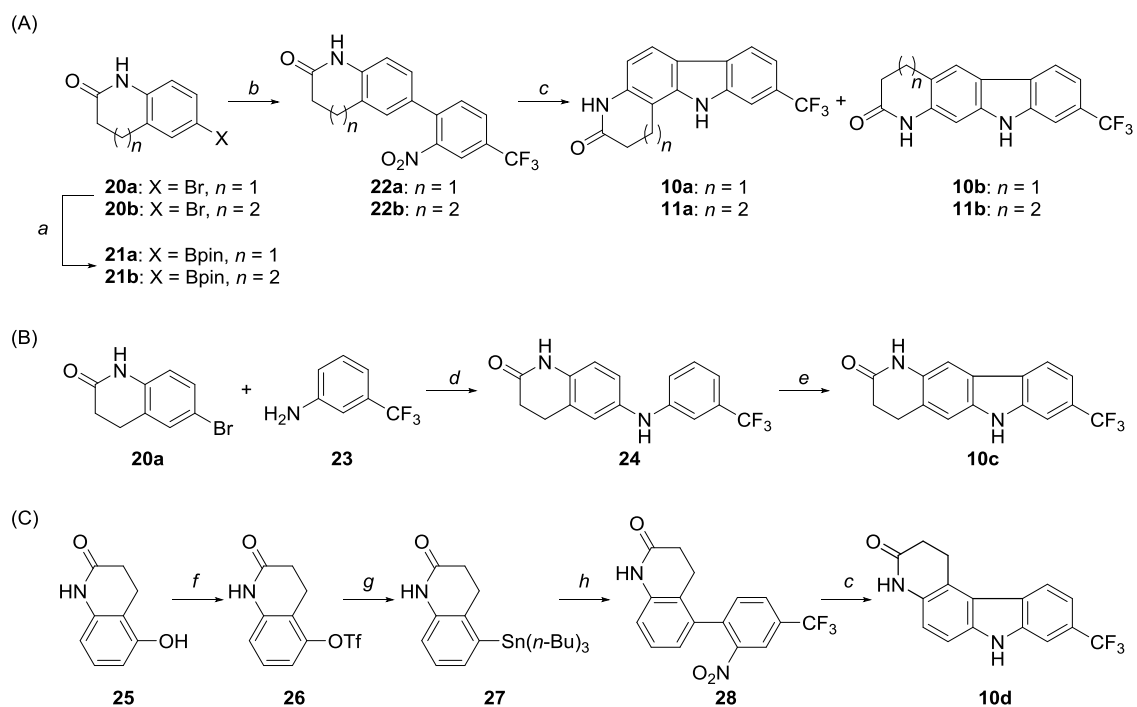
Scheme 2. Synthesis of carbazole derivatives with a lactam-fused structure. *Reagents and conditions:* (a) (pinB)$_2$, PdCl$_2$(dppf), KOAc, DMSO, 80 °C; (b) 4-bromo-3-nitrobenzotrifluoride, PdCl$_2$(dppf), K$_2$CO$_3$, 1,4-dioxane, 90 °C; (c) PPh$_3$, *o*-DCB, 165 °C; (d) Pd$_2$(dba)$_3$·CHCl$_3$, DavePhos, NaO*t*-Bu, toluene, 100 °C; (e) Pd(OAc)$_2$, O$_2$, AcOH, 120 °C; (f) Tf$_2$O, pyridine, CH$_2$Cl$_2$, rt; (g) Pd(PPh$_3$)$_4$, LiCl, (Bu$_3$Sn)$_2$, 1,4-dioxane, 100 °C; (h) 4-bromo-3-nitrobenzotrifluoride, Pd$_2$(dba)$_3$·CHCl$_3$, P(*t*-Bu)$_3$·HBF$_4$, CsF, toluene, 110 °C.

lactam **20a** and *m*-CF$_3$ substituted aniline **23** followed by oxidative biaryl coupling (Scheme 2B).[11] For the preparation of carbazole **10d**, phenol derivative **25** was initially
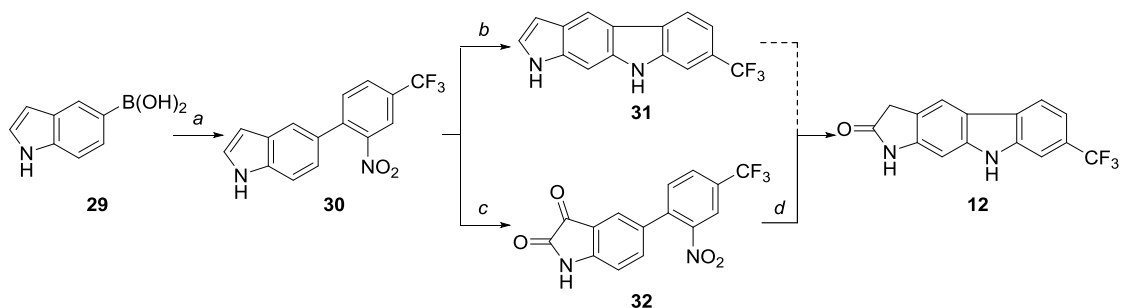
Scheme 3. Synthesis of carbazole derivatives with a five-membered lactam ring or pyrrole-fused structure. *Reagents and conditions:* (a) 4-bromo-3-nitrobenzotrifluoride, Pd(OAc)$_2$, XPhos, K$_2$CO$_3$, 1,4-dioxane, 60 °C; (b) 4-(dimethylamino)triphenylphosphine, *o*-DCB, 160 °C; (c) PCC, 1,2-DCE, 80 °C; (d) 4-(dimethylamino)triphenylphosphine, *o*-DCB, 140 °C.
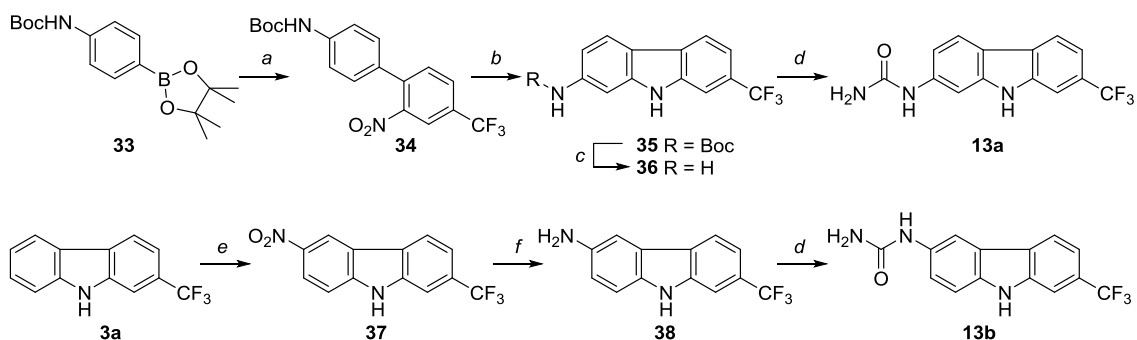
Scheme 4. Synthesis of carbazole derivatives with a urea group. *Reagents and conditions*: (a) 4-bromo-3-nitrobenzotrifluoride, PdCl$_2$(dppf), K$_2$CO$_3$, 1,4-dioxane, 80 °C; (b) PPh$_3$, *o*-DCB, 165 °C; (c) 4 N HCl in 1,4-dioxane, rt; (d) KOCN, AcOH, H$_2$O, rt; (e) HNO$_3$, AcOH, 60 °C; (f) Pd/C, HCO$_2$NH$_4$, EtOH, reflux

converted to the corresponding trifluoromethanesulfonate **26** (Scheme 2C).[12] Next, organotin compound **27** was obtained by treatment of **26** with bis(tributyltin) in the presence of palladium catalyst and LiCl,[13] and subsequent Stille coupling with aryl bromide provided compound **28**.[14] The desired carbazole **10d** was prepared under the identical conditions for the reductive cyclization.

The synthesis of carbazole **12** with a five-membered lactam was undertaken via indole derivative **30**, which was prepared using Suzuki–Miyaura coupling from commercially available boronic acid **29** (Scheme 3). Compound **30** was converted to carbazole **31** by phosphine-mediated reductive cyclization. However, separation of the byproduct, triphenylphosphine oxide, from the product **31** by repeated column chromatography failed. When 4-(dimethylamino)triphenylphosphine was used as the reducing reagent, the purification of carbazole **31** was readily achieved by a single round of column chromatography. Unfortunately, the efforts to obtain the desired
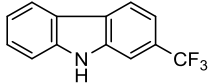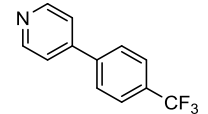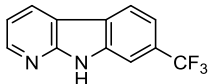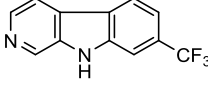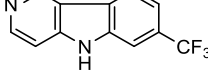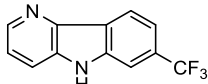
carbazole **12** upon treatment with various oxidative reagents resulted only in the recovery or decomposition of **31**. As an alternative, an isatin derivative **32** was prepared by the oxidation of compound **30** using pyridinium chlorochromate (PCC).[15] Interestingly, when compound **32** was treated with 4-(dimethylamino)triphenylphosphine, the carbonyl group at the isatin 3-position was reduced to the methylene group concomitantly with the formation of a carbazole core structure to provide the desired carbazole **12**.

The synthesis of compound **13a** with a urea group at the carbazole 2-position began from commercially available pinacolboronate ester **33** (Scheme 4). Compound **33** was converted to the 2-nitrobiphenyl derivative **34** by Suzuki–Miyaura coupling, which underwent reductive cyclization to afford Boc-protected aminocarbazole **35**. After deprotection, compound **36** was converted to the expected carbazole **13a** by using KOCN.[16] For compound **13b** with a urea group at the carbazole 3-position, compound **37** was prepared by nitration of carbazole derivative **3a**. Compound **37** was reduced to the corresponding amine **38**, which was converted to the desired carbazole **13b**.

The resulting carbolines and carbazoles were evaluated for inhibition of KSP ATPase and cytotoxicity toward HeLa cells. Among carboline derivatives **9a–d** having a 7-trifluoromethyl group, no inhibitory effect was observed with the α-carboline derivative **9a**, whereas β- and γ-carbolines **9b,c** exerted enhanced KSP ATPase inhibitory activity compared with the corresponding carbazole derivative **3a** or biaryl-type derivative **4** [IC_{50}(**9b**) = 0.052 μM; IC_{50}(**9c**) = 0.095 μM] (Table 1). δ-Carboline **9d** exhibited similar inhibitory potency to the parent carbazole **3a**. A positive correlation between KSP ATPase inhibition and cytotoxicity toward HeLa cells was observed among carboline derivatives **9a–d**; for example, the cytotoxicity of β-carboline **9b** was the most potent (IC_{50} = 0.81 μM). This investigation revealed that the introduction of accessory groups into the 2- or 3-position of carbazole **3a** is a promising approach to design potent KSP inhibitors.

Carbazole derivatives **10a–d** with a lactam-fused structure were then investigated (Table 2). The accessory amide group at the carbazole 2-position (**10a,b**) improved KSP ATPase inhibitory activity compared with **5**. Interestingly, carbazole **10b** with a 2,3-fused lactam ring showed remarkably potent cytotoxicity (IC_{50} = 0.091 μM) in comparison with carbazole **10a** fused at the 1- and 2-positions, although **10b** showed approximately equipotent KSP ATPase inhibitory activity to **10a**.[17] An identical modification at the carbazole 3-position (**10c,d**) was less effective, which showed similar or slightly greater potency compared with the parent carbazole **3a**. This may be due to the inappropriate orientations of the lactam amide moiety and/or the electron

Table 1. Structure–activity relationships of carboline derivatives

compound		KSP ATPase IC$_{50}$ (µM) ^{a,b}	cell growth IC$_{50}$ (µM) ^{a,c}
	3a	0.21	7.8
	4	>6.3^d	–^{e}
	9a	>6.3	>200
	9b	0.052	0.81
	9c	0.095	1.4
	9d	0.33	16
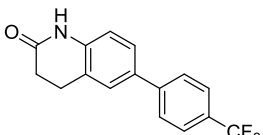
^{a}IC$_{50}$ values were derived from the dose–response curves generated from triplicate data points. ^{b}Inhibition of microtubule-activated KSP ATPase activity. ^{c}Cytotoxic activity against HeLa cells after 72-hour exposure to each compound. ^{d}IC$_{50}$ was ~10 µM. ^{e}Not tested.

donating effect to the carbazole scaffold. The 2,3-fused lactam **10c** did not show the bioactivity in the cell-based assay, which was in contrast with **10b**, which had similar fused ring systems. The orientation of the lactam NH group in **10c** was disadvantageous to the interaction with KSP and cellular effects.

The biological activities of the urea-containing compounds were also examined (Table 3).[6] The urea group at the carbazole 2-position in **13a** improved KSP ATPase inhibitory activity and cytotoxicity compared with the parent carbazole **3a** and the biphenyl-type inhibitors **6a,b**. 3-Carbamidylcarbazole **13b** was less potent than the 2-substituted congener **13a**, which was consistent with the SAR profile of the series of carbolines **9a–d** and lactam-fused compounds **10a–d**.

Subsequently, optimization of the lactam ring was carried out for the highly
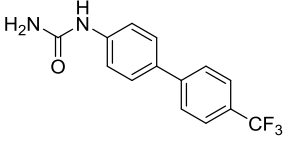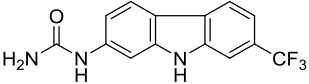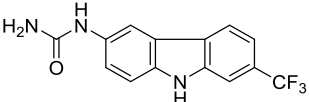
Table 2. Structure–activity relationships of carbazole derivatives with a lactam-fused structure

compound		KSP ATPase	cell growth
		IC$_{50}$ (μM) ^{a,b}	IC$_{50}$ (μM) ^{a,c}
	5	0.046	0.28
	10a	0.040	0.61
	10b	0.031	0.091
	10c	0.18	>63
	10d	0.084	5.0

^{a}IC$_{50}$ values were derived from the dose–response curves generated from triplicate data points. ^{b}Inhibition of microtubule-activated KSP ATPase activity. ^{c}Cytotoxic activity against HeLa cells after 72-hour exposure to each compound.

potent carbazoles **10a,b** (Table 4). Carbazole derivatives **12** and **11b**, which fused at the carbazole 2,3-positions with a five- and seven-membered lactam, respectively, exerted slightly less bioactivities compared with the six-membered lactam **10b**, suggesting the possible flexibility of the lactam carbonyl placement. Inhibitory activity was also dependent upon the position of ring-fusion. Carbazole **11a**, which fused with a seven-membered lactam at the 1- and 2-positions, showed less KSP inhibition and cytotoxicity than the 2,3-fused congener **11b**. This was consistent with the bioactivity profiles of compounds **10a,b** with a six-membered lactam. The less potent activities of pyrrolocarbazole derivative **31** than **12** indicate that a lactam carbonyl group at this position is a pivotal functional group for bioactivity.

Table 3. Structure–activity relationships of carbazole derivatives with a urea group

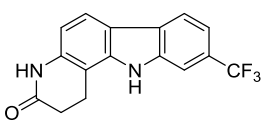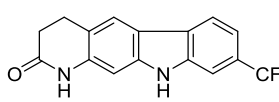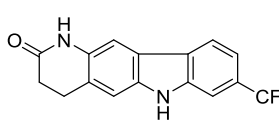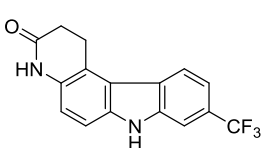| compound		KSP ATPase IC$_{50}$ (μM)^{a,b}	cell growth IC$_{50}$ (μM)^{a,c}
	6a	0.10	1.1
	6b	0.14	1.5
	13a	0.085	0.38
	13b	0.12	4.0

[a]IC$_{50}$ values were derived from the dose–response curves generated from triplicate data points. [b]Inhibition of microtubule-activated KSP ATPase activity. [c]Cytotoxic activity against HeLa cells after 72-hour exposure to each compound.

Examinations by three series of carboline and carbazole derivatives revealed that the coplanar conformation and appropriate bidirectional arrangements of two accessory groups provide favorable effects on KSP ATPase inhibitory activity and cytotoxicity. Although the twisted bioactive conformations of two phenyl rings in biphenyl **5** for KSP were proposed,[4a] the potent analogs **10a,b** suggest that the planar conformations could provide another favorable interaction for bioactivity. In particular, modification at the carbazole 2-position with a polar group such as a nitrogen atom (for β-carboline), lactam amide or urea group improved the inhibitory activities. The lactam-fused carbazole **10b** with a linear 6-6-5-6 fused ring system was the most potent KSP inhibitor in this investigation.

Potent KSP inhibitors (**10a,b**, and **13a**) were evaluated for inhibitory effects against the other motor proteins: centromere-associated protein E (CENP-E), Kid, mitotic kinesin-like protein 1 (MKLP-1) and KIF-4 (Table 5). The compounds did not inhibit these kinesins even at 20 μM, indicating that they are specific KSP inhibitors.
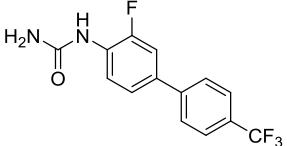
Table 4. Structure–activity relationships of carbazole derivatives with five-, six-, and seven-membered lactam-fused or pyrrole-fused structures

compound	KSP ATPase IC$_{50}$ (μM) [a,b]	cell growth IC$_{50}$ (μM) [a,c]
12	0.037	0.11
10b	0.031	0.091
11b	0.045	0.11
11a	0.058	1.1
31	0.17	2.7

[a]IC$_{50}$ values were derived from the dose–response curves generated from triplicate data points. [b]Inhibition of microtubule-activated KSP ATPase activity. [c]Cytotoxic activity against HeLa cells after 72-hour exposure to each compound.

Furthermore, the author investigated the effects of these compounds on cell cycle progression (Table 6). All of these compounds triggered cell-cycle arrest of HeLa cells to accumulate mitotic cells and, in particular, lactam-fused carbazole **10b** was effective in a low MI$_{50}$ (50% mitotic index induction concentration).

In the microscopic analysis of the mitotic phenotype of the cells treated with highly potent β-carboline **9b** and lactam-fused carbazole **10b**, the formation of monopolar spindles (the typical phenotype of KSP inhibition) was observed in all of the mitotic arrest cells (Figure 3). Although β-carbolines were reported to inhibit topoisomerases I/II,[18] the possible off-target effects were not observed by treatment with **9b**.

It has been reported that most KSP inhibitors (e.g., monastrol, *S*-trityl-L-cysteine) bind to the allosteric pocket formed by helices α2 and α3 and loop L5.[19,20] For example, tetrahydrocarboline-based inhibitors such as **2** (which was a lead compound for the carbazole-based inhibitors **3a–c**) also bind to the same allosteric

Table 5. % Inhibition of ATPase activity of five motor proteins[a]

compound	KSP	CENP-E	Kid	MKLP-1	KIF-4
5	93	1	0	0	0
6b	92	0	0	0	0
10a	96	1	0	1	0
10b	96	0	0	1	0
13a	96	0	0	0	0

[a]The inhibition values were determined by ATPase assay and are indicated as a percentage of the solvent only control. The final concentration of the compounds in the assay was 20 μM.

Table 6. Effects of KSP inhibitors on cell cycle progression of HeLa cells

compound	MI_{50} (μM)[a]
5	0.29
6b	3.7
10a	1.1
10b	0.13
13a	1.3

[a]MI_{50} values indicate the concentration of 50% induction in mitotic HeLa cells after 24-hour exposure to each compound. Values were derived from dose–response curves generated from triplicate data points.

pocket to show ATP-uncompetitive behavior.[21] In contrast, the biphenyl-type inhibitors **5** and **6a** (which work in an ATP-competitive manner) bind at the interface of helices α4 and α6 of the KSP ATPase domain (not at the ATP binding site).[4a] The carboline- and carbazole-based inhibitors **9–13** were designed by a combination of two distinct scaffolds (carbazole derivative **3a** and biaryl compounds **4–6**) so the inhibitory mechanism and binding site of KSP inhibitors **9–13** would be of interest.

To provide valuable insights into the inhibitory mode of β-carboline **9b** and lactam-fused carbazole **10b**, KSP ATPase activity was assessed in the absence or presence of inhibitors when incubating with variable ATP concentrations (Figure 4).
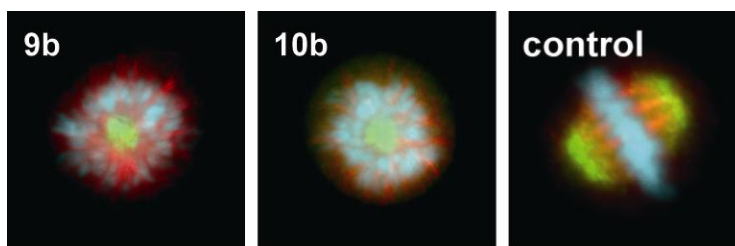
Figure 3. Mitotic phenotype of HeLa cells treated with fused indole derivatives **9b** (8.0 μM) and **10b** (0.25 μM). Chromosomes are colored blue, microtubules red and KSP green.
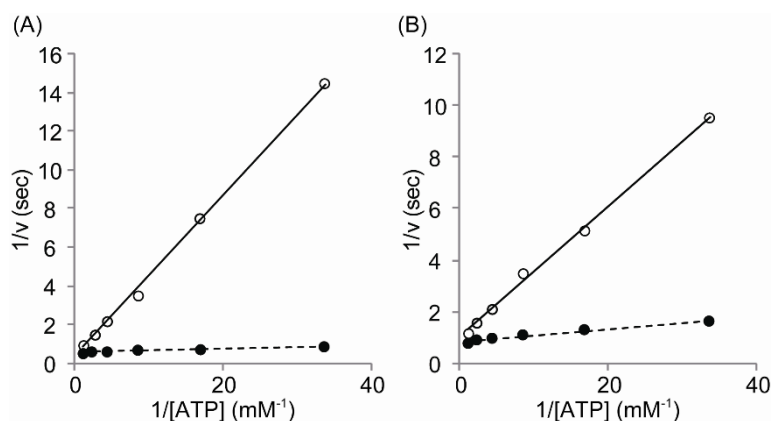
Figure 4. Lineweaver–Burk plots of the kinetics of KSP ATPase. ATPase activity of 80 nM KSP motor domain with 400 nM microtubules as a function of ATP concentration in the absence (closed circle) and presence (open circle) of inhibitors were measured by steady-state KSP ATPase assay. (A) β-carboline **9b** (56 nM); (B) lactam-fused carbazole **10b** (32 nM). Each data point is the average of two independent experiments. Enzyme velocities at the same inhibitor concentration were fitted to the Michaelis–Menten equation to obtain V_{max}.

Lineweaver–Burk plots revealed consistent V_{max} values independent of the presence of the inhibitors. This indicated that compounds **9b** and **10b** functionally compete with ATP binding.[22] It is of interest that these inhibitors **9b** and **10b** worked in a similar mode of inhibition to biphenyl-type **4–6** even though these belong to different types of scaffolds. This is the first observation of β-carboline and carbazole scaffolds for potent ATP-competitive KSP inhibitors.

Preliminary docking simulation study of these inhibitors demonstrated that the adenine binding pocket at the ATP binding site was too small to accommodate the potent lactam-fused carbazole **10b**. In addition, reported crystal structure analyses[23] revealed that the structures of the ATP binding site were highly conserved between KSP and CENP-E. This suggested that possible binding of these inhibitors to the nucleotide site would be contradictory to high KSP selectivity. Accordingly, it is likely that these carboline and carbazole derivatives bind to the interface of helices α4 and α6 in a

similar binding mode to biphenyl-type inhibitors.

In conclusion, the author identified a novel class of small-molecule KSP inhibitors. Studies of the structure–activity relationship of carboline and carbazole derivatives indicated that the coplanar conformations of biphenyl groups favorably contribute to potent KSP inhibition. In addition, hydrophilic groups (e.g., lactam amide group) at the appropriate position are also indispensable functional groups for potent KSP inhibition. The carbazole derivative **10b** fused with a six-membered lactam at the 2- and 3-positions exhibited the most potent KSP ATPase inhibitory activity and the consequent cytotoxicity by effective cell-cycle arrest at the M-phase. It can be concluded from the biochemical studies and selectivity profiles for several kinesins that the carbolines and carbazoles work as ATP-competitive KSP inhibitors by presumably binding at the same site to the one for the biphenyl-type inhibitors. These investigations suggest that similar fused indole scaffolds may provide two distinctive KSP inhibitors which work through separate inhibitory modes: tetrahydrocarboline-based ATP-uncompetitive inhibitors such as **2**; and planar carboline/carbazole-based ATP-competitive inhibitors such as **9b** and **10b**.

Experimental Section

General Method. ^{1}H NMR spectra were recorded using a JEOL AL-400 or a JEOL ECA-500 spectrometer. Chemical shifts are reported in δ (ppm) relative to Me_4Si as an internal standard. ^{13}C NMR spectra were referenced to the residual solvent signal. Exact mass (HRMS) spectra were recorded on a JMS-HX/HX 110A mass spectrometer. Melting points were measured by a hot stage melting point apparatus (uncorrected). For flash chromatography, Wakogel C-300E (Wako) or Chromatorex® NH was employed. For analytical HPLC, a Cosmosil 5C18-ARII column (4.6 x 250 mm, Nacalai Tesque, Inc., Kyoto, Japan) was employed with a linear gradient of CH_3CN containing 0.1% (v/v) TFA at a flow rate of 1 mL/min on a Shimadzu LC-10ADvp (Shimadzu Corp., Ltd., Kyoto, Japan), and eluting products were detected by UV at 254 nm. The purity of the compounds was determined by combustion analysis or HPLC analysis (> 95%).

7-Trifluoromethyl-9*H*-α-carboline (9a). Toluene (2.0 mL) was added to a flask containing $Pd(OAc)_2$ (44.9 mg, 0.20 mmol) and Xantphos (116 mg, 0.20 mmol) under an argon atmosphere. The mixture was stirred for 15 min. 2-iodopyridine **14** (410 mg, 2.0 mmol), 2-bromo-5-(trifluoromethyl)aniline **15** (309 μL, 2.20 mmol), NaO*t*-Bu (269 mg, 2.80 mmol) were added to the reaction mixture, and heated to reflux. After 24 h, the reaction mixture was concentrated *in vacuo*. Crude material was purified by flash chromatography with *n*-hexane/EtOAc (2:1 to 1:1) to afford the desired carboline **9a** (52.9 mg, 11% yield): pale yellow powder; mp 218–219 °C; IR (neat) cm^{-1}: 3438 (NH); ^{1}H NMR (500 MHz, THF-d_8): δ 6.94 (dd, *J* = 6.6, 6.6 Hz, 1H; Ar), 7.51 (dd, *J* = 9.2, 6.6 Hz, 1H; Ar), 7.59 (d, *J* = 8.3 Hz, 1H; Ar), 7.67 (d, *J* = 9.2 Hz, 1H; Ar), 8.15 (s, 1H; NH), 8.25 (d, *J* = 8.3 Hz, 1H; Ar), 8.84 (d, *J* = 6.6 Hz, 1H; Ar); ^{13}C NMR (125 MHz, THF-d_8): δ 111.6, 112.8, 117.6, 118.1, 118.9, 126.0 (q), 127.3, 127.9 (q), 131.1, 132.0, 145.3, 150.9; *Anal.* calcd for $C_{12}H_7F_3N_2$: C, 61.02; H, 2.99; N, 11.86. Found: C, 61.05; H, 2.97; N, 11.96.

7-Trifluoromethyl-9*H*-β-carboline (9b). *N*-Arylation was carried out using 3-iodopyridine **16** (164 mg, 0.80 mmol) and **15** (126 μL, 0.88 mmol) by the identical procedure for compound **9a**. After *N*-arylation, crude material was used in the subsequent steps without further purification. DMA (20 mL) was added to a flask containing the crude material, $Pd(OAc)_2$ (4.25 mg, 0.02 mmol), PCy_3·HBF_4 (14.0 mg, 0.04 mmol), K_2CO_3 (73.3 mg, 0.53 mmol) and *t*-$BuCO_2H$ (11.6 mg, 0.11 mmol) under an argon atmosphere. The mixture was stirred at 130 °C for 4 h. After cooling, the

reaction mixture was concentrated *in vacuo*. Crude material was purified by flash chromatography with *n*-hexane/EtOAc (1:1 to 0:1) to afford the desired carboline **9b** (58.6 mg, 31% yield): pale yellow needle crystal; mp 238–239 °C; IR (neat) cm^{-1}: 3567 (NH); ^{1}H NMR (500 MHz, CD$_3$OD); δ 7.52 (d, J = 8.3 Hz, 1H; Ar), 7.88 (s, 1H; Ar), 8.17 (d, J = 5.4 Hz, 1H; Ar), 8.37 (m, 2H; Ar), 8.89 (s, 1H; Ar); ^{13}C NMR (125 MHz, CD$_3$OD): δ 110.3, 116.8, 117.1, 123.8, 124.9, 126.1 (q), 129.4, 131.3 (q), 135.0, 138.7, 139.2, 141.8; *Anal.* calcd for C$_{12}$H$_7$F$_3$N$_2$: C, 61.02; H, 2.99; N, 11.86. Found: C, 61.06; H, 3.29; N, 11.73.

7-Trifluoromethyl-9*H*-γ-carboline (9c). Following the procedure described for **9b**, the carboline **9c** was obtained (88.9 mg, 51% yield): pale yellow powder; mp 240–241 °C; IR (neat) cm^{-1}: 3680 (NH); ^{1}H NMR (500 MHz, CD$_3$OD); δ 7.51–7.55 (m, 2H; Ar), 7.82 (s, 1H; Ar), 8.33 (d, J = 8.3 Hz, 1H; Ar), 8.43 (d, J = 5.7 Hz, 1H; Ar), 9.29 (s, 1H; Ar); ^{13}C NMR (125 MHz, CD$_3$OD): δ 108.0, 109.7, 118.1, 120.7, 122.4, 125.3, 126.1 (q), 129.9 (q), 140.7, 143.9, 145.7, 146.8; *Anal.* calcd for C$_{12}$H$_7$F$_3$N$_2$: C, 61.02; H, 2.99; N, 11.86. Found: C, 60.81; H, 2.91; N, 11.86.

7-Trifluoromethyl-9*H*-δ-carboline (9d). DMF (6.0 mL) was added to a flask containing 1-iodo-3-(trifluoromethyl)benzene **19** (846 mg, 3.11 mmol), 3-amino-2-chloropyridine **18** (400 mg, 3.11 mmol), CuI (59.2 mg, 0.31 mmol), 1,10-phenanthroline (84.1 mg, 0.47 mmol) and K$_2$CO$_3$ (860 mg, 6.22 mmol) under an argon atmosphere. The mixture was stirred at 110 °C for 24 h. After cooling, the reaction mixture was filtered though a pad of Celite and concentrated *in vacuo*. Crude material was purified by short silicagel chromatography with *n*-hexane/EtOAc (6:1) to afford the diarylamine (22.4 mg, <26% yield). DMA (8.2 mL) was added to a flask containing the crude amine, Pd(OAc)$_2$ (9.20 mg, 0.04 mmol), PCy$_3$·HBF$_4$ (30.2 mg, 0.08 mmol), K$_2$CO$_3$ (159 mg, 1.15 mmol) and *t*-BuCO$_2$H (25.1 mg, 0.25 mmol) under an argon atmosphere. The mixture was stirred at 130 °C for 10 h. After cooling, the reaction mixture was concentrated *in vacuo*. Crude material was purified by preparative TLC plate with *n*-hexane/EtOAc (1:2) to afford the desired carboline **9d** (76.1 mg, 10% yield): pale yellow powder; mp 228–229 °C; IR (neat) cm^{-1}: 3685 (NH); ^{1}H NMR (500 MHz, THF-d_8); δ 7.36 (dd, J = 8.3, 4.6 Hz, 1H; Ar), 7.51 (d, J = 8.0 Hz, 1H; Ar), 7.78 (s, 1H; Ar), 7.82 (dd, J = 8.3, 1.4 Hz, 1H; Ar), 8.41 (d, J = 8.0 Hz, 1H; Ar), 8.52 (dd, J = 4.6, 1.4 Hz, 1H; Ar), 10.79 (br, 1H; NH); ^{13}C NMR (125 MHz, THF-d_8): δ 109.3, 116.6, 118.7, 121.9 (2C), 126.0 (q), 126.3, 129.4 (q), 135.4, 140.8, 142.1, 143.4; *Anal.* calcd for C$_{12}$H$_7$F$_3$N$_2$: C, 61.02; H, 2.99; N, 11.86. Found: C, 60.74; H, 3.16; N, 11.63.

6-[2-Nitro-4-(trifluoromethyl)phenyl]-3,4-dihydroquinolin-2(1*H*)-one **(22a).**
1,4-Dioxane (1.5 mL) was added to a flask containing 4-bromo-3-nitrobenzotrifluoride
(51.0 µL, 0.33 mmol), 6-(4,4,5,5-tetramethyl-1,3,2-dioxaborolan-2-yl)-
3,4-dihydroquinolin-2(1*H*)-one **21a** (99.1 mg, 0.36 mmol), PdCl$_2$(dppf) (10.8 mg, 0.01
mmol), and K$_2$CO$_3$ (100 mg, 0.73 mmol) under an argon atmosphere. The mixture was
stirred at 90 °C for 24 h. After cooling, the reaction mixture was diluted with EtOAc,
and filtered. The filtrate was concentrated *in vacuo*. Crude material was purified by
flash chromatography with *n*-hexane/EtOAc (3:2) to afford **22a** (96.4 mg, 80% yield):
yellow solid; mp 230–231 °C; IR (neat) cm^{-1}: 1707 (C=O), 3055 (NH); ^{1}H NMR (500
MHz, DMSO-*d$_6$*) δ 2.50 (t, *J* = 7.7 Hz, 2H; CH$_2$), 2.93 (t, *J* = 7.7 Hz, 2H; CH$_2$), 6.95 (d,
J = 8.3 Hz, 1H; Ar), 7.17 (dd, *J* = 8.3, 1.7 Hz, 1H; Ar), 7.25 (d, *J* = 1.7 Hz, 1H; Ar),
7.79 (d, *J* =8.3 Hz, 1H; Ar), 8.11 (d, *J* = 8.3 Hz, 1H; Ar), 8.39 (s, 1H; Ar), 10.27 (s, 1H;
NH). ^{13}C NMR (125 MHz, DMSO-*d$_6$*) δ 24.6, 30.1, 115.4, 121.3, 123.0 (q), 124.2,
126.7, 127.2, 128.6 (q), 128.7, 129.0, 133.0, 138.4, 139.2, 148.9, 170.2; *Anal.* calcd for
C$_{16}$H$_{11}$F$_3$N$_2$O$_3$: C, 57.15; H, 3.30; N, 8.33. Found: C, 56.88; H, 3.26; N, 8.12.

**9-(Trifluoromethyl)-4,11-dihydro-1*H*-pyrido[3,2-*a*]carbazol-3(2*H*)-one (10a) and
8-(trifluoromethyl)-3,4-dihydro-1*H*-pyrido[2,3-*b*]carbazol-2(10*H*)-one (10b).** A
solution of 6-[2-nitro-4-(trifluoromethyl)phenyl]-3,4-dihydroquinolin-2(1*H*)-one **22a**
(600 mg, 1.78 mmol) and PPh$_3$ (1.17 g, 4.46 mmol) in *o*-DCB (3.6 mL) was heated at
165 °C with vigorous stirring for 13 h. After cooling, the solution was purified by
column chromatography on amino silica gel with *n*-hexane/EtOAc (1:2) to afford the
desired carbazoles **10a** (83.6 mg, 15% yield) and **10b** (109 mg, 20% yield) as white
solids; compound **10a**: mp 275–276 °C; IR (neat) cm^{-1}: 1702 (C=O), 3190 (NH), 3425
(NH); ^{1}H NMR (500 MHz, DMSO-*d$_6$*) δ 2.62 (t, *J* = 8.0 Hz, 2H; CH$_2$), 3.15 (t, *J* = 8.0
Hz, 2H; CH$_2$), 6.82 (d, *J* = 8.3 Hz, 1H; Ar), 7.43 (dd, *J* = 8.3, 0.9 Hz, 1H; Ar), 7.70 (d, *J*
= 0.9 Hz, 1H; Ar), 7.98 (d, *J* = 8.3 Hz, 1H; Ar), 8.20 (d, *J* = 8.3 Hz, 1H; Ar), 10.25 (s,
1H; NH), 11.54 (s, 1H; NH); ^{13}C NMR (125 MHz, DMSO-*d$_6$*) δ 20.0, 29.8, 105.1, 107.4,
108.8, 115.1, 116.7, 119.7, 120.2, 124.5 (q), 125.1 (q), 126.0, 137.5, 139.1, 139.4,
169.9; *Anal.* calcd for C$_{16}$H$_{11}$F$_3$N$_2$O: C, 63.16; H, 3.64; N, 9.21. Found: C, 62.87; H,
3.82; N, 9.03; compound **10b**: mp > 300 °C; IR (neat) cm^{-1}: 1658 (C=O), 2966 (NH),
3680 (NH); ^{1}H NMR (500 MHz, DMSO-*d$_6$*) δ 2.52 (t, *J* = 7.7 Hz, 2H; CH$_2$), 3.03 (t, *J* =
7.7 Hz, 2H; CH$_2$), 7.07 (s, 1H; Ar), 7.41 (d, *J* = 8.0 Hz, 1H; Ar), 7.70 (s, 1H; Ar), 7.99
(s, 1H; Ar), 8.18 (d, *J* = 8.0 Hz, 1H; Ar), 10.27 (s, 1H; NH), 11.45 (s,1H; NH); ^{13}C
NMR (125 MHz, DMSO-*d$_6$*) δ 25.2, 30.9, 97.0, 107.5, 114.8, 116.3, 116.6, 119.8, 120.0,
124.4 (q), 125.2 (q), 125.5, 138.2, 138.7, 140.5, 170.6; HRMS (FAB): calcd for

$C_{16}H_{11}F_3N_2O$ (M^+) 304.0823; found: 304.0822.

7-(4,4,5,5-Tetramethyl-1,3,2-dioxaborolan-2-yl)-4,5-dihydro-1*H*-benzo[*b*]azepin-2(3*H*)-one (21b). DMSO (14.2 mL) was added to a flask containing 7-bromo-4,5-dihydro-1*H*-benzo[*b*]azepin-2(3*H*)-one **20b**[24] (1.70 g, 7.08 mmol), bis(pinacolato)diboron (1.98 g, 7.80 mmol), PdCl$_2$(dppf) (289 mg, 0.35 mmol) and KOAc (2.08 g, 21.2 mmol) under an argon atmosphere. The mixture was stirred at 85 °C for 21 h. After cooling, the reaction mixture was concentrated *in vacuo* and filtered through silica gel. Crude material was purified by flash chromatography with *n*-hexane/EtOAc (1:1) to afford **21b** (1.97 g, 97% yield): white solid; mp 177–178 °C; IR (neat) cm^{-1}: 1656 (C=O), 3161 (NH); ^{1}H NMR (500 MHz, CDCl$_3$); δ 2.20–2.25 (m, 2H; CH$_2$), 2.36 (t, J = 7.4 Hz, 2H; CH$_2$), 2.82 (t, J = 7.4 Hz, 2H; CH$_2$), 6.95 (d, J = 8.3 Hz, 1H; Ar), 7.52 (br, 1H; NH), 7.67 (s, 1H; Ar), 7.68 (d, J = 8.3 Hz, 1H; Ar); ^{13}C NMR (125 MHz, CDCl$_3$): δ 24.9, 28.4, 30.3, 33.0, 83.9, 120.9, 133.4, 134.2, 136.5, 140.5, 174.9; *Anal.* calcd for $C_{16}H_{22}BNO_3$: C, 66.92; H, 7.72; N, 4.88. Found: C, 66.81; H, 7.70; N, 4.91.

7-[2-Nitro-4-(trifluoromethyl)phenyl]-4,5-dihydro-1*H*-benzo[*b*]azepin-2(3*H*)-one (22b). Following the procedure described for **22a**, **22b** was obtained (153 mg, 34% yield): yellow solid; mp 228–229 °C; IR (neat) cm^{-1}: 1686 (C=O), 3173 (NH); ^{1}H NMR (500 MHz, CDCl$_3$) δ 2.24–2.30 (m, 2H; CH$_2$), 2.43 (t, J = 7.4 Hz, 2H; CH$_2$), 2.85 (t, J = 7.4 Hz, 2H; CH$_2$), 7.05 (d, J = 8.0 Hz, 1H; Ar), 7.19 (s, 1H; Ar), 7.20 (d, J = 8.0 Hz, 1H; Ar), 7.54 (br, 1H; NH), 7.61 (d, J = 8.0 Hz, 1H; Ar), 7.88 (d, J = 8.0 Hz, 1H; Ar), 8.13 (s, 1H; Ar); ^{13}C NMR (125 MHz, CDCl$_3$) δ 28.2, 30.6, 32.8, 121.6, 122.2, 122.8 (q), 127.1, 128.9, 129.4, 131.0 (q), 132.8, 133.3, 135.0, 138.7, 139.0, 149.1, 174.6; HRMS (FAB): *m/z* calcd for $C_{17}H_{14}F_3N_2O_3$ [M + H]$^+$ 351.0957; found: 351.0961.

10-(Trifluoromethyl)-2,3,5,12-tetrahydroazepino[3,2-*a*]carbazol-4(1*H*)-one (11a) and 9-(trifluoromethyl)-3,4,5,11-tetrahydroazepino[2,3-*b*]carbazol-2(1*H*)-one (11b). Following the procedure described for **10a,b**, desired carbazoles **11a** (21.1 mg, 19% yield) and **11b** (35.8 mg, 33% yield) were obtained as white solids; compound **11a**: mp 294–295 °C; IR (neat) cm^{-1}: 1666 (C=O), 2927 (NH), 3189 (NH); ^{1}H NMR (500 MHz, DMSO-d_6) δ 2.24–2.27 (m, 4H; CH$_2$ × 2), 3.06 (t, J = 6.6 Hz, 2H; CH$_2$), 6.92 (d, J = 8.0 Hz, 1H; Ar), 7.45 (d, J = 8.0 Hz, 1H; Ar), 7.74 (s, 1H; Ar), 8.05 (d, J = 8.0 Hz, 1H; Ar), 8.27 (d, J = 8.0 Hz, 1H; Ar), 9.70 (s, 1H; NH), 11.68 (s, 1H; NH); ^{13}C NMR (125 MHz, DMSO-d_6) δ 24.2, 27.6, 33.4, 107.6, 114.5, 115.0, 115.9, 118.3, 119.2, 120.6, 125.0 (q),

125.1 (q), 125.8, 137.9, 139.1, 140.3, 173.5; HRMS (FAB): calcd for $C_{17}H_{13}F_3N_2O$ (M^+) 318.0980; found: 318.0985; compound **11b**: mp 290–291 °C; IR (neat) cm^{-1}: 1651 (C=O), 3283 (NH); ^{1}H NMR (400 MHz, DMSO-d_6) δ 2.14–2.19 (m, 4H; CH$_2$ × 2), 2.84 (t, J = 6.8 Hz, 2H; CH$_2$), 7.17 (s, 1H; Ar), 7.44 (d, J = 8.0 Hz, 1H; Ar), 7.76 (s, 1H; Ar), 8.08 (s, 1H; Ar), 8.25 (d, J = 8.0 Hz, 1H; Ar), 9.71 (br, 1H; NH), 11.53 (br, 1H; NH); ^{13}C NMR (125 MHz, DMSO-d_6) δ 28.1, 30.1, 32.8, 104.0, 107.8, 114.9, 118.4, 120.5, 121.4, 125.0 (q), 125.1 (q), 125.2, 125.8, 138.4, 139.0, 140.2, 173.3; HRMS (FAB): calcd for $C_{17}H_{13}F_3N_2O$ (M^+) 318.0980; found: 318.0977.

6-[3-(Trifluoromethyl)phenylamino]-3,4-dihydroquinolin-2(1H)-one (24). Toluene (7.0 mL) was added to a flask containing 6-bromo-3,4-dihydroquinolin-2(1H)-one **20a** (800 mg, 3.54 mmol), 3-(trifluoromethyl)aniline **23** (482 μL, 3.89 mmol), Pd$_2$(dba)$_3$·CHCl$_3$ (183 mg, 0.18 mmol), 2-dicyclohexylphosphino-2'-(N,N-dimethyl-amino)biphenyl (104 mg, 0.27 mmol) and NaOt-Bu (477 mg, 4.96 mmol) under an argon atmosphere. The mixture was stirred at 100 ºC for 6 h. After cooling, the reaction mixture was diluted with EtOAc, and filtered though a pad of Celite. The filtrate was concentrated *in vacuo*. Crude material was purified by flash chromatography with n-hexane/EtOAc (1:1) to afford **24** (668 mg, 62% yield): pale yellow solid; mp 190–191 °C; IR (neat) cm^{-1}: 1652 (C=O), 3045 (NH), 3317 (NH); ^{1}H NMR (500 MHz, DMSO-d_6) δ 2.45 (t, J = 7.4 Hz, 2H; CH$_2$), 2.86 (t, J = 7.4 Hz, 2H; CH$_2$), 6.85 (d, J = 8.0 Hz, 1H; Ar), 6.96 (d, J = 8.0 Hz, 1H; Ar), 6.97 (s, 1H; Ar), 7.00 (d, J = 8.0 Hz, 1H; Ar), 7.16 (s, 1H; Ar), 7.20 (d, J = 8.0 Hz, 1H; Ar), 7.37 (t, J = 8.0 Hz, 1H; Ar), 8.30 (s, 1H; NH), 10.02 (s, 1H; NH); ^{13}C NMR (125 MHz, DMSO-d_6) δ 25.0, 30.4, 110.5, 114.0, 115.8, 117.6, 118.8, 119.7, 124.3 (q), 124.7, 130.0 (q), 130.2, 133.2, 136.1, 145.9, 169.8; *Anal.* calcd for $C_{16}H_{13}F_3N_2O$: C, 62.74; H, 4.28; N, 9.15. Found: C, 62.94; H, 4.36; N, 8.91.

8-(Trifluoromethyl)-3,4-dihydro-1H-pyrido[3,2-b]carbazol-2(6H)-one (10c). AcOH (3.3 mL) was added to a flask containing 6-[3-(trifluoromethyl)phenylamino]-3,4-dihydroquinolin-2(1H)-one **24** (100 mg, 0.33 mmol) and Pd(OAc)$_2$ (73.3 mg, 0.33 mmol) and an oxygen balloon was connected to the reaction vessel. The mixture was stirred at 120 °C for 8 h. After cooling, the reaction mixture was diluted with EtOAc, washed with saturated NaHCO$_3$, dried over Na$_2$SO$_4$, and concentrated *in vacuo*. Crude material was purified by flash chromatography with n-hexane/EtOAc (1:2) to afford the desired carbazole **10c** (52.7 mg, 52% yield): white solid; mp > 300 °C; IR (neat) cm^{-1}: 1666 (C=O), 3439 (NH); ^{1}H NMR (500 MHz,

DMSO-d_6) δ 2.50 (t, J = 7.7 Hz, 2H; CH$_2$), 3.06 (t, J = 7.7 Hz, 2H; CH$_2$), 7.41 (d, J = 8.3 Hz, 1H; Ar), 7.42 (s, 1H; Ar), 7.59 (s, 1H; Ar), 7.77 (s, 1H; Ar), 8.17 (d, J = 8.3 Hz, 1H; Ar), 10.18 (s, 1H; NH), 11.46 (s, 1H; NH); ^{13}C NMR (125 MHz, DMSO-d_6) δ 25.9, 30.6, 105.9, 107.9, 110.5, 114.4, 120.0, 120.6, 125.0, 125.1 (q), 125.2 (q), 125.3, 131.7, 136.9, 139.0, 170.1; HRMS (FAB): calcd for C$_{16}$H$_{11}$F$_3$N$_2$O (M$^+$) 304.0823; found: 304.0826.

2-Oxo-1,2,3,4-tetrahydroquinolin-5-yl trifluoromethanesulfonate (26). To 5-hydroxy-3,4-dihydroquinolin-2(1H)-one **25** (800 mg, 4.90 mmol) in anhydrous CH$_2$Cl$_2$ (10 mL) was added pyridine (793 μL, 9.80 mmol) and the solution was cooled to 0 °C. Tf$_2$O (989 μL, 5.88 mmol) was added dropwise and the mixture was warmed to room temperature. After stirring for 2 h, the mixture was neutralized with sat. NaHCO$_3$, extracted into CHCl$_3$, washed with saturated brine, and dried over Na$_2$SO$_4$. The organic solvent was removed under reduced pressure and the crude residue was purified by flash chromatography with n-hexane/EtOAc (3:2) to afford **26** (1.20 g, 83% yield): white solid; mp 149–150 °C; IR (neat) cm^{-1}: 1686 (C=O), 3077 (NH); ^{1}H NMR (500 MHz, DMSO-d_6) δ 2.51 (t, J = 7.7 Hz, 2H; CH$_2$), 2.92 (t, J = 7.7 Hz, 2H; CH$_2$), 6.98 (d, J = 8.3 Hz, 1H; Ar), 7.01 (d, J = 8.3 Hz, 1H; Ar), 7.34 (t, J = 8.3 Hz, 1H; Ar), 10.45 (s, 1H; NH); ^{13}C NMR (125 MHz, DMSO-d_6) δ 19.5, 29.0, 114.4, 115.3, 116.5, 118.1 (q), 128.9, 140.9, 146.7, 169.6; HRMS (FAB): calcd for C$_{10}$H$_9$F$_3$NO$_4$S [M + H]$^+$ 296.0204; Found: 296.0207.

5-(Tributylstannyl)-3,4-dihydroquinolin-2(1H)-one (27). To 2-oxo-1,2,3,4-tetra-hydroquinolin-5-yl trifluoromethanesulfonate **26** (70.0 mg, 0.24 mmol) in 1,4-dioxane (2.4 mL) at room temperature was added LiCl (50.4 mg, 1.19 mmol), Pd(PPh$_3$)$_4$ (13.9 mg, 0.01 mmol) and (n-Bu$_3$Sn)$_2$ (243 μL, 0.48 mmol). After stirring for 11 h at 100 °C, the reaction mixture was cooled to room temperature and concentrated in $vacuo$. The residue was purified by flash chromatography with n-hexane/EtOAc (3:1) to afford **27** (68.2 mg, 65% yield): off-white solid; mp 83–84 °C; IR (neat) cm^{-1}: 1671(C=O), 2921 (NH); ^{1}H NMR (500 MHz, CDCl$_3$) δ 0.89 (t, J = 7.3 Hz, 9H; CH$_3$ × 3), 1.07–1.10 (m, 6H), 1.29–1.37 (m, 6H), 1.49–1.55 (m, 6H), 2.64 (t, J = 7.7 Hz, 2H; CH$_2$), 2.93 (t, J = 7.7 Hz, 2H; CH$_2$), 6.79 (d, J = 7.4 Hz, 1H; Ar), 7.09 (d, J = 7.4 Hz, 1H; Ar), 7.14 (t, J = 7.4 Hz, 1H; Ar), 8.94 (s, 1H; NH); ^{13}C NMR (125 MHz, CDCl$_3$) δ 10.2, 13.6, 27.3, 28.6, 29.1, 31.0, 116.0, 126.9, 129.9, 131.2, 136.8, 142.0, 171.9; HRMS (FAB): calcd for C$_{21}$H$_{36}$NOSn [M + H]$^+$ 438.1819; found: 438.1820.

5-[2-Nitro-4-(trifluoromethyl)phenyl]-3,4-dihydroquinolin-2(1*H*)-one (28). Toluene (5 mL) was added to a flask containing 4-bromo-3-nitrobenzotrifluoride (63.3 μL, 0.41 mmol), 5-(tributylstannyl)-3,4-dihydroquinolin-2(1*H*)-one **27** (180 mg, 0.41 mmol), Pd$_2$(dba)$_3$·CHCl$_3$ (128 mg, 0.12 mmol), P(*t*-Bu)$_3$·HBF$_4$ (72 mg, 0.25 mmol) and CsF (439 mg, 2.89 mmol) under an argon atmosphere. The mixture was stirred at 110 °C for 21 h. After cooling, the reaction mixture was diluted with EtOAc, and filtered. The filtrate was concentrated *in vacuo*. Crude material was purified by flash chromatography with *n*-hexane/EtOAc (1:2) to afford **28** (77.3 mg, 56% yield): yellow solid; mp 240–241 °C; IR (neat) cm^{-1}: 1676 (C=O), 3066 (NH); ^{1}H NMR (400 MHz, CDCl$_3$) δ 2.55–2.60 (m, 2H; CH$_2$), 2.64–2.68 (m, 2H; CH$_2$), 6.82 (d, *J* = 7.8 Hz, 1H; Ar), 6.87 (d, *J* = 8.0 Hz, 1H; Ar), 7.25 (t, *J* = 7.8 Hz, 1H; Ar), 7.53 (d, *J* = 7.8 Hz, 1H; Ar), 7.92 (d, *J* = 8.0 Hz, 1H; Ar), 8.28 (s, 1H; Ar), 8.33 (br, 1H; NH); ^{13}C NMR (125 MHz, CDCl$_3$) δ 23.2, 30.3, 116.1, 121.6, 121.9, 122.7 (q), 123.0, 127.7, 129.2, 131.6 (q), 133.1, 135.6, 137.8, 138.6, 149.0, 171.2; HRMS (FAB): *m/z* calcd for C$_{16}$H$_{12}$F$_3$N$_2$O$_3$ [M + H]$^+$ 337.0800; found: 337.0806.

9-(Trifluoromethyl)-4,7-dihydro-1*H*-pyrido[2,3-*c*]carbazol-3(2*H*)-one (10d). A solution of 5-[2-nitro-4-(trifluoromethyl)phenyl]-3,4-dihydroquinolin-2(1*H*)-one **28** (54.8 mg, 0.16 mmol) and PPh$_3$ (107 mg, 0.41 mmol) in *o*-DCB (1 mL) was heated at 165 °C with vigorous stirring. After 14 h, the solution was purified by flash chromatography with *n*-hexane/EtOAc (1:3) to afford the desired carbazole **10d** (19.6 mg, 40% yield): white solid; mp > 300 °C; IR (neat) cm^{-1}: 1662 (C=O), 3195 (NH), 3483 (NH); ^{1}H NMR (500 MHz, DMSO-d_6) δ 2.62 (t, *J* = 7.7 Hz, 2H; CH$_2$), 3.51 (t, *J* = 7.7 Hz, 2H; CH$_2$), 7.09 (d, *J* = 8.3 Hz, 1H; Ar), 7.40 (d, *J* = 8.3 Hz, 1H; Ar), 7.42 (d, *J* = 8.3 Hz, 1H; Ar), 7.79 (s, 1H; Ar), 8.33 (d, *J* = 8.3 Hz, 1H; Ar), 10.05 (s, 1H; NH), 11.56 (s, 1H; NH); ^{13}C NMR (125 MHz, DMSO-d_6) δ 22.3, 29.9, 107.8, 109.8, 114.3, 116.0, 117.3, 118.9, 122.9, 124.9, 125.0 (q), 125.2 (q), 131.2, 137.0, 139.4, 169.2; HRMS (FAB): *m/z* calcd for C$_{16}$H$_{11}$F$_3$N$_2$O (M$^+$) 304.0823; found: 304.0822.

5-[2-Nitro-4-(trifluoromethyl)phenyl]-1*H*-indole (30). 1,4-Dioxane (1 mL) was added to a flask containing 4-bromo-3-nitrobenzotrifluoride (28.4 μL, 0.19 mmol), (1*H*-indol-5-yl)boronic acid **29** (35.8 mg, 0.22 mmol), Pd(OAc)$_2$ (2.1 mg, 0.01 mmol), XPhos (8.8 mg, 0.02 mmol) and K$_2$CO$_3$ (56.3 mg, 0.41 mmol) under an argon atmosphere. The mixture was stirred at 60 °C for 4 h. After cooling, the reaction mixture was diluted with EtOAc, and filtered. The filtrate was concentrated *in vacuo*. Crude material was purified by flash chromatography with *n*-hexane/EtOAc (5:1) to

afford **30** (31.2 mg, 55% yield): yellow solid; 155–156 °C; IR (neat) cm^{-1}: 1532 (NO$_2$), 3437 (NH); ^{1}H NMR (500 MHz, CDCl$_3$) δ 6.59–6.60 (m, 1H; Ar), 7.11 (dd, J = 8.0, 1.7 Hz, 1H; Ar), 7.26 (dd, J = 3.2, 2.6 Hz, 1H; Ar), 7.41 (d, J = 8.0 Hz, 1H; Ar), 7.62 (d, J = 1.7 Hz, 1H; Ar), 7.67 (d, J = 8.0 Hz, 1H; Ar), 7.84 (dd, J = 8.0, 1.7 Hz, 1H; Ar), 8.07 (d, J = 1.7 Hz, 1H; Ar), 8.27 (br, 1H; NH); ^{13}C NMR (125 MHz, CDCl$_3$) δ 103.2, 111.6, 120.4, 121.2, 121.7, 123.0 (q), 125.5, 127.4, 128.2, 128.4, 129.9 (q), 133.3, 135.9, 140.9, 149.6; *Anal.* calcd for C$_{15}$H$_9$F$_3$N$_2$O$_2$: C, 58.83; H, 2.96; N, 9.15. Found: C, 59.03; H, 2.83; N, 9.17.

7-(Trifluoromethyl)-1,9-dihydropyrrolo[2,3-*b*]carbazole (31). A solution of 5-[2-nitro-4-(trifluoromethyl)phenyl]-1*H*-indole **30** (405 mg, 1.32 mmol) and 4-(dimethylamino)triphenylphosphine (1.01 g, 3.30 mmol) in *o*-DCB (2.6 mL) was heated at 160 °C with vigorous stirring. After 10 h, the solution was purified by flash chromatography with amino silica gel with *n*-hexane/EtOAc (3:2) to afford the desired carbazole **31** (269 mg, 74% yield): white solid; mp 274–275 °C; IR (neat) cm^{-1}: 3412 (NH), 3486 (NH); ^{1}H NMR (500 MHz, DMSO-d_6) δ 6.82 (s, 1H; Ar), 7.32 (d, J = 8.3 Hz, 1H; Ar), 7.39 (t, J = 2.6 Hz, 1H; Ar), 7.43 (d, J = 8.3 Hz, 1H; Ar), 7.78 (s, 1H; Ar), 7.87 (d, J = 8.3 Hz, 1H; Ar), 8.21 (d, J = 8.3 Hz, 1H; Ar), 11.43 (s, 1H; NH), 11.91 (s, 1H; NH); ^{13}C NMR (125 MHz, DMSO-d_6) δ 99.0, 105.5, 107.4, 112.6, 112.8, 114.2, 114.7, 119.2, 122.8 (q), 123.5, 125.4 (q), 127.0, 134.8, 135.6, 137.3; *Anal.* calcd for C$_{15}$H$_9$F$_3$N$_2$: C, 65.69; H, 3.31; N, 10.21. Found: C, 65.83; H, 3.29; N, 10.30.

5-[2-Nitro-4-(trifluoromethyl)phenyl]indoline-2,3-dione (32). PCC (2.64 g, 12.2 mmol) was added to a solution of 5-[2-nitro-4-(trifluoromethyl)phenyl]-1*H*-indole **30** (1.50 g, 4.90 mmol) in 1,2-DCE (12 mL). The reaction mixture was stirred at 80 °C for 1 h, then filtered. The filtrate was concentrated *in vacuo*. Crude material was purified by flash chromatography with *n*-hexane/EtOAc (3:2) to afford **32** (465 mg, 28% yield): orange solid; mp 248–249 °C; IR (neat) cm^{-1}: 1624 (C=O), 3154 (NH); ^{1}H NMR (400 MHz, CDCl$_3$) δ 7.02 (d, J = 8.0 Hz, 1H; Ar), 7.50 (dd, J = 8.0, 1.7 Hz, 1H; Ar), 7.58 (d, J = 8.0 Hz, 1H; Ar), 7.61 (d, J = 1.7 Hz, 1H; Ar), 7.93 (d, J = 8.0 Hz, 1H; Ar), 8.23 (s, 1H; Ar); ^{13}C NMR (125 MHz, CDCl$_3$) δ 112.7, 118.5, 122.1, 122.7 (q), 125.1, 129.4, 131.8 (q), 132.2, 132.7, 137.8, 137.9, 148.8, 149.3, 158.6, 182.1; HRMS (FAB): *m/z* calcd for C$_{15}$H$_8$F$_3$N$_2$O$_4$ [M + H]$^+$ 337.0436; found: 337.0438.

7-(Trifluoromethyl)-3,9-dihydropyrrolo[2,3-*b*]carbazol-2(1*H*)-one (12). A solution of 5-[2-nitro-4-(trifluoromethyl)phenyl]indoline-2,3-dione **32** (354 mg, 1.05 mmol) and

4-(dimethylamino)triphenylphosphine (1.28 g, 4.20 mmol) in *o*-DCB (2 mL) was heated at 140 °C with vigorous stirring. After 8 h, the solution was purified by flash chromatography with amino silica gel with EtOAc to afford the desired carbazole **12** (46.4 mg, 15% yield): white solid; mp > 300 °C; IR (neat) cm^{-1}: 1685 (C=O), 3177 (NH); ^{1}H NMR (400 MHz, DMSO-d_6) δ 3.58 (s, 2H; CH$_2$), 6.96 (s, 1H; Ar), 7.40 (d, *J* = 8.0 Hz, 1H; Ar), 7.73 (s, 1H; Ar), 8.02 (s, 1H; Ar), 8.19 (d, *J* = 8.0 Hz, 1H; Ar), 10.54 (s, 1H; NH), 11.44 (s, 1H; NH); ^{13}C NMR (125 MHz, DMSO-d_6) δ 35.3, 92.0, 107.5, 114.8, 115.7, 117.0, 118.4, 119.6, 124.0 (q), 125.2 (q), 125.8, 138.0, 140.9, 143.6, 176.7; *Anal.* calcd for C$_{15}$H$_9$F$_3$N$_2$O: C, 62.07; H, 3.13; N, 9.65. Found: C, 61.91; H, 3.29; N, 9.48.

***tert*-Butyl [2'-nitro-4'-(trifluoromethyl)-(1,1'-biphenyl)-4-yl]carbamate (34).** 1,4-Dioxane (8 mL) was added to a flask containing 4-bromo-3-nitrobenzotrifluoride (358 μL, 2.34 mmol), *tert*-butyl *N*-[4-(4,4,5,5-tetramethyl-1,3,2-dioxaborolane-2-yl)phenyl]carbamate **33** (798 mg, 2.50 mmol), PdCl$_2$(dppf) (76.4 mg, 0.09 mmol) and K$_2$CO$_3$ (710 mg, 5.14 mmol) under an argon atmosphere. The mixture was stirred at 80 °C for 23 h. After cooling, the reaction mixture was diluted with EtOAc, and filtered. The filtrate was concentrated *in vacuo*. Crude material was purified by flash chromatography with *n*-hexane/EtOAc (10:1) to afford **34** (708 mg, 79% yield): yellow solid; mp 147–148 °C; IR (neat) cm^{-1}: 1698 (C=O), 3369 (NH); ^{1}H NMR (500 MHz, CDCl$_3$) δ 1.53 (s, 9H; *t*-Bu), 6.63 (br, 1H; NH), 7.25 (d, *J* = 8.6 Hz, 2H; Ar), 7.47 (d, *J* = 8.6 Hz, 2H; Ar), 7.58 (d, *J* = 8.0 Hz, 1H; Ar), 7.84 (d, *J* = 8.0 Hz, 1H; Ar), 8.08 (s, 1H; Ar); ^{13}C NMR (125 MHz, CDCl$_3$) δ 28.3 (3C), 81.0, 118.6, 121.4, 122.9(q), 128.6, 128.7, 130.1, 130.4 (q), 132.8, 139.2, 139.4, 149.1, 152.5; *Anal.* calcd for C$_{18}$H$_{17}$F$_3$N$_2$O$_4$: C, 56.55; H, 4.48; N, 7.33. Found: C, 56.65; H, 4.31; N, 7.36.

***tert*-Butyl [7-(trifluoromethyl)-9*H*-carbazol-2-yl]carbamate (35).** A solution of *tert*-butyl [2'-nitro-4'-(trifluoromethyl)-(1,1'-biphenyl)-4-yl]carbamate **34** (40.0 mg, 0.10 mmol) and PPh$_3$ (68.6 mg, 0.26 mmol) in *o*-DCB (1 mL) was heated at 165 °C with vigorous stirring. After 12 h, the solution was purified by flash chromatography with *n*-hexane/EtOAc (8:1) to afford **35** (21.7 mg, 62% yield): white solid; mp 249–250 °C; IR (neat) cm^{-1}: 1702 (C=O), 3359 (NH), 3406 (NH); ^{1}H NMR (500 MHz, DMSO-d_6) δ 1.52 (s, 9H; *t*-Bu), 7.25 (d, *J* = 8.0 Hz, 1H; Ar), 7.42 (d, *J* = 8.0 Hz, 1H; Ar), 7.72 (s, 1H; Ar), 7.88 (s, 1H; Ar), 8.05 (d, *J* = 8.0 Hz, 1H; Ar), 8.19 (d, *J* = 8.0 Hz, 1H; Ar), 9.55 (s, 1H; NH), 11.47 (s, 1H; NH); ^{13}C NMR (125 MHz, DMSO-d_6) δ 28.1

(9C), 79.1, 99.9, 107.4, 111.3, 114.7, 116.2, 120.0, 121.1, 124.4 (q), 125.1 (q), 125.5, 138.8, 139.0, 141.6, 152.8; *Anal.* calcd for $C_{18}H_{17}F_3N_2O_2$: C, 61.71; H, 4.89; N, 8.00. Found: C, 61.85; H, 4.90; N, 7.99.

7-(Trifluoromethyl)-9*H*-carbazol-2-amine (36). 4 N HCl/1,4-dioxane (4 mL) was added to a flask containing *tert*-butyl [7-(trifluoromethyl)-9*H*-carbazol-2-yl]carbamate **35** (92.0 mg, 0.26 mmol). The mixture was stirred at room temperature for 1 h. The reaction mixture was neutralized with 2N NaOH aqueous solution, then evaporated *in vacuo*. The mixture was extracted into EtOAc, washed with water, and dried over Na_2SO_4. The organic solvent was removed under reduced pressure to give **36** (65.3 mg, 100% yield): white solid; mp 274–275 °C; IR (neat) cm^{-1}: 3414 (NH); ^{1}H NMR (500 MHz, DMSO-d_6) δ 5.39 (br, 2H; NH$_2$), 6.56 (dd, J = 1.7, 8.0 Hz, 1H; Ar), 6.66 (d, J = 1.7 Hz, 1H; Ar), 7.32 (d, J = 8.0 Hz, 1H; Ar), 7.59 (s, 1H; Ar), 7.81 (d, J = 8.0 Hz, 1H; Ar), 7.99 (d, J = 8.0 Hz, 1H; Ar), 11.08 (br, 1H; NH); ^{13}C NMR (125 MHz, DMSO-d_6) δ 93.9, 106.6, 109.1, 111.9, 114.5, 118.4, 121.4, 122.7 (q), 125.4 (q), 126.6, 138.3, 143.3, 149.2; HRMS (FAB): *m/z* calcd for $C_{13}H_9F_3N_2$ (M$^+$) 250.0718; found: 250.0721.

***N*-[7-(Trifluoromethyl)-9*H*-carbazol-2-yl]urea (13a).** To a stirred solution of 7-(trifluoromethyl)-9*H*-carbazol-2-amine **36** (135 mg, 0.54 mmol) in AcOH (6.8 mL) was added KOCN (131 mg, 1.62 mmol) and water (540 μL). The reaction mixture was stirred at room temperature for 12 h, then evaporated to dryness under vacuum. Crude material was purified by flash chromatography with *n*-hexane/EtOAc (1:10) to afford the desired carbazole **13a** (43.0 mg, 27% yield): white solid; mp > 300 °C; IR (neat) cm^{-1}: 1664 (C=O), 3412 (NH); ^{1}H NMR (500 MHz, CD$_3$OD) δ 7.01 (dd, J = 8.3, 2.0 Hz, 1H; Ar), 7.35 (d, J = 8.3 Hz, 1H; Ar), 7.65 (s, 1H; Ar), 7.81 (d, J = 2.0 Hz, 1H; Ar), 7.95 (d, J = 8.3 Hz, 1H; Ar), 8.05 (d, J = 8.3 Hz, 1H; Ar); ^{13}C NMR (125 MHz, CD$_3$OD) δ 102.4, 108.5, 113.3, 116.2, 118.7, 120.7, 121.9, 126.6 (q), 127.2, 127.2 (q), 140.2, 140.7, 143.4, 159.6; HRMS (FAB): calcd for $C_{14}H_{10}F_3N_3O$ (M$^+$) 293.0776; found: 293.0781.

6-Nitro-2-(trifluoromethyl)-9*H*-carbazole (37). To a suspension of 2-(trifluoromethyl)-9*H*-carbazole **3a** (2.00 g, 8.50 mmol) in AcOH (53 mL) was added, dropwise with stirring at room temperature, 60% HNO$_3$ (677 μL, 9.35 mmol). The reaction was heated to 60 °C for 4.5 h. After cooling, the reaction mixture was concentrated *in vacuo*. Crude material was purified by flash chromatography with *n*-hexane/EtOAc (15:1 to 3:1) to afford the desired compound **37** (978 mg, 41% yield)

along with the regioisomeric 1-nitro-7-(trifluoromethyl)-9*H*-carbazole (667 mg, 28% yield): yellow solid **37**; mp = 294–295 °C; IR (neat) cm^{-1}: 1215 (NO$_2$), 3021 (NH); ^{1}H NMR (500 MHz, DMSO-d_6) δ 7.60 (d, J = 8.0 Hz, 1H; Ar), 7.75 (d, J = 8.0 Hz, 1H; Ar), 7.94 (s, 1H; Ar), 8.37 (dd, J = 8.0, 2.3 Hz, 1H; Ar), 8.61 (d, J = 8.0 Hz, 1H; Ar), 9.29 (d, J = 2.3 Hz, 1H; Ar), 12.34 (s, 1H; NH); ^{13}C NMR (125 MHz, DMSO-d_6) δ 109.0, 111.8, 116.4, 118.4, 121.2, 122.4 (2C), 124.7 (q), 125.4, 127.2 (q), 140.1, 140.4, 144.1; HRMS (FAB): calcd for C$_{13}$H$_7$F$_3$N$_2$O$_2$ (M$^+$) 280.0460; found: 280.0450.

7-(Trifluoromethyl)-9*H*-carbazol-3-amine   (38). To a stirred solution of 6-Nitro-2-(trifluoromethyl)-9*H*-carbazole **37** (600 mg, 2.14 mmol) and ammonium formate (1.62 g, 25.7 mmol) in EtOH (7.1 mL) at room temperature was added 10% Pd/C (114 mg, 0.11 mmol). The mixture was heated under reflux for 2 h. After cooling, the reaction mixture was diluted with EtOAc, and filtered through a pad of Celite. The filtrate was concentrated *in vacuo*. Crude material was purified by flash chromatography with *n*-hexane/EtOAc (1:1) to afford compound **38** (497 mg, 93% yield): pale yellow solid; mp = 282–283 °C; IR (neat) cm^{-1}: 3418 (NH); ^{1}H NMR (500 MHz, DMSO-d_6) δ 4.80 (s, 2H; NH$_2$), 6.89 (dd, J = 8.0, 2.3 Hz, 1H; Ar), 7.30 (d, J = 8.0 Hz, 1H; Ar), 7.31 (s, 1H; Ar), 7.33 (d, J = 8.0 Hz, 1H; Ar), 7.69 (s, 1H; Ar), 8.11 (d, J = 8.0 Hz, 1H; Ar), 11.12 (s, 1H; NH); ^{13}C NMR (125 MHz, DMSO-d_6) δ 103.8, 107.6, 111.7, 113.6, 116.9, 120.5, 122.1, 124.8 (q), 124.9, 125.2 (q), 133.8, 139.0, 142.0; *Anal*. calcd for C$_{13}$H$_9$F$_3$N$_2$: C, 62.40; H, 3.63; N, 11.20. Found: C, 62.21; H, 3.81; N, 11.24.

N-[7-(trifluoromethyl)-9*H*-carbazol-3-yl]urea   (13b). Following the procedure described for **13a**, compound **13b** (85.5 mg, 30% yield) was synthesized from 7-(trifluoromethyl)-9*H*-carbazol-3-amine **38**: white solid; mp > 300 °C; IR (neat) cm^{-1}: 1638 (C=O), 3282 (NH), 3519 (NH); ^{1}H NMR (500 MHz, CD$_3$OD) δ 7.37 (d, J = 8.6 Hz, 1H; Ar), 7.37 (d, J = 8.6 Hz, 1H; Ar), 7.43 (d, J = 8.6 Hz, 1H; Ar), 7.70 (s, 1H; Ar), 8.14 (d, J = 8.6 Hz, 1H; Ar), 8.15 (s, 1H; Ar); ^{13}C NMR (125 MHz, CD$_3$OD) δ 109.0, 112.3, 114.2, 115.9, 121.6, 122.9, 123.5, 126.5 (q), 126.9, 128.3 (q), 132.7, 139.3, 141.1, 160.4; HRMS (FAB): calcd for C$_{14}$H$_{10}$F$_3$N$_3$O (M$^+$) 293.0776; found: 293.0768.

Tubulin purification and the polymerization of mictrotubule

Tubulin was purified from pig brains as described.[25] The concentration of prepared tubulin was determined by the Bradford assay using BSA as the standard. Microtubules were polymerized *in vitro* using 30 μM of purified pig brain tubulin in the PM buffer [100 mM PIPES (pH6.8), 1 mM MgSO$_4$, 2 mM EGTA) containing 1 mM GTP (Sigma)

at 37 °C for 10 min. Polymerized microtubules were then stabilized by the addition of paclitaxel (Sigma) in DMSO at 70 μM final concentration and further incubated at 37 °C for at least 12 h. The resulting microtubule solution was used for the KSP ATPase assay.

KSP ATPase Assay

The microtubules-stimulated KSP ATPase reaction was performed in a reaction buffer [20 mM PIPES-KOH (pH 6.8), 25 mM KCl, 2 mM $MgCl_2$, 1 mM EGTA-KOH (pH 8.0)] containing 38 nM of bacteria-expressed KSP motor domain (1–369) fused to histidine-tag at carboxyl-terminus and 350 nM microtubules in 96-well half-area plates (Corning). Each chemical compound in DMSO at different concentrations was diluted 12.5-fold with the chemical dilution buffer [10 mM Tris-OAc (pH7.4), 0.04% (v/v) NP-40]. After pre-incubation of 9.7 μL of the enzyme solution with 3.8 μL of each chemical solution at 25 °C for 20 min, the ATPase reaction was initiated by the addition of 1.5 μL of 0.3 mM ATP solution, and followed by incubation at 25 °C for further 15 min. The reaction was terminated by the addition of 10 μL of the Kinase-Glo Plus reagent (Promega). The ATP consumption in each reaction was measured as the luciferase-derived luminescence by ARVO Light (PerkinElmer). At least three experiments were performed per condition and the averages and standard deviations of inhibition rates in each condition were evaluated to determine IC_{50} values using the GraphPad Prism software.

Growth Inhibition Assay

HeLa cells were cultured in DMEM medium supplemented with 10% (v/v) FCS and antibiotics at 37 °C in a 5% CO_2-incubator. Growth inhibition assays using HeLa cells were performed in 96-well plates (Greiner). HeLa cells were seeded at 5000 cells/well in 50 μL of DMEM, and placed for 6 h. Chemical compounds in DMSO were diluted 100-fold with the culture medium in advance. Following the addition of 40 μL of the fresh culture medium, 30 μL of the chemical diluents were also added to the cell cultures. The final volume of DMSO in the medium was equal to 0.25% (v/v). The cells under chemical treatment were incubated for further 72 h. The wells in the plates were washed twice with the cultured medium without phenol-red. After 1 h incubation with 100 μL of the medium, the cell culture in each well was supplemented with 20 μL of the MTS reagent (Promega), followed by incubation for additional 40 min. Absorbance at 495 nm of each well was measured using a VersaMax plate reader (Molecular Devices). At least three experiments were performed per condition and the averages and standard

deviations of inhibition rates in each condition were evaluated to determine IC_{50} values using the GraphPad Prism software.

Evaluation of Mitotic Arrest

HeLa cells were seeded at 10^5 cells/well in 500 μL of the medium on Lab-Tek II 8-well CC2 glass chamber slides (Nalge Nunc). After 6-hour incubation at 37 °C in a 5% CO_2 incubator, the culture medium was exchanged with 400 μL of fresh medium containing different inhibitors or DMSO, and the cells were placed at 37 °C in 5% CO_2 for 24 h. The final volume of inhibitor dissolved in DMSO in the medium was 0.4% (v/v). Before processing for immunofluorescence, HeLa cells were washed once with PBS(−) and then fixed with 3% paraformaldehyde/PBS(−) for 3 min and then with MeOH at −20 °C for 10 min. Microtubules was stained with a primary mouse monoclonal anti-α-tubulin antibody DM1A and a secondary rabbit polyclonal AlexaFluor594-conjugated anti-mouse antibody (Molecular Probes). Mitotic chromosomes were stained with a primary polyclonal rabbit anti-phospho-Histone H3 (Ser10) antibody (Upstate) followed by a secondary polyclonal AlexaFluor488-conjugated anti-rabbit antibody. DNA was counterstained with DAPI. Cells were classified as "mitotic", "interphase", or "other" by visual inspection to calculate the percentage of mitotic cells at each inhibitor concentration. At least 500 cells were examined per condition, and MI_{50} values were evaluated using Microsoft Excel and GraphPad Prism software. Fluorescent images were taken by a DP30BW CCD camera coupled to an IX71 microscope (Olympus) and superimposed using Adobe Photoshop software.

Steady-state KSP ATPase Assay

An enzyme-coupled system that regenerates ADP to ATP was used to measure ATP hydrolysis by KSP, with NADH absorbance at 340 nm as an indirect measurement of ATP turnover. To measure KSP ATPase activity in a reaction, the assay buffer [2.5 mM KCl, 50 mM PIPES (pH 6.9), 1 mM $MgCl_2$, 3 mM potassium phophoenol pyruvate, 450 μM Na_2·NADH, 1 mM dithiothreitol, 8 μM taxol, 9 U/mL lactate dehydrogenase, 15 U/mL pyruvate kinase, and 400 nM taxol-stabilized microtubules, and 80 nM bacteria-expressed KSP motor domain; K_m(ATP) = 15–35 μM] was supplemented with various concentrations of ATP along with KSP inhibitor solution. The optical density of a reaction at 340 nm was measured every 5 second using a UV-2450 photometer (Shimadzu). The steady-state rate of absorbance reduction was calculated using a linear least squares fitting method by Shimadzu UVProbe ver. 2.10 and Microsoft Excel. The

coupling activity of the ATP regeneration enzyme system was 100-fold greater than the ATPase activity measured in these experiments. Enzyme velocities were fitted to the Michealis–Menten equation as a function of ATP concentration at a particular drug concentration: $V = ([ATP] \times V_{max})/([ATP] + K_m)$. The observed Vmax values were 1.62 s^{-1} or 1.67 s^{-1} in the absence or presence of compound **9b**, and 1.19 s^{-1} or 0.94 s^{-1} in the absence or presence of compound **10b**, respectively.

References and Footnotes

(1)   Oishi, S.; Watanabe, T.; Sawada, J.; Asai, A.; Ohno, H.; Fujii, N. *J. Med. Chem.* **2010**, *53*, 5054–5058.

(2)   Nakazawa, J.; Yajima, J.; Usui, T.; Ueki, M.; Takatsuki, A.; Imoto, M.; Toyoshima, Y.; Osada, H. *Chem. Biol.* **2003**, *10*, 131–137.

(3)   Hotha, S.; Yarrow, J. C.; Yang, J. G.; Garrett, S.; Renduchintala, K. V.; Mayer, T. U.; Kapoor, T. M. *Angew. Chem., Int. Ed.* **2003**, *42*, 2379–2382.

(4)   (a) Luo, L.; Parrish, C. A.; Nevins, N.; McNulty, D. E.; Chaudhari, A. M.; Carson, J. D.; Sudakin, V.; Shaw, A. N.; Lehr, R.; Zhao, H.; Sweitzer, S.; Lad, L.; Wood, K. W.; Sakowicz, R.; Annan, R. S.; Huang, P. S.; Jackson, J. R.; Dhanak, D.; Copeland, R. A.; Auger, K. R. *Nat. Chem. Biol.* **2007**, *33*, 722–726. (b) Parrish, C. A.; Adams, N. D.; Auger, K. R.; Burgess, J. L.; Carson, J. D.; Chaudhari, A. M.; Copeland, R. A.; Diamond, M. A.; Donatelli, C. A.; Duffy, K. J.; Faucette, L. F.; Finer, J. T.; Huffman, W. F.; Hugger, E. D.; Jackson, J. R.; Knight, S. D.; Luo, L.; Moore, M. L.; Newlander, K. A.; Ridgers, L. H.; Sakowicz, R.; Shaw, A. N.; Sung, C. M. M.; Sutton, D.; Wood, K. W.; Zhang, S. Y.; Zimmerman, M. N.; Dhanak, D. *J. Med. Chem.* **2007**, *50*, 4939–4952.

(5)   Rickert, K. W.; Schaber, M.; Torrent, M.; Neilson, L. A.; Tasber, E. S.; Garbaccio, R.; Coleman, P. J.; Harvey, D.; Zhang, Y.; Yang, Y.; Marshall, G.; Lee, L.; Walsh, E. S.; Hamilton, K.; Buser, C. A. *Arch. Biochem. Biophys.* **2008**, *469*, 220–231.

(6)   Matsuno, K.; Sawada, J.; Sugimoto, M.; Ogo, N.; Asai, A. *Bioorg. Med. Chem. Lett.* **2009**, *19*, 1058–1061.

(7)   Ackermann, L.; Althammer, A. *Angew. Chem., Int. Ed.* **2007**, *46*, 1627–1629.

(8)   Owens, A. P.; Nadin, A.; Talbot, A. C.; Clarke, E. E.; Harrison, T.; Lewis, H. D.; Reilly, M.; Wrigley, J. D. J.; Castro, J. L. *Bioorg. Med. Chem. Lett.* **2003**, *13*, 4143–4145.

(9)   (a) Ishiyama, T.; Murata, M.; Miyaura, N. *J. Org. Chem.* **1995**, *60*, 7508–7510. (b) Ishiyama, T.; Miyaura, N. *J. Organomet. Chem.* **2000**, *611*, 392–402.

(10) Freeman, A. W.; Urvoy, M.; Criswell, M. E. *J. Org. Chem.* **2005**, *70*, 5014–5019.

(11) (a) Watanabe, T.; Ueda, S.; Inuki, S.; Oishi, S.; Fujii, N.; Ohno, H. *Chem. Commun.* **2007**, 4516–4518. (b) Watanabe, T.; Oishi, S.; Fujii, N.; Ohno, H. *J. Org. Chem.* **2009**, *74*, 4720–4726.

(12) Thompson, A. L. S.; Kabalka, G. W.; Akula, M. R.; Huffman, J. W. *Synthesis* **2005**, *4*, 547–550.

(13) (a) Azizian, H.; Eaborn, C.; Pidcock, A. *J. Organometal. Chem.* **1981**, *215*, 49–58.

(b) Furuya, T.; Strom, A. E.; Ritter, T. *J. Am. Chem. Soc.* **2009**, *131*, 1662–1663.

(14) Scott, W. J.; Crisp, G. T.; Stille, J. K. *J. Am. Chem. Soc.* **1984**, *106*, 4630–4632.

(15) Kumar, C. N. S. S. P.; Devi, C. L.; Rao, V. J.; Palaniappan, S. *Synlett* **2008**, *13*, 2023–2027.

(16) Wang, H.; Liu, L.; Wang, Y.; Peng, C.; Zhang, J.; Zhu, Q. *Tetrahedron Lett.* **2009**, *50*, 6841–6843.

(17) The varied cell membrane permeability could be attributable to the incompatible results between the in vitro KSP inhibition and cytotoxicity.

(18) Funayama, Y.; Nishio, K.; Wakabayashi, K.; Nagao, M.; Shimoi, K.; Ohira, T.; Hasegawa, S.; Saijo, N. *Mutat. Res.* **1996**, *349*, 183–191.

(19) Yan, Y.; Sardana, V.; Xu, B.; Homnick, C.; Halczenko, W.; Buser, C. A.; Schaber, M.; Hartman, G. D.; Huber, H. E.; Kuo, L. C. *J. Mol. Biol.* **2004**, *335*, 547–554.

(20) (a) Kaan, H. Y. K.; Ulaganathan, V.; Hackney, D. D.; Kozielski, F. *Biochem. J.* **2010**, *425*, 55–60. (b) Kim, E. D.; Buckley, R.; Learman, S.; Richard, J.; Parke, C.; Worthylake, D. K.; Wojcik, E. J.; Walker, R. A.; Kim, S. *J. Biol. Chem.* **2010**, *285*, 18650–18661.

(21) Barsanti, P. A.; Ni, W. W. Z.; Duhl, D.; Brammeier, N.; Martin, E.; Bussiere, D.; Walter, A. O. *Bioorg. Med. Chem. Lett.* **2010**, *20*, 157–160.

(22) Although the plots in the presence and absence of inhibitors converged, the possible mixed mode of inhibition by binding to the second site cannot be ruled out.

(23) Garcia-Saez, I.; Yen, T.; Wade, R. H.; Kozielski, F. *J. Mol. Biol.* **2004**, *340*, 1107–1116.

(24) Tomasi, S.; Renault, J.; Martin, B.; Duhieu, S.; Cerec, V.; Roch, M. L.; Uriac, P.; Delcros, J. G. *J. Med. Chem.* **2010**, *53*, 7647–7663.

(25) Williams, R. C. Jr.; Lee, J. C. *Methods Enzymol.* **1982**, *85*, 376–385.

Chapter 2.   Development of Novel Kinesin Spindle Protein
Inhibitors with Diaryl Amine Scaffolds

Section 1.   Improvement of Aqueous Solubility of Kinesin
Spindle Protein Inhibitors by Modification of
Ring-fused Scaffolds

Diaryl amine derivatives have been designed and synthesized for novel KSP inhibitors based on planar carboline/carbazole-type KSP inhibitors with poor aqueous solubility. This new generation of inhibitors showed comparable inhibitory activity and high selectivity for KSP accompanied with improved solubility. Comparative structural investigations on a series of compounds revealed that the higher solubility of diaryl amine-type inhibitors was attributed to fewer van der Waals interactions in the crystal packing, as well as a hydrogen-bond acceptor nitrogen in the aniline moiety for favorable solvation.
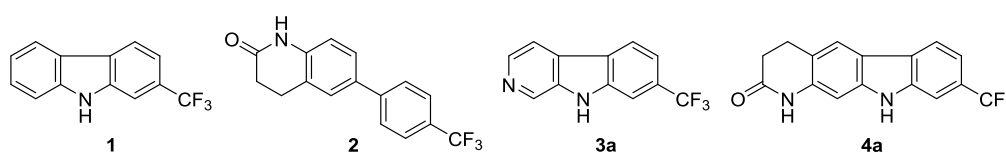

Figure 1. Structures of carbazole- and carboline-based KSP inhibitors **1**, **3a** and **4a**, and biphenyl-type KSP inhibitor **2**.

As described in chapter 1, the author has identified β-carboline derivative **3a** (= **9b** in chapter 1) and lactam-fused carbazole derivative **4a** (= **10b** in chapter 1) as novel potent KSP inhibitors by the structure–activity relationship studies from carbazole **1** in combination with the known biphenyl-type KSP inhibitors like **2** (Figure 1).[1] During the course of the studies of the antitumor effects of these carboline- and carbazole-based KSP inhibitors,[2] the author found that these inhibitors exhibited low solubility in the aqueous solvents employed for in vivo studies. To overcome the inherent drawbacks of carbazole-based KSP inhibitors, the author undertook the development of novel diaryl amine-type KSP inhibitors to simultaneously satisfy the potent inhibitory activity requirements, as well as obtain better solubility in aqueous solution. The structural basis of the solubility of a series of compounds was also investigated by single crystal X-ray diffraction studies and free energy calculations.

The melting points of carboline- and carbazole-type KSP inhibitors **3–5**, as described in chapter 1, were extremely high (Figure 2); for example, the melting points of carbazoles **4a,b** and **5c,f** were > 300 °C. The author speculated that the poor

solubility of compounds **3–5** would be attributable to the significant intermolecular interactions in the crystals, since the melting point is correlated with the crystal packing of the molecule, which is one of the major contributing factors to solubility.[3] With the aim of disrupting the possible intermolecular π–π stacking interactions to lower the melting point and in turn to improve the solubility, the design of more nonplanar analogs from planar compounds **3–5** was expected to be a promising approach.[3] Alternatively, the addition of polar or ionizable functional group(s) is also an effective modification to enhance solubility.[4] To satisfy these two criteria, the author designed diaryl amine derivatives **6–8**, in which the pyrrole C–C bond in the central part of carbolines and carbazoles **3–5** was cleaved (Figure 2). Diaryl amines **6a,b** with a pyridine ring were designed based on carbolines **3a,b** with potent KSP inhibitory activity (Figure 2A). Diphenylamines **7a–f** with a nitro, amino or urea group at the 3- or 4-position on the left-hand phenyl ring were similarly investigated, which represent the cleaved analogs of carbazoles **5b–f** (Figure 2B). Diphenylamines **8a,b** with a 3,4-fused lactam structure on the left-hand phenyl ring were also designed based on carbazoles **4a,b** (Figure 2C). It was expected that highly flexible conformations of the two aryl rings in **6–8** would prevent intermolecular π–π stacking interactions and that the newly available aniline would enhance solubility in an aqueous environment.
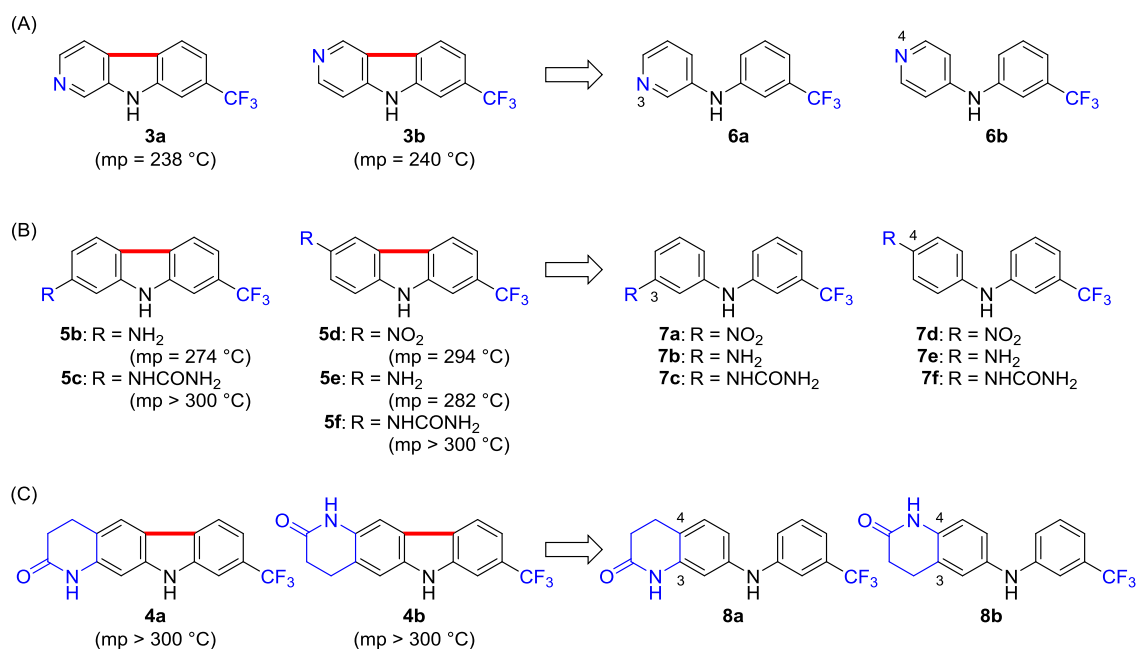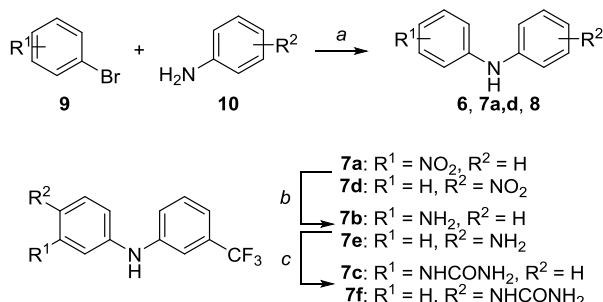

Figure 2. Design of novel KSP inhibitors **6–8** with diaryl amine scaffolds. Melting points of parent compounds **3–5** are shown in parentheses.
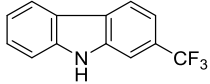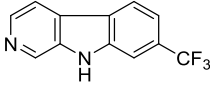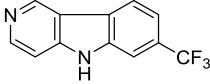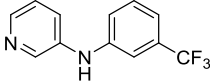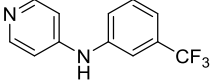
A series of diaryl amine derivatives **6**, **7a,d** and **8** were prepared by palladium-catalyzed *N*-arylation using aryl bromides **9** and substituted anilines **10**

(Scheme 1).[5] For the preparation of compounds **7c,f** with a urea group, nitro derivatives **7a,d** were reduced to the corresponding amines **7b,e** using Pd/C and ammonium formate, which were converted to the expected compounds **7c,f** by KOCN.

7a: $R^1 = NO_2$, $R^2 = H$
7d: $R^1 = H$, $R^2 = NO_2$
7b: $R^1 = NH_2$, $R^2 = H$
7e: $R^1 = H$, $R^2 = NH_2$
7c: $R^1 = NHCONH_2$, $R^2 = H$
7f: $R^1 = H$, $R^2 = NHCONH_2$

Scheme 1. Synthesis of diaryl amine derivatives. *Reagents and conditions*: (a) $Pd_2(dba)_3$, biaryl phosphine ligand, NaOt-Bu, toluene, 100 °C; (b) Pd/C, HCO_2NH_4, EtOH, reflux; (c) KOCN, AcOH, H_2O, rt.

Table 1. KSP inhibitory activities and thermodynamic aqueous solubility of diaryl amines with a pyridine ring and the related compounds
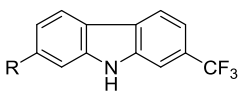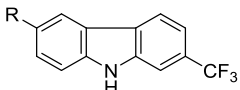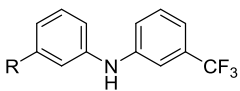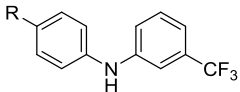
compound		KSP ATPase IC_{50} (μM)^{a,b}	solubility	
			50% EtOH^c (mg/mL)	phosphate buffer (pH 7.4) (μg/mL)
	1	0.21	0.424	<1
	3a	0.052	0.472	<1
	3b	0.095	1.76	3.16
	6a	>6.3^d	14.3	10.8
	6b	>6.3	24.0	264

^{a}Inhibition of microtubule-activated KSP ATPase activity. ^{b}IC_{50} values were derived from the dose–response curves generated from triplicate data points. ^{c}Solubility in an equal volume of EtOH and 1/15 M phosphate buffer (pH 7.4). ^{d}IC_{50} was $\approx$7.0 μM.

KSP ATPase inhibitory activity of the diaryl amine derivatives **6–8** was evaluated. First, compounds **6a,b** with a pyridine ring in the left-hand part were comparatively assessed with the parent carboline-type inhibitors **3a,b** (Table 1). Unfortunately, the cleavage of the pyrrole C–C bond in carboline was accompanied by a

significant decrease or loss of KSP ATPase inhibitory activity. Diphenylamine derivatives **7a–f** with a nitro, amino or urea group at the 3- or 4-position on the left-hand phenyl group were next examined (Table 2). The 3-substituted anilines **7a–c** showed no KSP inhibitory activity at 6.3 μM. Among the 4-substituted analogs, compound **7f** with a urea group exhibited moderate inhibitory activity ($IC_{50} = 0.39$ μM), while compounds **7d,e** with a nitro or amino group had weak or no potency. The potency of **7f** was approximately three times lower than that of the parent carbazole **5f**.

Table 2. KSP inhibitory activities of diphenylamines with a nitro, amino or urea group and the related carbazoles
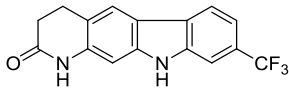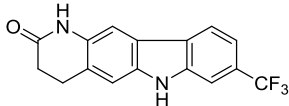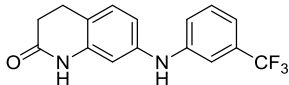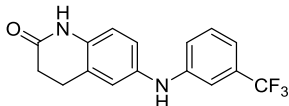
compound		R	KSP ATPase IC_{50} (μM)^{a,b}
R—carbazole—CF₃ (N-H)	**5b**	NH_2	0.27
	5c	$NHCONH_2$	0.085
R—carbazole—CF₃ (N-H)	**5d**	NO_2	0.043
	5e	NH_2	0.55
	5f	$NHCONH_2$	0.12
R—phenyl—NH—phenyl—CF₃	**7a**	NO_2	>6.3
	7b	NH_2	>6.3
	7c	$NHCONH_2$	>6.3
R—phenyl—NH—phenyl—CF₃	**7d**	NO_2	3.2
	7e	NH_2	>6.3
	7f	$NHCONH_2$	0.39

^{a}Inhibition of microtubule-activated KSP ATPase activity. ^{b}IC_{50} values were derived from the dose–response curves generated from triplicate data points.

Next, diphenylamine derivatives **8a,b**, which were fused with a lactam at the 3- and 4-positions on the left-hand phenyl group, were investigated (Table 3). Diphenylamine **8a** with the accessory amide group at the 3-position on the left-hand phenyl group showed no KSP inhibitory activity, although the parent carbazole **4a** showed highly potent activity. On the other hand, diphenylamine **8b** (= **24** in chapter 1)

with the amide group at the 4-position exhibited four times more potency ($IC_{50} = 0.045$ μM) than the parent carbazole **4b**. This potency was comparable to that of the most potent carbazole-type inhibitor **4a**. Diphenylamine **8b** showed a moderate inhibitory effect on the proliferation of A549 cells ($IC_{50} = 4.2$ μM).

Table 3. KSP inhibitory activities of diphenylamines with a 3,4-fused lactam structure on the left-hand phenyl group and the related carbazoles

compound		KSP ATPase IC_{50} (μM)[a,b]
	4a	0.031
	4b	0.18
	8a	>6.3
	8b	0.045

[a]Inhibition of microtubule-activated KSP ATPase activity. [b]IC_{50} values were derived from the dose–response curves generated from triplicate data points.

To investigate the selectivity of diphenylamine **8b**, inhibitory activities were evaluated for a number of the other kinesins. The ATPase activities of centromere-associated protein E (CENP-E), Kid, mitotic kinesin-like protein 1 (MKLP-1), KIF4A, KIFC3, KIF14, KIF15 and KIF2A were not inhibited by **8b** at 20 μM (Table 4), which is consistent with the selectivity profile of carbazole-type inhibitor **4a**. No inhibitory activity of β-carboline **3a** against these kinesins was also observed.

Next, the diphenylamine **8b** was screened in comparison with the parent β-carboline **3a** and carbazole **4a** against a panel of 117 kinases to assess the selectivity profiles (Table 5). β-Carboline **3a** showed >50% inhibition against four kinases (CDK6/cyclinD3, IKKβ, PRK2, ROCK-II) at 10 μM, which is consistent with previous studies showing that carboline is a well-known scaffold of kinase inhibitors.[6] On the other hand, no more than 50% inhibition against any kinases was observed in **4a** and **8b** (10 μM), suggesting that newly identified diphenylamine-type inhibitor **8b** has high selectivity for KSP.

Table 4. ATPase inhibitory activity against nine kinesin motor proteins

motor protein	% Inhibition[a]		motor protein	% Inhibition[a]	
	3a	**8b**		**3a**	**8b**
KSP	97	97	KIFC3	<3	<3
CENP-E	<3	<3	KIF14	4	<3
Kid	<3	<3	KIF15	<3	<3
MKLP-1	<3	<3	KIF2A	<3	<3
KIF4A	<3	<3			

[a]The inhibition values were determined by ATPase assay and are indicated as a percentage of the solvent only control. The final concentration of the compounds in the assay was 20 μM.
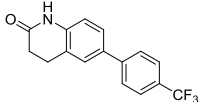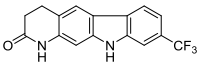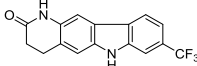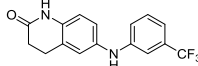
Table 5. Kinase selectivity profile of β-carboline **3a**, carbazole **4a** and diphenylamine **8b**

kinase	% Inhibition[a]		
	3a	**4a**	**8b**
CDK6/cyclinD3	53	0	2
GSK3β	22	32	3
IKKβ	51	10	0
Mnk2	22	41	0
Pim-1	37	9	0
PKCα	26	9	0
PRK2	52	0	0
ROCK-II	63	0	0

[a]% Inhibition was determined from the duplicate data points of the *in-vitro* assay for each kinase. The final concentration of the compounds was 10 μM.

The solubility of a series of potent KSP inhibitors was evaluated by a thermodynamic method.[7] A mixture of EtOH–phosphate buffer (pH 7.4) (1:1) [50% EtOH] and phosphate buffer (pH 7.4) were employed as aqueous media.[7] In these solutions, the parent carbazole-type inhibitor **1** was moderately soluble (0.424 mg/mL) and insoluble (<1 μg/mL), respectively (Table 1). First, the solubility of aminopyridine

Table 6. KSP inhibitory activities and physicochemical properties of biphenyl **2**, carbazole **4a,b** and diphenylamine **8b** with a lactam-fused structure

	2	**4a**	**4b**	**8b**
KSP ATPase IC$_{50}$ (μM)[a,b]	0.046	0.031	0.18	0.045
solubility (mg/mL)[c]	0.339	0.457	0.468	1.80
melting point (°C)	221	>300	>300	190
crystal packing energy (kcal/mol)[d]	−55.2 (vdW: −37.6; ele: −17.6)	−58.8 (vdW: −31.8; ele: −27.0)	−[e]	−53.7 (vdW: −29.7; ele: −24.0)
ClogP[f]	4.2	3.9	3.9	4.2
HPLC retention time (min)[g]	29.0	25.9	21.7	24.4

[a]Inhibition of microtubule-activated KSP ATPase activity. [b]IC$_{50}$ values were derived from the dose–response curves generated from triplicate data points. [c]Solubility in 50% EtOH [an equal volume of EtOH and 1/15 M phosphate buffer (pH 7.4)]. [d]Contributions of vdW and electrostatic energies were shown in the brackets. Electrostatic energies were abbreviated to "ele". [e]Not tested. [f]CLogP values were calculated with ChemBioDraw Ultra 12.0. [g]HPLC analysis was carried out on a Cosmosil 5C18-ARII column (4.6 × 250 mm) and the material eluted by a linear MeCN gradient (70:30 to 30:70 over 40 min) in 0.1% TFA; flow rate of 1 mL/min.

derivatives **6a,b** were investigated. *N*-(Pyridin-3-yl)amine **6a** showed the anticipated improvement in thermodynamic solubility, being 30 times more soluble in 50% EtOH (14.3 mg/mL) compared with the corresponding carboline **3a**. *N*-(Pyridin-4-yl)amine **6b** also exhibited approximately 14 times greater solubility in 50% EtOH (24.0 mg/mL) than the parent carboline **3b**. Of note, compound **6b** had moderate solubility (264 μg/mL) even in phosphate buffer, which was 80 times or more soluble compared with **3a** and **3b**, respectively. Although these pyridinylamine derivatives **6a,b** were inert in KSP inhibition, it was suggested that cleavage of the pyrrole C–C bond in carboline and carbazole derivatives could be a promising approach to improve the solubility in
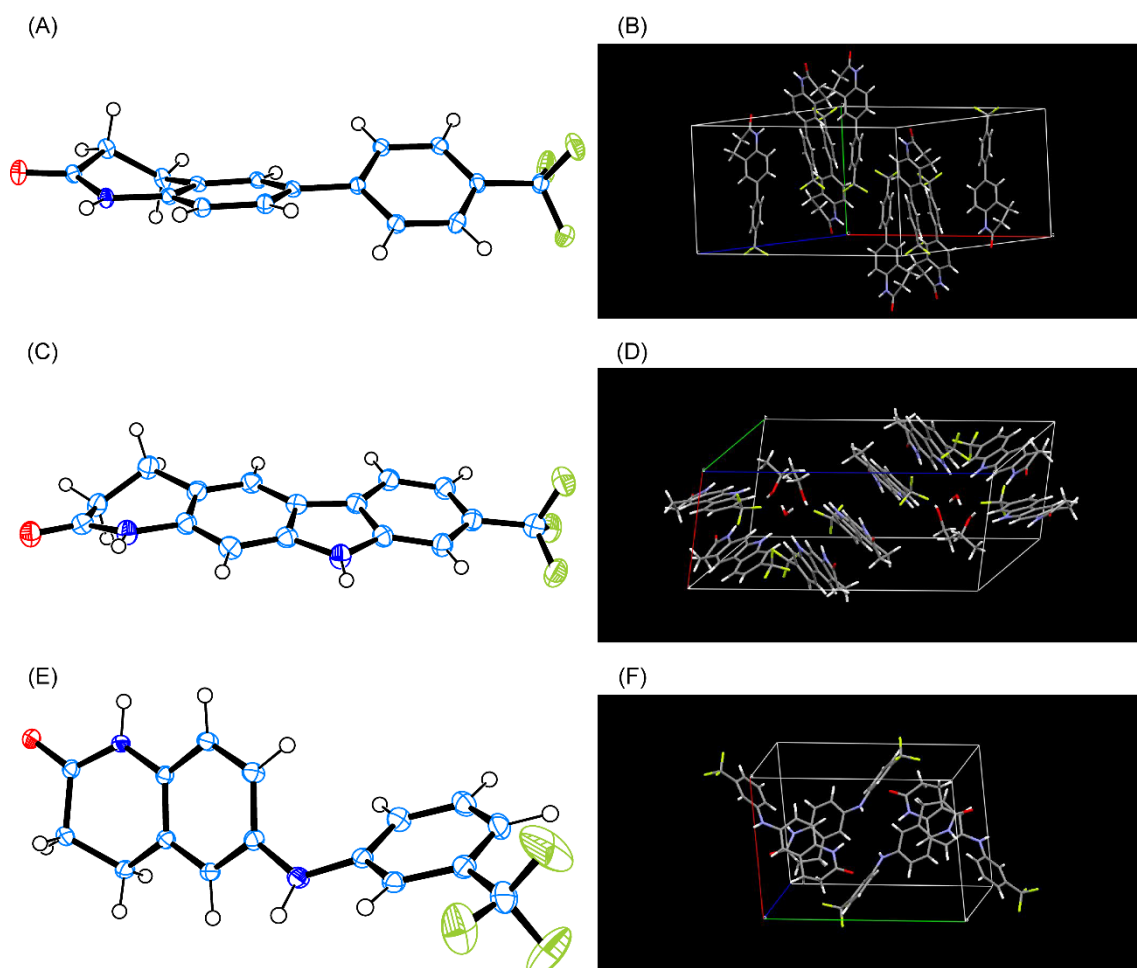
Figure 3. X-ray crystal structures of biphenyl-type (**2**), carbazole-type (**4a**) and diphenylamine-type (**8b**) KSP inhibitors. (A) ORTEP diagram of **2**; (B) Crystal packing of **2**. (C) ORTEP diagram of **4a**; (D) Crystal packing of **4a**. (E) ORTEP diagram of **8b**; (F) Crystal packing of **8b**.

aqueous solution.

The thermodynamic aqueous solubility of biphenyl **2**, carbazoles **4a,b** and diphenylamine **8b** with potent KSP inhibitory activity was next evaluated (Table 6). Biphenyl compound **2** showed the lowest solubility in this examination (0.339 mg/mL in 50% EtOH). Carbazoles **4a,b** were slightly more soluble (0.457 mg/mL and 0.468 mg/mL, respectively, in 50% EtOH) compared with biphenyl **2**. Diphenylamine **8b** was approximately four times more soluble (1.80 mg/mL in 50% EtOH) than carbazoles **4a**,**b**. The physicochemical parameters such as melting point and retention time on a reversed-phase HPLC column were also investigated to estimate the underlying factors contributing to the solubility. The melting point of diphenylamine **8b** (190 °C) was significantly lower than those of biphenyl **2** (221 °C) and carbazoles **4a,b** (>300 °C). In

contrast, there were no correlations between the solubility in 50% EtOH and HPLC retention time. ClogP values in an uncharged form of a series of compounds were similar (3.9–4.2).

The solubility of a solid inhibitor in water depends on two factors: the crystallinity of the compound and the ability of the compound to interact with water.[8] Recently, trials to address solubility issues of drug candidates based on X-ray crystal structures have been reported.[9] Thus, the author analyzed the crystal structures of the series of inhibitors to investigate the possible correlation with solubility (Figure 3). First, single crystals of biphenyl-type inhibitor **2** were prepared by slow evaporation of Et_2O for X-ray structural analysis. Eight biphenyl molecules **2** in a unit cell exhibited a slightly twisted conformation with a relatively small dihedral angle between the two phenyl groups (34.0°) (Figure 3A, B). Two phenyl groups of **2** are involved in a number of CH/π interactions with the methylene groups on lactam moieties or with the phenyl groups of adjacent molecules, which would possibly contribute to large van der Waals interactions for crystal packing (Figure 4A). The electrostatic stabilization in this packing mainly came from two intermolecular hydrogen bonds between the lactam amide groups across a pair of molecules. The packing energy of **2** calculated from the crystal structure by the MM method was −55.2 kcal/mol (vdW: −37.6 kcal/mol; electrostatic: −17.6 kcal/mol) (Table 6).

Single crystals of carbazole **4a**, which were obtained from an EtOH solution,[10] contained eight carbazole molecules, four EtOH molecules and two water molecules in a unit cell (Figure 3C, D). In the packing modes of crystals, intermolecular π–π stacking interactions with the adjacent carbazoles were clearly observed (average distance between two carbazole rings: 3.81 Å). The carbazole moiety also formed CH/π interactions with other molecules of **4a** (Figure 4C–F), but the number of interactions was less when compared with that of **2** (Figure 4A). Regarding electrostatic interactions, there were two hydrogen bonds between the lactam amide groups across a pair of molecules of **4a** as observed in the biphenyl **2** crystal. Additionally, the carbazole NH group in **4a** also interacted with an oxygen atom of EtOH or water via a hydrogen bond, leading to an increase in the electrostatic interaction contribution for the total packing energy when compared with biphenyl **2**. The average value from four unique carbazole molecules in a unit cell was calculated for the packing energies of **4a** [−58.8 kcal/mol (vdW: −31.8 kcal/mol; electrostatic: −27.0 kcal/mol)].

Crystal structure analysis of **8b** was then performed using colorless single crystals from EtOAc, in which four equivalent molecules were included in a unit cell (Figure 3E, F). No π–π interactions of the aryl groups in **8b** with the adjacent molecules
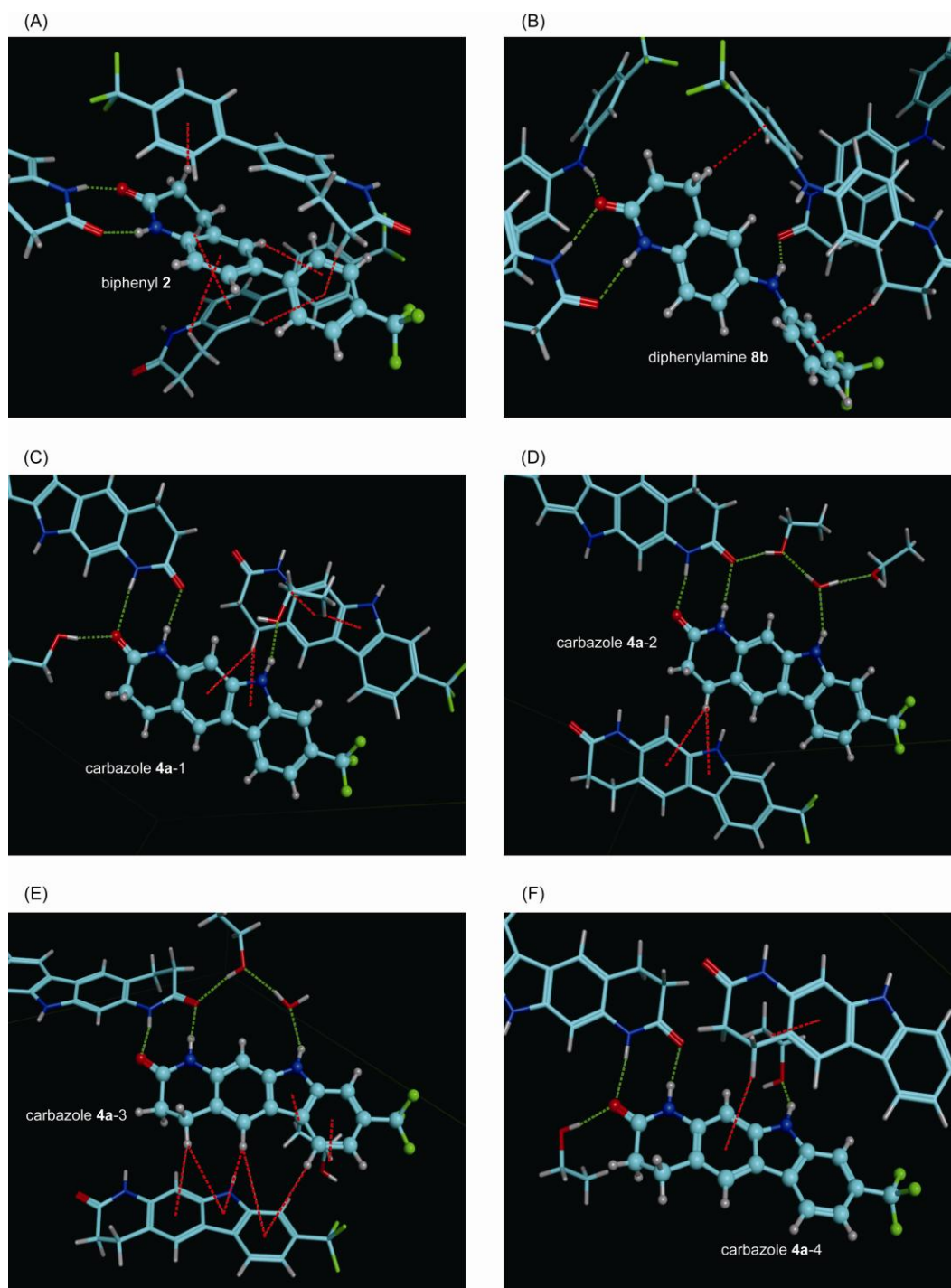
Figure 4. Intermolecular interactions of biphenyl-type (**2**), diphenylamine-type (**8b**) and carbazole-type (**4a**) KSP inhibitors. (A) Biphenyl **2**. (B) Diphenylamine **8b**. (C)–(F) Four carbazole molecules (**4a**) in different environments in a unit cell. Hydrogen bonds are shown in green dashed line and CH/π interactions red.

were involved in the crystal packing, as the author expected given that the possibly large torsion angle between the two phenyl groups in the diphenylamine **8b** would

collapse the intermolecular π–π stacking of planar carbazole **4a**. Two intermolecular CH/π interactions in a pair of molecules of **8b** between a CF_3-phenyl group and a methylene C–H group of the lactam rings were observed (Figure 4B). The aniline NH group in **8b** formed an intermolecular hydrogen bond with a lactam carbonyl oxygen. A pair of intermolecular hydrogen bonds between the lactam amides as observed in biphenyl **2** and carbazole **4a** were observed. The total energy of the crystal packing of **8b** was found to be the lowest [−53.7 kcal/mol (vdW: −29.7 kcal/mol; electrostatic: −24.0 kcal/mol)] among three KSP inhibitors.

Taken together, the packing modes of the crystals of the three KSP inhibitors were revealed by X-ray crystal structure analysis. All crystal structures share common intermolecular hydrogen bonds across the lactam amide groups of two molecules to affect the crystal packings (Figure 3B, D, F). The total energies of the crystal packings correlated with the order of the melting points. For example, the higher total packing energy may rationalize the higher melting point of carbazole **4a**. However, the thermodynamic solubility of a series of compounds was not estimated directly from the total energy of the crystal packing nor the melting points. The lower solubility of **2** could be explained by the high energy of the crystal packing from van der Waals interactions via a number of CH/π and π–π interactions in the periodic lattice. Because electrostatic interactions, including intermolecular hydrogen bonds, in the crystals can be offset in aqueous solution by interactions with the surrounding solvent, the energy from electrostatic interactions may have less of an impact to the solubility. In the course of the calculation of the packing energies, the uncharged forms of three inhibitors were compared.[11] The hydrogen-bond acceptor nitrogen of the aniline moiety in diphenylamine **8b**, which is not involved in electrostatic interactions in the crystal, may have a favorable effect on solvation for the increased solubility. Indeed, the solubility of **8b** was much higher than that of carbazole **4a**, even though the difference between the packing energies of **4a** and **8b** from van der Waals interactions was small.

In conclusion, the author has designed a new class of KSP inhibitors with a diaryl amine scaffold to improve aqueous solubility from carboline- and carbazole-based KSP inhibitors. The structure–activity relationship studies of a series of derivatives demonstrated that diaryl amines with a urea group (**7f**) or a fused lactam (**8b**) at the appropriate position exhibited potent KSP inhibitory activity with high selectivity. As expected, the diphenylamine **8b** showed four times greater solubility than the parent carbazoles **4a**,**b**. The investigations on the physicochemical properties and packing energy calculations of the crystals of a series of compounds revealed that the improvement in solubility of **8b** resulted from the reduction in van der Waals

interactions of CH/π and π–π interactions, as well as increased solvation by a hydrogen-bond acceptor nitrogen of aniline moiety.

Experimental Section

General Methods. ^{1}H NMR spectra were recorded using a JEOL AL-400 or a JEOL ECA-500 spectrometer. Chemical shifts are reported in δ (ppm) relative to Me$_4$Si as an internal standard. ^{13}C NMR spectra were referenced to the residual DMSO signal. Exact mass (HRMS) spectra were recorded on a JMS-HX/HX 110A mass spectrometer. Melting points were measured by a hot stage melting point apparatus (uncorrected). For flash chromatography, Wakogel C-300E (Wako) was employed. For analytical HPLC, a Cosmosil 5C18-ARII column (4.6 x 250 mm, Nacalai Tesque, Inc., Kyoto, Japan) was employed with a linear gradient of CH$_3$CN containing 0.1% (v/v) TFA at a flow rate of 1 mL/min on a Shimadzu LC-10ADvp (Shimadzu Corp., Ltd., Kyoto, Japan), and eluting products were detected by UV at 254 nm. The purity of the compounds was determined by combustion analysis or HPLC analysis (> 95%).

General Procedure of *N*-Arylation for Preparation of Diaryl Amine Compounds: Synthesis of *N*-[3-(Trifluoromethyl)phenyl]pyridin-3-amine (6a). Toluene (10.5 mL) was added to a flask containing 3-bromopyridine (500 mg, 3.16 mmol), 3-(trifluoromethyl)aniline (510 μL, 4.11 mmol), Pd$_2$(dba)$_3$ (28.9 mg, 0.03 mmol), 2-dicyclohexylphosphino-2′,4′,6′-triisopropylbiphenyl (60.3 mg, 0.13 mmol) and NaO*t*-Bu (456 mg, 4.75 mmol) under an argon atmosphere. The mixture was stirred at 100 °C for 11 h. After cooling, the reaction mixture was diluted with EtOAc, and filtered through a pad of Celite. The filtrate was concentrated *in vacuo*. Crude material was purified by flash chromatography with *n*-hexane/EtOAc (1:1) to afford the desired diaryl amine **6a** (689 mg, 92% yield): white solid; mp 122–123 °C; IR (neat) cm^{-1}: 3048 (NH); ^{1}H NMR (500 MHz, DMSO-d_6) δ 7.17 (d, *J* = 8.0 Hz, 1H; Ar), 7.31–7.33 (m, 2H; Ar), 7.38 (d, *J* = 8.0 Hz, 1H; Ar), 7.46 (t, *J* = 8.0 Hz, 1H; Ar), 8.15–8.17 (m, 1H; Ar), 8.16 (dd, *J* = 4.6, 1.7 Hz, 1H; Ar), 8.44 (d, *J* = 2.3 Hz, 1H; Ar), 8.75 (s, 1H; NH); ^{13}C NMR (125 MHz, DMSO-d_6) δ 112.1, 116.0, 119.3, 123.9 (2C), 124.2 (q), 130.2 (q), 130.4, 138.8, 140.3, 141.9, 143.8; *Anal.* calcd for C$_{12}$H$_9$F$_3$N$_2$: C, 60.51; H, 3.81; N, 11.76. Found: C, 60.78; H, 3.83; N, 11.78.

***N*-[3-(Trifluoromethyl)phenyl]pyridin-4-amine (6b).** Following the general procedure for **6a**, compound **6b** (540 mg, 88% yield) was synthesized from 4-bromopyridine hydrochloride and 3-(trifluoromethyl)aniline: white solid; mp 130–131 °C; IR (neat) cm^{-1}: 2902 (NH); ^{1}H NMR (500 MHz, DMSO-d_6) δ 7.01 (d, *J* = 6.3 Hz, 2H; Ar), 7.34 (d, *J* = 6.9 Hz, 1H; Ar), 7.48 (s, 1H; Ar), 7.53–7.59 (m, 2H; Ar), 8.31 (d, *J*

= 6.3 Hz, 2H; Ar), 9.17 (s, 1H; NH); ^{13}C NMR (125 MHz, DMSO-d_6) δ 109.8 (2C), 115.3, 118.1, 122.5, 124.0 (q), 130.2 (q), 130.5, 141.6, 149.2, 150.3 (2C); *Anal.* calcd for $C_{12}H_9F_3N_2$: C, 60.51; H, 3.81; N, 11.76. Found: C, 60.79; H, 3.77; N, 11.82.

3-Nitro-*N*-[3-(trifluoromethyl)phenyl]aniline (7a). Following the general procedure for **6a**, compound **7a** (365 mg, 97% yield) was synthesized from 1-bromo-3-(trifluoromethyl)benzene and 3-nitroaniline: orange solid; mp 69–71 °C; IR (neat) cm^{-1}: 1526 (NO$_2$), 3379 (NH); ^{1}H NMR (500 MHz, DMSO-d_6) δ 7.27 (d, J = 7.4 Hz, 1H; Ar), 7.39 (s, 1H; Ar), 7.47 (d, J = 7.4 Hz, 1H; Ar), 7.53–7.57 (m, 3H; Ar), 7.70 (d, J = 7.4 Hz, 1H; Ar), 7.86 (s, 1H; Ar), 9.08 (s, 1H; NH); ^{13}C NMR (125 MHz, DMSO-d_6) δ 110.2, 113.7, 114.5, 117.2, 120.8, 122.6, 124.1 (q), 130.2 (q), 130.6, 130.7, 142.8, 144.0, 148.7; HRMS (FAB): *m/z* calcd for $C_{13}H_9F_3N_2O_2$ (M$^+$) 282.0616; found: 282.0621.

N^1-[3-(Trifluoromethyl)phenyl]benzene-1,3-diamine (7b). To a stirred solution of 3-nitro-*N*-[3-(trifluoromethyl)phenyl]aniline **7a** (190 mg, 0.67 mmol) and ammonium formate (509 mg, 8.07 mmol) in EtOH (2.2 mL) at room temperature was added 10% Pd/C (35.8 mg, 0.03 mmol). The mixture was heated under reflux for 2 h. After cooling, the reaction mixture was diluted with EtOAc, and filtered through a pad of Celite. The filtrate was concentrated *in vacuo*. Crude material was purified by flash chromatography with *n*-hexane/EtOAc (3:1) to afford compound **7b** (165 mg, 97%): brown oil; IR (neat) cm^{-1}: 3035 (NH), 3377 (NH); ^{1}H NMR (400 MHz, DMSO-d_6) δ 4.96 (s, 2H; NH$_2$), 6.19 (d, J = 8.0 Hz, 1H; Ar), 6.28 (d, J = 8.0 Hz, 1H; Ar), 6.37 (s, 1H; Ar), 6.92 (t, J = 8.0 Hz, 1H; Ar), 7.01 (d, J = 8.0 Hz, 1H; Ar), 7.22 (s, 1H; Ar), 7.25 (d, J = 8.2 Hz, 1H; Ar), 7.37 (t, J = 8.0 Hz, 1H; Ar), 8.13 (s, 1H; NH); ^{13}C NMR (125 MHz, DMSO-d_6) δ 104.0, 106.5, 107.8, 111.3, 114.3, 118.8, 124.3 (q), 129.6, 129.8 (q), 130.0, 142.5, 145.2, 149.7; HRMS (FAB): *m/z* calcd for $C_{13}H_{11}F_3N_2$ (M$^+$) 252.0874; found: 252.0874.

1-(3-{[3-(Trifluoromethyl)phenyl]amino}phenyl)urea (7c). To a stirred solution of N^1-[3-(trifluoromethyl)phenyl]benzene-1,3-diamine **7b** (80.0 mg, 0.32 mmol) in AcOH (4.0 mL) was added KOCN (77.2 mg, 0.95 mmol) and water (80.0 µL). The reaction mixture was stirred at room temperature for 18 h, then evaporated to dryness under vacuum. Crude material was purified by flash chromatography with amino silica gel with CHCl$_3$/MeOH (20:1 to 10:1) to afford compound **7c** (31.9 mg, 34% yield): yellow oil; IR (neat) cm^{-1}: 1661 (C=O), 3225 (NH), 3351 (NH); ^{1}H NMR (500 MHz, DMSO-d_6) δ 5.82 (br, 2H; NH$_2$), 6.66 (d, J = 8.0 Hz, 1H; Ar), 6.84 (d, J = 8.0 Hz, 1H;

Ar), 7.06 (d, J = 8.0 Hz, 1H; Ar), 7.12 (t, J = 8.0 Hz, 1H; Ar), 7.28 (s, 1H; Ar), 7.30 (d, J = 8.0 Hz, 1H; Ar), 7.41 (s, 1H; Ar), 7.42 (t, J = 8.0 Hz, 1H; Ar), 8.50 (br, 2H; NH); ^{13}C NMR (125 MHz, DMSO-d_6) δ 107.4, 110.7, 110.9, 111.5, 114.8, 118.9, 124.2 (q), 129.3, 129.8 (q), 130.1, 141.5, 142.2, 144.6, 155.8; HRMS (FAB): m/z calcd for $C_{14}H_{12}F_3N_3O$ (M$^+$) 295.0932; found: 295.0926.

N-(4-Nitrophenyl)-3-(trifluoromethyl)aniline (7d). Following the general procedure for **6a**, compound **7d** (2.20 g, 70% yield) was synthesized from 1-bromo-3-(trifluoromethyl)benzene and 4-nitroaniline: yellow solid; mp 141–143 °C; IR (neat) cm^{-1}: 1587 (NO$_2$), 3327 (NH); ^{1}H NMR (500 MHz, DMSO-d_6) δ 7.13 (d, J = 9.2 Hz, 2H; Ar), 7.36 (d, J = 6.9 Hz, 1H; Ar), 7.46 (s, 1H; Ar), 7.53–7.60 (m, 2H; Ar), 8.12 (d, J = 9.2 Hz, 2H; Ar), 9.51 (s, 1H; NH); ^{13}C NMR (125 MHz, DMSO-d_6) δ 114.3 (2C), 116.0, 119.0, 123.2, 124.0 (q), 126.0 (2C), 130.3 (q), 130.6, 138.9, 141.3, 149.6; HRMS (FAB): m/z calcd for $C_{13}H_9F_3N_2O_2$ (M$^+$) 282.0616; found: 282.0612.

N^1-[3-(Trifluoromethyl)phenyl]benzene-1,4-diamine (7e). Following the procedure described for **7b**, compound **7e** (1.75 g, 98% yield) was synthesized from N-(4-nitrophenyl)-3-(trifluoromethyl)aniline **7d**: brown solid; mp 58–60 °C; IR (neat) cm^{-1}: 3027 (NH), 3393 (NH); ^{1}H NMR (500 MHz, DMSO-d_6) δ 4.91 (s, 2H; NH$_2$), 6.61 (d, J = 8.0 Hz, 2H; Ar), 6.85–6.89 (m, 3H; Ar), 6.98 (s, 1H; Ar), 6.99 (d, J = 8.0 Hz, 1H; Ar), 7.27 (t, J = 8.0 Hz, 1H; Ar), 7.90 (s, 1H; NH); ^{13}C NMR (125 MHz, DMSO-d_6) δ 108.8, 112.6, 114.8 (2C), 116.4, 124.0 (2C), 124.5 (q), 129.9 (q), 129.9 (2C), 145.1, 147.9; HRMS (FAB): m/z calcd for $C_{13}H_{11}F_3N_2$ (M$^+$) 252.0874; found: 252.0876.

1-(4-{[3-(Trifluoromethyl)phenyl]amino}phenyl)urea (7f). Following the procedure described for **7c**, compound **7f** (109 mg, 37% yield) was synthesized from N^1-[3-(trifluoromethyl)phenyl]benzene-1,4-diamine **7e**: off-white solid; mp 165–166 °C; IR (neat) cm^{-1}: 1660 (C=O), 3217 (NH), 3331 (NH), 3445 (NH); ^{1}H NMR (500 MHz, DMSO-d_6) δ 5.80 (br, 2H; NH$_2$), 6.98 (d, J = 8.0 Hz, 1H; Ar), 7.04 (d, J = 8.6 Hz, 2H; Ar), 7.13 (s, 1H; Ar), 7.16 (d, J = 8.0 Hz, 1H; Ar), 7.34 (t, J = 8.0 Hz, 1H; Ar), 7.37 (d, J = 8.6 Hz, 2H; Ar), 8.28 (br, 1H; NH), 8.44 (s, 1H; NH); ^{13}C NMR (125 MHz, DMSO-d_6) δ 110.0, 113.8, 117.5, 119.2 (2C), 120.7 (2C), 124.4 (q), 130.0 (q), 130.2, 135.2, 135.4, 146.1, 156.1; HRMS (FAB): m/z calcd for $C_{14}H_{12}F_3N_3O$ (M$^+$) 295.0932; found: 295.0932.

7-{[3-(Trifluoromethyl)phenyl]amino}-3,4-dihydroquinoline-2(1*H*)-one **(8a).**
Following the general procedure for **6a**, compound **8a** (1.27 g, 63% yield) was synthesized from 7-bromo-3,4-dihydroquinolin-2(1*H*)-one and 3-(trifluoromethyl)aniline: white solid; mp 164–165 °C; IR (neat) cm^{-1}: 1675 (C=O), 3219 (NH), 3338 (NH); ^{1}H NMR (500 MHz, DMSO-d_6) δ 2.44 (t, J = 7.4 Hz, 2H; CH$_2$), 2.81 (t, J = 7.4 Hz, 2H; CH$_2$), 6.67 (dd, J = 8.0, 2.3 Hz, 1H; Ar), 6.71 (d, J = 2.3 Hz, 1H; Ar), 7.05–7.08 (m, 2H; Ar), 7.24 (s, 1H; Ar), 7.27 (d, J = 8.0 Hz, 1H; Ar), 7.41 (t, J = 8.0 Hz, 1H; Ar), 8.48 (s, 1H; NH), 10.04 (s, 1H; NH); ^{13}C NMR (125 MHz, DMSO-d_6) δ 24.2, 30.7, 105.1, 111.4, 112.0, 114.9, 116.4, 118.8, 124.3 (q), 129.6, 130.0 (q), 130.2, 139.1, 141.0, 144.8, 170.2; *Anal.* calcd for C$_{16}$H$_{13}$F$_3$N$_2$O: C, 62.74; H, 4.28; N, 9.15. Found: C, 62.47; H, 3.98; N, 9.14.

KSP ATPase Assay
The microtubules-stimulated KSP ATPase assay was performed as described in Chapter 1.

Growth Inhibition Assay
A549 cells were cultured in Dulbecco's modified Eagle's medium (DMEM; Sigma) supplemented with 10% (v/v) fetal bovine serum at 37 °C in a 5% CO$_2$-incubator. Growth inhibition assays using A549 cells were performed in 96-well plates (BD Falcon). A549 cells were seeded at 500 cells/well in 50 μL of DMEM, and were cultured for 6 h. Chemical compounds in DMSO were diluted 250-fold with the culture medium in advance. Following the addition of 40 μL of the fresh culture medium to the cell cultures, 30 μL of the chemical diluents were also added. The final volume of DMSO in the medium was equal to 0.1% (v/v). The cells under chemical treatment were incubated for further 72 h. The wells in the plates were washed twice with the cultured medium without phenol-red. After 1 h incubation with 100 μL of the medium, the cell culture in each well was supplemented with 20 μL of the MTS reagent (Promega), followed by incubation for an additional 40 min. Absorbance at 490 nm of each well was measured using a Wallac 1420 ARVO SX multilabel counter (Perkin Elmer). At least three experiments were performed per condition and the averages and standard deviations of inhibition rates in each condition were evaluated to determine IC$_{50}$ values using the GraphPad Prism software.

Thermodynamic Solubility in Aqueous Solution
An equal volume of a mixture of 1/15 M phosphate buffer (pH 7.4, 0.5 mL) and EtOH

(0.5 mL), or 1/15 M phosphate buffer (pH 7.4, 1.0 mL) was added to a compound in a vial. The suspension was then shaken for 48 h at 25 °C, and undissolved material was separated by filtration. *m*-Cresol was added as an internal standard (final concentration: 0.05 mg/mL) and the mixture was diluted in DMF and injected onto the HPLC column. The peak area ratio of the sample to the standard was recorded by UV detection at 254 nm. The concentration of the sample solution was calculated using a previously determined calibration curve, corrected for the dilution factor of the sample.

Crystallography

The data of **2** ($C_{16}H_{12}F_3NO$) was collected with a Rigaku R-AXIS RAPID diffractometer using graphite monochromated Mo-Kα radiation at -180 °C. The substance was crystallized from Et$_2$O and solved in C-centered monoclinic space group *C2/c* with $Z = 8$. The unit cell dimensions are $a = 19.133(2)$, $b = 11.3254(6)$, $c = 15.2117(9)$ Å, $\beta = 128.273(9)°$, $V = 2587.8(5)$ Å^3, $D_{calc} = 1.495$ g/cm^3, Mw: 291.27. $R = 0.0491$, GOF = 1.001.

The data of **4a**·1/2EtOH·1/4H$_2$O ($C_{17}H_{14.5}F_3N_2O_{1.75}$) was collected with a Rigaku R-AXIS RAPID diffractometer using multi-layer mirror monochromated Cu-Kα radiation at -180 °C. The substance was crystallized from EtOH and solved in primitive triclinic space group *P-1* with $Z = 8$. The unit cell dimensions are $a = 8.6132(2)$, $b = 16.1152(3)$, $c = 22.3470(4)$ Å, $\alpha = 92.163(7)$, $\beta = 96.975(7)$, $\gamma = 104.059(8)°$, $V = 2979.4(2)$ Å^3, $D_{calc} = 1.479$ g/cm^3, Mw: 331.81. $R = 0.0512$, GOF = 1.451.

The data of **8b** ($C_{16}H_{13}F_3N_2O$) was collected with a Rigaku R-AXIS RAPID diffractometer using graphite monochromated Mo-Kα radiation at -180 °C. The substance was crystallized from EtOAc and solved in primitive monoclinic space group *P2$_{1/C}$* with $Z = 4$. The unit cell dimensions are $a = 11.212(4)$, $b = 15.181(5)$, $c = 8.307(3)$ Å, $\beta = 95.31(1)°$, $V = 1407.9(8)$ Å^3, $D_{calc} = 1.445$ g/cm^3, Mw: 306.29. $R = 0.0640$, GOF = 1.676.

Calculation of Crystal Packing Energies

A virtual crystal model which reproduces the periodic lattice and contains compound molecules within 40 Å from one unit cell was constructed based on the crystal structure of each compound. As a packing energy, the interaction energy between one molecule in the cell and other molecules in the model was calculated by the MMFF94x forcefield. For compound **4a**, which exists as four independent molecules in the asymmetric unit, the averaged interaction energy of the four molecules was calculated.

Table 7. Crystal packing energies of four carbazole molecules of **4a** in different environments in a unit cell

compound **4a**[a]	crystal packing energy (kcal/mol)	van der Waals energy (kcal/mol)	electrostatic energy (kcal/mol)
carbazole **4a**-1	–59.2	–30.7	–28.5
carbazole **4a**-2	–55.2	–30.9	–24.3
carbazole **4a**-3	–57.5	–32.7	–24.8
carbazole **4a**-4	–63.0	–33.0	–30.0

[a]Carbazoles **4a**-1–**4a**-4 correspond to Figure 4C–F.

Kinase selectivity profile

Panel profiling was conducted using Merck Millipore's KinaseProfiler service. The inhibitory activities for 117 kinases were measured as percentage inhibition in the presence of β-carboline **3a**, carbazole **4a** or diphenylamine **8b**. The typical inhibitory effects caused by 10 μM of **3a**, **4a** or **8b** are shown in Table 5 ($n = 2$). Compounds **3a**, **4a** and **8b** did not inhibit kinases other than listed in Table 5.

Kinases (117): Abl, Abl(T315I), ALK, Arg, AMPKα1, ASK1, Aurora-A, Axl, Blk, Bmx, BTK, CaMKI, CaMKIIβ, CaMKIV, CDK1/cyclinB, CDK2/cyclinA, CDK2/cyclinE, CDK3/cyclinE, CDK5/p35, CDK6/cyclinD3, CDK7/cyclinH/MAT1, CDK9/cyclinT1, CHK1, CHK2, CK1γ1, CK1δ, CK1, CK2, CK2α2, CSK, c-RAF, cSRC, DRAK1, eEF-2K, EGFR, EphA5, EphB2, EphB4, Fes, FGFR3, Flt3, Fms, Fyn, GSK3β, IGF-1R, IKKα, IKKβ, IRAK4, JAK2, JNK1α1, JNK2α2, JNK3, KDR, Lck, LOK, Lyn, MAPK1, MAPK2, MAPKAP-K2, MEK1, Met, MKK4, MKK6, MKK7β, MLK1, Mnk2, MSK1, MSK2, MST1, MST2, mTOR, NEK2, p70S6K, PAK2, PAR-1Bα, PDGFRα, PDGFRβ, PDK1, Pim-1, PKA, PKBα, PKBβ, PKBγ, PKCα, PKCβII, PKCγ, PKCδ, PKCε, PKCη, PKCι, PKCμ, PKCθ, PKCζ, PKD2, PKG1α, Plk3, PRAK, PRK2, ROCK-I, ROCK-II, Ros, Rse, Rsk1, Rsk2, Rsk3, SAPK2a, SAPK2b, SAPK3, SAPK4, SGK, SRPK1, Syk, TAK1, Tie2, Yes, ZAP-70.

References and Footnotes

(1) Takeuchi, T.; Oishi, S.; Watanabe, T.; Ohno, H.; Sawada, J.; Matsuno, K.; Asai, A.; Asada, N.; Kitaura, K.; Fujii, N. *J. Med. Chem.* **2011**, *54*, 4839–4846.

(2) (a) Ding, S.; Nishizawa, K.; Kobayashi, T.; Oishi, S.; Lv, J.; Fujii, N.; Ogawa, O.; Nishiyama, H. *J. Urol.* **2010**, *15*, 314–318. (b) Xing, N. D.; Ding, S. T.; Saito, R.; Nishizawa, K.; Kobayashi, T.; Inoue, T.; Oishi, S.; Fujii, N.; Lv, J. J.; Ogawa, O.; Nishiyama, H. *Asian J. Androl.* **2011**, *13*, 236–241.

(3) For a recent review, see: Ishikawa, M.; Hashimoto, Y. *J. Med. Chem.* **2011**, *54*, 1539–1554.

(4) (a) Milbank, J. B. J.; Tercel, M.; Atwell, G. J.; Wilson, W. R.; Hogg, A.; Denny, W. A. *J. Med. Chem.* **1999**, *42*, 649–658. (b) Xie, L.; Yu, D.; Wild, C.; Allaway, G.; Turpin, J.; Smith, P. C.; Lee, K. *J. Med. Chem.* **2004**, *47*, 756–760. (c) Kim, I. H.; Morisseau, C.; Watanabe, T.; Hammock, B. D. *J. Med. Chem.* **2004**, *47*, 2110–2122.

(5) Anderson, K. W.; Tundel, R. E.; Ikawa, T.; Altman, R. A.; Buchwald, S. L. *Angew. Chem., Int. Ed.* **2006**, *45*, 6523–6527.

(6) (a) Song, Y.; Wang, J.; Teng, S. F.; Kesuma, D.; Deng, Y.; Duan, J.; Wang, J. H.; Qi, R. Z.; Sim, M. M. *Bioorg. Med. Chem. Lett*. **2002**, *12*, 1129–1132. (b) Xin, B.; Tang, W.; Wang, Y.; Lin, G.; Liu, H.; Jiao, Y.; Zhu, Y.; Yuan, H.; Chen, Y.; Lu, T. *Bioorg. Med. Chem. Lett*. **2012**, *22*, 4783–4786.

(7) Avdeef, A.; Testa, B. *Cell Mol. Life Sci.* **2002**, *59*, 1681–1689.

(8) Jain, N.; Yalkowsky, S. H. *J. Pharm. Sci.* **2001**, *90*, 234–252.

(9) (a) Scott, J. S.; Birch, A. M.; Brocklehurst, K. J.; Broo, A.; Brown, H. S.; Butlin, R. J.; Clarke, D. S.; Davidsson, Ö.; Ertan, A.; Goldberg, K.; Groombridge, S. D.; Hudson, J. A.; Laber, D.; Leach, A. G.; MacFaul, P. A.; McKerrecher, D.; Pickup, A.; Schofield, P.; Svensson, P. H.; Sorme, P.; Teague, J. *J. Med. Chem.* **2012**, *55*, 5361–5379. (b) Wenglowsky, S.; Moreno, D.; Rudolph, J.; Ran, Y.; Ahrendt, K. A.; Arrigo, A.; Colson, B.; Gloor, S. L.; Hastings, G. *Bioorg. Med. Chem. Lett*. **2012**, *22*, 912–915.

(10) The single crystals of carbazole **4a** were easily collapsed to give amorphous powder. The solubility of this single crystal was identical (0.423 mg/mL in 50% EtOH, <0.001 mg/mL in phosphate buffer) to that of the powder form.

(11) The charged form of diphenylamine **8b** in solution was not considered because the pK_a value of protonated diphenylamine was reported to be 0.78, see: Dolman, D.; Stewart, R. *Can. J. Chem.* **1967**, *45*, 903–910.

Chapter 2.   Development of Novel Kinesin Spindle Protein Inhibitors with Diaryl Amine Scaffolds

Section 2.   Optimization Studies of Diaryl Amine Derivatives as Kinesin Spindle Protein Inhibitors

In this section, the author describes the optimization of diaryl amine-type KSP inhibitors by the structure–activity relationship studies. The aniline NH group and 3-CF$_3$ phenyl group were indispensable for potent KSP inhibition. Substitution with a seven-membered lactam-fused phenyl group and a 4-(trifluoromethyl)pyridin-2-yl group improved aqueous solubility while maintaining potent KSP inhibitory activity. From these studies, the author identified diaryl amine derivatives with a favorable balance of potency and solubility. Kinetic analysis and molecular modeling studies suggested that diaryl amine-type inhibitors work in an ATP-competitive manner via binding to the secondary allosteric site formed by the α4 and α6 helices of KSP.

As described in section 1, the author identified novel KSP inhibitor **2a** (= **8b** in section 1) with a diphenylamine scaffold by modification of planar ring-fused indoles such as carbazole **1** (Figure 1). Diphenylamine **2a** exhibits highly potent KSP inhibitory activity and four times better solubility in 50% EtOH than carbazole **1**. However, the aqueous solubility of diphenylamine **2a** was still not enough to be employed for in vivo studies (solubility in phosphate buffer < 1 μg/mL). In this section, the author describes optimization studies of diphenylamine **2a** to develop novel KSP inhibitors with high potency and improved aqueous solubility.

The author planned to investigate the structure–activity relationship and the further refinement of **2a** for novel potent KSP inhibitors in terms of: (i) the linkage
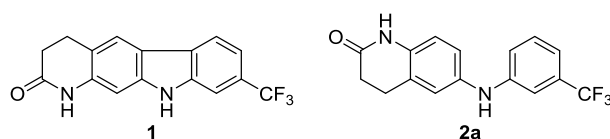

Figure 1. Structures of carbazole-type (**1**) and diphenylamine-type (**2a**) KSP inhibitors.
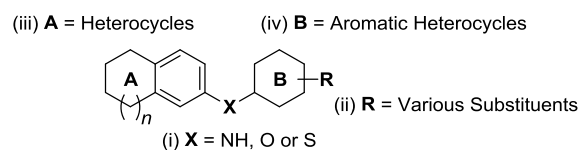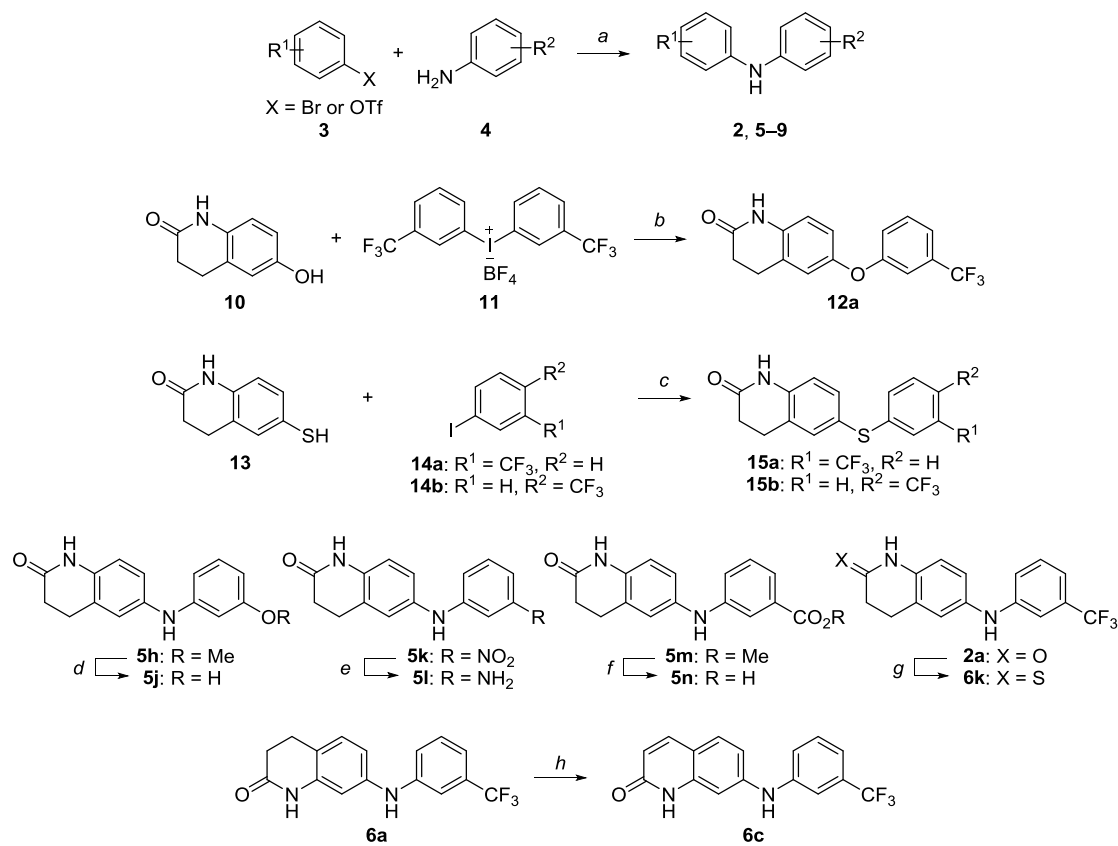

Figure 2. Strategy for the structure–activity relationship study of diaryl amine-type KSP inhibitors.
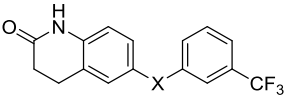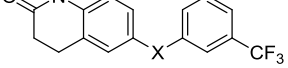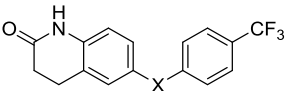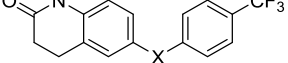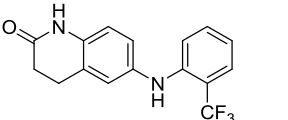
Scheme 1. Synthesis of diaryl amine derivatives. *Reagents and conditions*: (a) Pd$_2$(dba)$_3$, biaryl phosphine ligand, NaOt-Bu, toluene, 100 °C; (b) KOt-Bu, DMF, 40 °C; (c) CuI, ethylene glycol, K$_2$CO$_3$, 2-propanol, 80 °C; (d) BBr$_3$, CH$_2$Cl$_2$, rt; (e) Zn, AcOH, rt; (f) LiOH·H$_2$O, MeOH, H$_2$O, 50 °C; (g) Lawesson's reagent, toluene, reflux; (h) Pd(OAc)$_2$, O$_2$, AcOH, 115 °C.

between the two aryl groups, (ii) the substituent on the right-hand phenyl group, (iii) the left-hand heterocycle, and (iv) the right-hand aromatic heterocycle (Figure 2).

A series of diaryl amine derivatives **2** and **5–9** were prepared by Buchwald–Hartwig *N*-arylation using aryl bromides or triflates **3** and substituted anilines **4**, except for the compounds (**5j,l,n** and **6c,k**) indicated below (Scheme 1).[1] Diphenylether derivative **12a** was obtained by treatment of phenol derivative **10** with diaryliodonium tetrafluoroborate **11**[2] in the presence of KOt-Bu.[3] Diphenylsulfide derivatives **15a,b** were prepared by the copper-catalyzed C–S bond-forming reaction using aryl thiol **13** and CF$_3$-substituted iodobenzenes **14a,b**.[4] Compounds **5j, 5l, 5n** and **6k** were obtained by simple transformations including BBr$_3$-mediated demethylation of **5h**, Zn-mediated reduction of **5k**, saponification of **5m**, and thiocarbonylation of **2a** using Lawesson's reagent,[5] respectively. Compound **6c** was prepared by treatment of **6a** (= **8a** in section 1) with O$_2$ in the presence of Pd(OAc)$_2$.

Table 1. KSP inhibitory activities of dihydroquinolinone derivatives

compound		X	KSP ATPase IC$_{50}$ (μM)^{a,b}
	2a	NH	0.045
	12a	O	2.0
	15a	S	>6.3
	2b	NH	0.33
	12b	O	>6.3
	15b	S	>6.3
	2c		>6.3

^{a}Inhibition of microtubule-activated KSP ATPase activity. ^{b}IC$_{50}$ values were derived from the dose–response curves generated from triplicate data points.

The author initially investigated the type of hetero atom in the central part of diphenylamine **2a** and the position of a substituent on the right-hand phenyl group (Table 1). Replacing the bridging NH group in compound **2a** with oxygen (**12a,b**: ether) or sulfur (**15a,b**: thioether) resulted in a significant reduction or loss of KSP inhibitory activity, indicating that the aniline NH group was an indispensable functional group as a hydrogen-bond donor. Regarding the position of CF$_3$ group on the right-hand phenyl ring of **2a**, 4-CF$_3$ compound **2b** was approximately 7 times less potent than **2a** and no KSP inhibition of 2-CF$_3$ compound **2c** was observed.

Next, the structure–activity relationship was examined by replacing 3-substituents on the right-hand phenyl group in **2a** (Table 2). Among compounds **5a–d** with a 3-alkyl substituent, the *tert*-butyl derivative **5d** exhibited the most potent inhibitory activity (IC$_{50}$ = 0.16 μM). The structure–activity relationship of the simple alkyl group correlated with that of the carbazole-type KSP inhibitors, suggesting that carbazoles and diphenylamine **2a** may occupy the same binding site of KSP.[6] Substitution with 3,5-di-CF$_3$ (**5e**), 3-phenyl (**5f**), 3-phenoxy (**5g**) and 3-methoxy (**5h**) groups were not effective. Introduction of a polar substituent such as 3-hydroxy (**5j**), 3-amino (**5l**), 3-methoxycarbonyl (**5m**), or 3-carboxylate (**5n**) also gave rise to inactive compounds. 3-Trifluoromethyloxy (**5i**) and 3-nitro (**5k**) derivatives showed moderate

Table 2. KSP inhibitory activities of diphenylamines with a 3-substituent or 3,5-substituents on the right-hand phenyl group
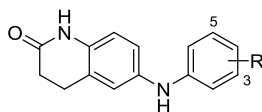
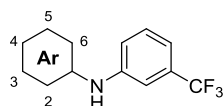| R		KSP ATPase IC$_{50}$ (μM)^{a,b}	R		KSP ATPase IC$_{50}$ (μM)^{a,b}
3-CF$_3$	**2a**	0.045	3-OMe	**5h**	>6.3
H	**5a**	>6.3	3-OCF$_3$	**5i**	1.2
3-Et	**5b**	0.81	3-OH	**5j**	>6.3
3-i-Pr	**5c**	0.43	3-NO$_2$	**5k**	0.44
3-t-Bu	**5d**	0.16	3-NH$_2$	**5l**	>6.3
3,5-di-CF$_3$	**5e**	>6.3	3-CO$_2$Me	**5m**	>6.3
3-Ph	**5f**	>6.3	3-CO$_2$H	**5n**	>6.3
3-OPh	**5g**	>6.3			

^{a}Inhibition of microtubule-activated KSP ATPase activity. ^{b}IC$_{50}$ values were derived from the dose–response curves generated from triplicate data points.

inhibitory activity. It is inferred from these data that the substituent at the 3-position on the right-hand phenyl part is buried in a relatively large hydrophobic pocket of KSP.

In the left part of the molecule, the position of accessory amide group was crucial for the potency (Table 3). Compounds **6a–d** with an amide group at the 3-position were less active or inactive, while the parent compound **2a** with the 4-position amide group showed potent KSP inhibitory activity. A five-membered ring thiocarbamate **6g** exhibited moderate inhibitory activity (IC$_{50}$ = 0.81 μM) in contrast to the ineffectiveness in lactam derivative **6e** and carbamate derivative **6f**, suggesting that the introduction of a sulfur atom into the lactam ring had favorable effects on the bioactivity. The addition of a sulfur atom (**6i**) into the six-membered lactam of **2a** also maintained potent KSP inhibitory activity (IC$_{50}$ = 0.051 μM), whereas an oxygen atom (**6h**) decreased the inhibitory activity. The loss of activity in the N-methylamide derivative **6j** indicates that the lactam NH group at this position is essential for KSP inhibition. Compound **6k**, with a thioamide group, had slightly reduced potency (IC$_{50}$ = 0.19 μM) compared with **2a**. Compound **6l**, with a seven-membered lactam, showed approximately equipotent KSP inhibitory activity (IC$_{50}$ = 0.050 μM) to **2a**, suggesting that some flexibility of the lactam carbonyl placement is tolerated. Substitution with a fluorine group on the 5- or 6-position (**6m,n**) resulted in a reduction in the inhibitory

activity, suggesting that modification at these positions was inappropriate for favorable interactions with KSP.
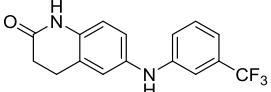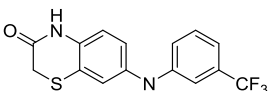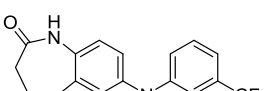
Table 3. KSP inhibitory activities of diphenylamines with a heterocycle on the left-hand phenyl group

Ar	KSP ATPase IC$_{50}$ (µM)^{a,b}	Ar	KSP ATPase IC$_{50}$ (µM)^{a,b}
2a	0.045	**6h**	0.29
6a	>6.3	**6i**	0.051
6b	>6.3	**6j**	>6.3
6c	4.6	**6k**	0.19
6d	>6.3	**6l**	0.050
6e	3.6	**6m**	0.43
6f	>6.3	**6n**	0.92
6g	0.81		

^{a}Inhibition of microtubule-activated KSP ATPase activity. ^{b}IC$_{50}$ values were derived from the dose–response curves generated from triplicate data points.

Table 4. KSP inhibitory activities and physicochemical properties of diphenylamines **2a** and **6i,l** with a heterocycle on the left-hand phenyl group

compound		KSP ATPase IC_{50} $(\mu M)^{a,b}$	solubility $(mg/mL)^c$	melting point (°C)	ClogP^d	HPLC retention time $(min)^e$
	2a	0.045	1.80	190	4.2	24.4
	6i	0.051	1.70	166	4.0	28.2
	6l	0.050	7.39	140	4.4	27.0

^{a}Inhibition of microtubule-activated KSP ATPase activity. ^{b}IC$_{50}$ values were derived from the dose–response curves generated from triplicate data points. ^{c}Solubility in 50% EtOH [an equal volume of EtOH and 1/15 M phosphate buffer (pH 7.4)]. ^{d}CLogP values were calculated with ChemBioDraw Ultra 12.0. ^{e}HPLC analysis was carried out on a Cosmosil 5C18-ARII column (4.6 × 250 mm) and the material eluted by a linear MeCN gradient (70:30 to 30:70 over 40 min) in 0.1% TFA; flow rate of 1 mL/min.

The thermodynamic solubility of potent diphenylamine derivatives **6i,l** in aqueous media was next evaluated (Table 4). Diphenylamine **6i** with a thiomorpholin-3-one structure was slightly less soluble (1.70 mg/mL in 50% EtOH) than the parent compound **2a**. The larger retention time on a reversed-phase HPLC column (28.2 min) of compound **6i** indicated that the introduction of a sulfur atom into the lactam ring of **2a** resulted in the increased hydrophobicity, thereby lowering the solubility in aqueous media. Interestingly, diphenylamine **6l** with a seven-membered lactam ring was approximately four times more soluble (7.39 mg/mL in 50% EtOH) than **2a**, although a high CLogP value and HPLC retention time suggested higher hydrophobicity. The lower melting point of compound **6l** (140 °C) suggested that the low energy of the crystal packing from van der Waals interactions mainly contributed to the observed improvement in solubility because the contribution of the electrostatic interactions seemed to be comparable to **2a**. These results indicated that the seven-membered lactam ring on the left-hand phenyl group was a promising structural unit for the development of KSP inhibitors that have a favorable balance of bioactivity and aqueous solubility.
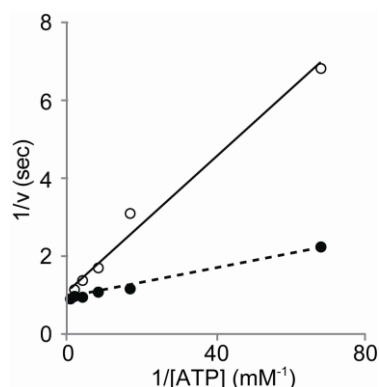
Figure 3. Lineweaver–Burk plots of the kinetics of KSP ATPase. KSP ATPase activity was measured by a steady-state ATPase assay as a function of ATP concentration in the absence (closed circle) and presence (open circle) of lactam-fused diphenylamine **2a** (48 nM) [80 nM KSP motor domain; 400 nM microtubules].

To estimate the possible binding pocket of the diaryl amine-type inhibitor **2a**, kinetic experiments of KSP ATPase were conducted as a function of ATP concentration in the absence or presence of **2a** (Figure 3). Lineweaver–Burk plots revealed that the maximum velocity (V_{max}) value in the presence of **2a** was identical to that in the absence of **2a**. This suggested that diphenylamine **2a** inhibited KSP ATPase activity in an ATP-competitive manner as observed for biphenyl-type, β-carboline-type and carbazole-type (**1**) inhibitors in chapter 1,[7] possibly by binding to the ATP binding site or the α4/α6 allosteric site.

To provide insights into the binding site of diaryl amine-type KSP inhibitors, possible interactions of diphenylamine **2a** to three possible binding sites (i.e., the ATP binding site, the α2/α3/L5 allosteric site and the α4/α6 allosteric site; see the text in Preface) were estimated by a simulated docking study using the MM/GBVI method. The predicted binding affinity (E_{bind}) of **2a** to the α4/α6 allosteric site (−24.7 kcal/mol) was higher than the values computed to the other sites (−20.3 kcal/mol for the ATP binding site; −19.7 kcal/mol for the α2/α3/L5 allosteric site). In addition, the high selectivity of **2a** for KSP compared with any other kinesins and kinases also supports the unlikely affinity to the ATP binding pocket, which is highly conserved among kinesins.[8]

The predicted docking pose of diphenylamine **2a** in the pocket formed by helices α4 and α6 is shown in Figure 4. Compound **2a** exhibited a twisted conformation of the two aryl groups, which were buried in the pocket. The aniline NH group forms a strong hydrogen bond with the backbone carbonyl oxygen of Leu292. The 3-trifluoromethyl group interacts with a large hydrophobic pocket formed by Tyr104, Ile299, Thr300, Ile332, Tyr352, Ala353 and Ala356 through van der Waals interactions.
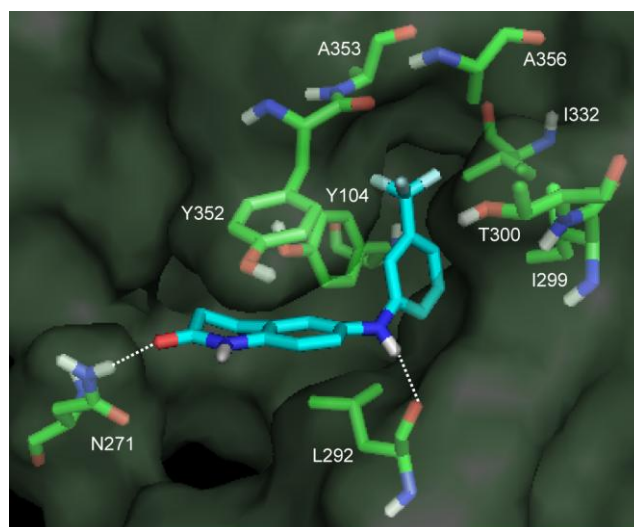
67

Figure 4. Docking mode of diphenylamine **2a** at the interface of helices α4 and α6.

A possible π–π stacking interaction between the trifluoromethylphenyl group in **2a** and the Tyr104 side chain was also observed. The lactam carbonyl group in **2a** forms a hydrogen bond with the side chain amide NH_2 group of Asn271. In addition, the lactam-fused phenyl group is likely to form a π–π interaction with the Tyr352 side chain. Combined with the structure–activity relationships of a series of compounds, two hydrogen bonds from the aniline NH and lactam carbonyl groups, and van der Waals interactions from the trifluoromethyl group particularly define the potency of the KSP inhibition of **2a**. This is supported by the findings that these three interactions are indispensable for potent KSP inhibitory activity. For example, diphenylsulfide **15a** without the central NH group, compound **6a** with a lactam amide group at an inappropriate position, and compound **5a** without the bulky hydrophobic group showed no KSP inhibitory activity.

Given the binding mode of diphenylamine-type KSP inhibitors, further optimization from diphenylamine **2a** was attempted for novel KSP inhibitors with more potent bioactivity and favorable properties. Since the left-hand lactam-fused phenyl group plays a pivotal role in KSP inhibition, replacement of the right-hand 3-CF_3-phenyl group with aromatic nitrogen heterocycles (**7a–e**) was examined (Table 5). 5-Pyridine **7c** and pyrazine derivatives **7e** with a nitrogen at the 5-position decreased the potency for KSP inhibition [IC_{50}(**7c**) = 0.71 μM; IC_{50}(**7e**) = 1.9 μM]. 2-Pyridine **7a** and pyrimidine derivatives **7d** also showed moderate inhibitory activity [IC_{50}(**7a**) = 0.41 μM; IC_{50}(**7d**) = 0.10 μM]. This suggests that the nitrogen atoms at these positions prevented the key hydrophobic interactions with the hydrophobic pocket of KSP. On the

Table 5. KSP inhibitory activities and thermodynamic solubility of diaryl amines with a right-hand aromatic heterocycle

Ar		KSP ATPase IC$_{50}$ (μM)^{a,b}	solubility	
			50% EtOH^c (mg/mL)	phosphate buffer (pH 7.4) (μg/mL)
	2a	0.045	1.80	<1
	7a	0.41	3.64	3.08
	7b	0.068	3.51	6.12
	7c	0.71	4.78	6.15
	7d	0.10	0.458	1.53
	7e	1.9	0.276	1.49

^{a}Inhibition of microtubule-activated KSP ATPase activity. ^{b}IC$_{50}$ values were derived from the dose–response curves generated from triplicate data points. ^{c}Solubility in an equal volume of EtOH and 1/15 M phosphate buffer (pH 7.4).

other hand, 6-pyridine **7b** retained the highly potent KSP inhibitory activity seen for the parent **2a** [IC$_{50}$(**7b**) = 0.068 μM].

The aqueous solubility of pyridine derivatives **7a–c** was significantly improved, as anticipated. Compound **7b** was approximately twice as soluble in 50% EtOH and more than six times as soluble in phosphate buffer compared with **2a**. In contrast, pyrimidine **7d** and pyrazine derivatives **7e** were less soluble in 50% EtOH and phosphate buffer compared with pyridine derivatives **7a–c**. This is partly because of the lower basicity of pyrimidine or pyrazine compared with that of pyridine. From these results, compound **7b** was identified to be a novel KSP inhibitor with potent bioactivity and improved aqueous solubility.
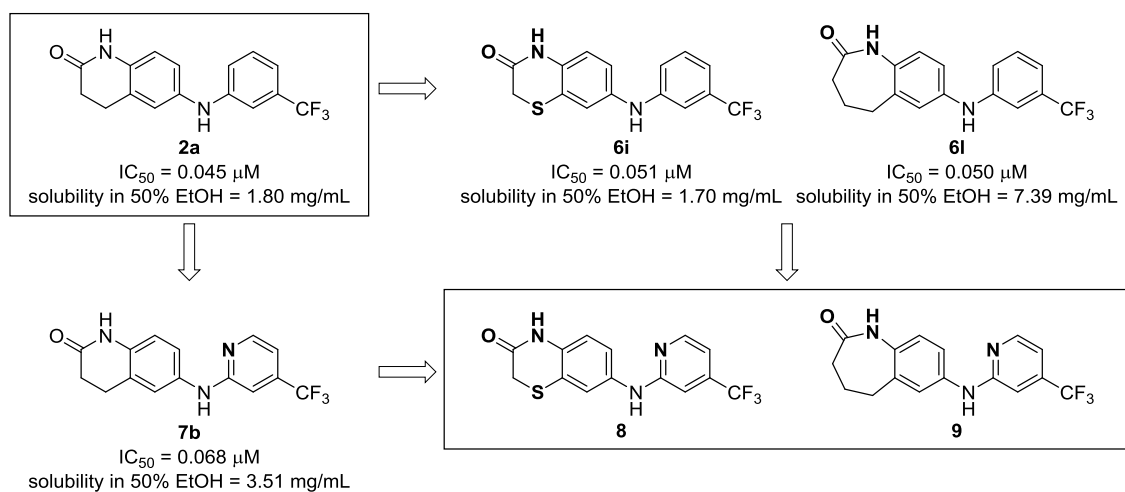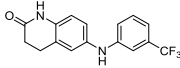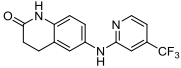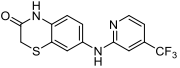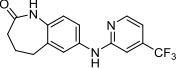
Figure 5. Design of novel diaryl amine-type KSP inhibitors **8** and **9**.

As such, the author identified benzothiomorpholin-3-one **6i** and benzoazepin-2-one **6l** as potent KSP inhibitors using structure–activity relationship studies of fused heterocycles on the left-hand phenyl group. Compound **6l** represents the lead compound for further structural refinements because of the improved solubility. Separately, examination of the right-hand phenyl group identified 6-pyridine derivative **7b** with potent KSP inhibitory activity and improved aqueous solubility. On the basis of these promising components, two diaryl amine derivatives were then designed (Figure 5). Diaryl amine **8** was designed based on compound **6i** with a thiomorpholin-3-one structure and compound **7b** with a 6-pyridine ring. Diaryl amine **9** was similarly designed based on compounds **6l** and **7b**.

Thiomorpholin-3-one **8** exhibited the most potent KSP inhibitory activity (IC_{50} = 0.035 μM) among the diaryl amine-type inhibitors that were examined in this study (Table 6). However, compound **8** was less soluble in 50% EtOH (0.669 mg/mL) and in phosphate buffer (1.11 μg/mL) than the parent compound **7b**. The high melting point of compound **8** (217 °C) indicated that the tight crystal packing might cause this decrease in aqueous solubility. Benzoazepin-2-one **9** maintained highly potent KSP inhibitory activity (IC_{50} = 0.050 μM) as seen for the parent compounds **2a**, **6l** and **7b**. Compound **9** exhibited greater solubility in 50% EtOH (4.82 mg/mL) and in phosphate buffer (8.07 μg/mL) than the corresponding compound **7b**. Taken together, compound **9** was identified to be a novel KSP inhibitor with a favorable balance of potency and aqueous solubility.

Compounds **2a**, **6i,l**, **7b**, **8** and **9** were tested for their inhibitory effect on the proliferation of cancer cell lines: lung cancer cells A549, colorectal cancer cells

Table 6. KSP inhibitory activities and physicochemical properties of diaryl amine derivatives **2a**, **7b**, **8** and **9**

	2a	7b	8	9
KSP ATPase IC$_{50}$ (μM)^{a,b}	0.045	0.068	0.035	0.050
solubility in 50% EtOH (mg/mL)^c	1.80	3.51	0.669	4.82
solubility in phosphate buffer (pH 7.4) (μg/mL)	<1	6.12	1.11	8.07
melting point (°C)	190	177	217	185
ClogP^d	4.2	3.4	3.2	3.6
HPLC retention time (min)^e	24.4	7.0	13.8	10.8

^{a}Inhibition of microtubule-activated KSP ATPase activity. ^{b}IC$_{50}$ values were derived from the dose–response curves generated from triplicate data points. ^{c}Solubility in 50% EtOH [an equal volume of EtOH and 1/15 M phosphate buffer (pH 7.4)]. ^{d}CLogP values were calculated with ChemBioDraw Ultra 12.0. ^{e}HPLC analysis was carried out on a Cosmosil 5C18-ARII column (4.6 × 250 mm) and the material eluted by a linear MeCN gradient (70:30 to 30:70 over 40 min) in 0.1% TFA; flow rate of 1 mL/min.

HCT-116, and breast cancer cells MCF-7 (Table 7). Cells were treated with increasing concentrations of the compounds, and viabilities were measured by the 3-(4,5-dimethylthiazol-2-yl)-5-(3-carboxymethoxyphenyl)-2-(4-sulfophenyl)-2*H*-tetrazolium (MTS) assay. All the tested diaryl amine derivatives were shown to be effective against these cell lines. In particular, thiomorpholin-3-one derivative **8** with the highest KSP inhibitory activity was found to be the most potent against all the cell lines tested.

Table 7. Inhibitory effects on cell proliferation of diaryl amine-type KSP inhibitors toward A549, HCT-116 and MCF-7

compound	IC$_{50}$ (μM)^a		
	A549	HCT-116	MCF-7
2a	4.2	8.9	11
6i	4.1	6.8	6.5
6l	4.5	5.7	3.9
7b	2.5	4.4	8.0
8	1.5	2.6	2.8
9	5.0	6.5	9.1

^{a}IC$_{50}$ values were derived from the dose–response curves generated from triplicate data points.

In conclusion, the author has carried out intensive structure–activity relationship studies from diphenylamine derivative **2a** for development of novel KSP inhibitors. The bridging NH group, 3-CF$_3$ group on the right-hand phenyl group, and the lactam amide group at 4-position on the left-hand phenyl group contribute to the potent KSP inhibitory activity. The kinetic analysis of KSP ATPase activity and molecular modeling studies suggested that diphenylamine **2a** binds to the interface of α4 and α6 via van der Waals interactions and two hydrogen bonds, working as an ATP-competitive inhibitor. Investigation into the right-hand CF$_3$-phenyl group in **2a** provided a potent and more soluble KSP inhibitor **7b** with a pyridinylamine moiety. The further optimization studies provided a novel KSP inhibitor **9** with the best balance of potency and aqueous solubility in this study. These diaryl amine-type selective KSP inhibitors represent promising therapeutic candidates for cancer treatment.

General Methods. ^{1}H NMR spectra were recorded using a JEOL AL-400 a JEOL ECA-500 spectrometer. Chemical shifts are reported in δ (ppm) relative to Me$_4$Si as an internal standard. ^{13}C NMR spectra were referenced to the residual DMSO signal. Exact mass (HRMS) spectra were recorded on a JMS-HX/HX 110A mass spectrometer. Melting points were measured by a hot stage melting point apparatus (uncorrected). For flash chromatography, Wakogel C-300E (Wako) was employed. For analytical HPLC, a Cosmosil 5C18-ARII column (4.6 x 250 mm, Nacalai Tesque, Inc., Kyoto, Japan) was employed with a linear gradient of CH$_3$CN containing 0.1% (v/v) TFA at a flow rate of 1 mL/min on a Shimadzu LC-10ADvp (Shimadzu Corp., Ltd., Kyoto, Japan), and eluting products were detected by UV at 254 nm. The purity of the compounds was determined by combustion analysis or HPLC analysis (> 95%).

General Procedure of *N*-Arylation for Preparation of Diaryl Amine Compounds: Synthesis of 6-{[3-(Trifluoromethoxy)phenyl]amino}-3,4-dihydroquinolin-2(1*H*)-one (5i). Toluene (4.5 mL) was added to a flask containing 6-bromo-3,4-dihydro-quinolin-2(1*H*)-one (300 mg, 1.33 mmol), 3-(trifluoromethoxy)aniline (231 μL, 1.73 mmol), Pd$_2$(dba)$_3$ (15.2 mg, 0.02 mmol), 2-dicyclohexylphosphino-2′,4′,6′-triisopropyl-biphenyl (31.6 mg, 0.07 mmol) and NaO*t*-Bu (192 mg, 2.00 mmol) under an argon atmosphere. The mixture was stirred at 100 °C for 9 h. After cooling, the reaction mixture was diluted with EtOAc, and filtered through a pad of Celite. The filtrate was concentrated *in vacuo*. Crude material was purified by flash chromatography with *n*-hexane/EtOAc (2:3) to afford the desired diaryl amine **5i** (292 mg, 68% yield): pale yellow solid; mp 160–162 °C; IR (neat) cm^{-1}: 1667 (C=O), 3219 (NH), 3315 (NH); ^{1}H NMR (500 MHz, DMSO-d_6) δ 2.43 (t, *J* = 6.9 Hz, 2H; CH$_2$), 2.85 (t, *J* = 6.9 Hz, 2H; CH$_2$), 6.63 (d, *J* = 8.0 Hz, 1H; Ar), 6.79 (s, 1H; Ar), 6.81 (d, *J* = 8.0 Hz, 1H; Ar), 6.91–6.96 (m, 3H; Ar), 7.25 (t, *J* = 8.0 Hz, 1H; Ar), 8.25 (s, 1H; NH), 9.99 (s, 1H; NH); ^{13}C NMR (125 MHz, DMSO-d_6) δ 25.0, 30.4, 106.3, 109.6, 113.1, 115.8, 118.7, 119.5, 120.1 (q), 124.7, 130.7, 133.1, 136.1, 146.9, 149.4, 169.8; *Anal.* calcd for C$_{16}$H$_{13}$F$_3$N$_2$O$_2$: C, 59.63; H, 4.07; N, 8.69. Found: C, 59.51; H, 4.12; N, 8.59.

6-{[4-(Trifluoromethyl)phenyl]amino}-3,4-dihydroquinolin-2(1*H*)-one (2b). Follow-ing the general procedure for **5i**, compound **2b** (122 mg, 30% yield) was synthesized from 6-bromo-3,4-dihydroquinolin-2(1*H*)-one and 4-(trifluoromethyl)aniline: pale yellow solid; mp 293–294 °C; IR (neat) cm^{-1}: 1650 (C=O), 3320 (NH); ^{1}H NMR (500

MHz, DMSO-d_6) δ 2.43 (t, J = 7.4 Hz, 2H; CH$_2$), 2.86 (t, J = 7.4 Hz, 2H; CH$_2$), 6.83 (d, J = 8.6 Hz, 1H; Ar), 6.97 (dd, J = 8.6, 2.3 Hz, 1H; Ar), 6.99–7.02 (m, 3H; Ar), 7.46 (d, J = 8.6 Hz, 2H; Ar), 8.46 (s, 1H; NH), 10.02 (s, 1H; NH); ^{13}C NMR (125 MHz, DMSO-d_6) δ 25.0, 30.4, 113.6 (2C), 115.8, 117.5 (q), 119.5, 120.2, 124.6, 125.0 (q), 126.5 (2C), 133.5, 135.5, 148.6, 169.8; HRMS (FAB): m/z calcd for C$_{16}$H$_{13}$F$_3$N$_2$O (M$^+$) 306.0980; found: 306.0982.

6-{[2-(Trifluoromethyl)phenyl]amino}-3,4-dihydroquinolin-2(1H)-one (2c). Following the general procedure for **5i**, compound **2c** (104 mg, 26% yield) was synthesized from 6-bromo-3,4-dihydroquinolin-2(1H)-one and 2-(trifluoromethyl)aniline: pale yellow solid; mp 167–169 °C; IR (neat) cm^{-1}: 1671 (C=O), 3205 (NH), 3440 (NH); ^{1}H NMR (500 MHz, DMSO-d_6) δ 2.42 (t, J = 7.4 Hz, 2H; CH$_2$), 2.82 (t, J = 7.4 Hz, 2H; CH$_2$), 6.79 (d, J = 8.0 Hz, 1H; Ar), 6.91 (dd, J = 8.0, 2.3 Hz, 1H; Ar), 6.93–6.97 (m, 2H; Ar), 7.11 (d, J = 8.0 Hz, 1H; Ar), 7.22 (s, 1H; NH), 7.42 (t, J = 8.0 Hz, 1H; Ar), 7.56 (d, J = 8.0 Hz, 1H; Ar), 10.00 (s, 1H; NH); ^{13}C NMR (125 MHz, DMSO-d_6) δ 24.9, 30.4, 115.7, 116.6 (q), 118.6, 119.3, 120.0, 120.8, 124.5 (q), 124.5, 126.7, 133.2, 133.4, 136.8, 143.3, 169.8; HRMS (FAB): m/z calcd for C$_{16}$H$_{13}$F$_3$N$_2$O (M$^+$) 306.0980; found: 306.0982.

6-(Phenylamino)-3,4-dihydroquinolin-2(1H)-one (5a). Following the general procedure for **5i**, compound **5a** (57.5 mg, 20% yield) was synthesized from 6-bromo-3,4-dihydroquinolin-2(1H)-one and aniline: white solid; mp 156–158 °C; IR (neat) cm^{-1}: 1665 (C=O), 3216 (NH), 3310 (NH); ^{1}H NMR (500 MHz, DMSO-d_6) δ 2.41 (t, J = 7.4 Hz, 2H; CH$_2$), 2.82 (t, J = 7.4 Hz, 2H; CH$_2$), 6.73 (t, J = 8.0 Hz, 1H; Ar), 6.75 (d, J = 8.0 Hz, 1H; Ar), 6.87 (dd, J = 8.0, 2.3 Hz, 1H; Ar), 6.91 (d, J = 2.3 Hz, 1H; Ar), 6.95 (d, J = 8.0 Hz, 2H; Ar), 7.17 (t, J = 8.0 Hz, 2H; Ar), 7.88 (s, 1H; NH), 9.90 (s, 1H; NH). ^{13}C NMR (125 MHz, DMSO-d_6) δ 25.1, 30.5, 115.4 (2C), 115.7, 117.1, 117.9, 118.6, 124.5, 129.1 (2C), 131.8, 137.6, 144.5, 169.7; HRMS (FAB): calcd for C$_{15}$H$_{14}$N$_2$O (M$^+$) 238.1106; found: 238.1099.

6-[(3-Ethylphenyl)amino]-3,4-dihydroquinolin-2(1H)-one (5b). Following the general procedure for **5i**, compound **5b** (76.2 mg, 22% yield) was synthesized from 6-bromo-3,4-dihydroquinolin-2(1H)-one and 3-ethylaniline: white solid; mp 179–181 °C; IR (neat) cm^{-1}: 1665 (C=O), 3195 (NH), 3307 (NH); ^{1}H NMR (500 MHz, DMSO-d_6) δ 1.15 (t, J = 7.4 Hz, 3H; CH$_3$), 2.41 (t, J = 7.4 Hz, 2H; CH$_2$), 2.81 (t, J = 7.4 Hz, 2H; CH$_2$), 6.59 (d, J = 7.4 Hz, 1H; Ar), 6.75 (d, J = 8.0 Hz, 1H; Ar), 6.78 (d, J = 8.0

Hz, 1H; Ar), 6.79 (s, 1H; Ar), 6.87 (d, J = 8.0 Hz, 1H; Ar), 6.89 (s, 1H; Ar), 7.07 (t, J = 7.4 Hz, 1H; Ar), 7.82 (s, 1H; NH), 9.90 (s, 1H; NH). ^{13}C NMR (125 MHz, DMSO-d_6) δ 15.6, 25.1, 28.3, 30.5, 112.8, 115.1, 115.6, 116.9, 117.8, 118.3, 124.4, 129.0, 131.6, 137.8, 144.5, 144.6, 169.7; HRMS (FAB): calcd for $C_{17}H_{18}N_2O$ (M$^+$) 266.1419; found: 266.1419.

6-[(3-Isopropylphenyl)amino]-3,4-dihydroquinolin-2(1H)-one (5c): Following the general procedure for **5i**, compound **5c** (66.7 mg, 36% yield) was synthesized from 6-bromo-3,4-dihydroquinolin-2(1H)-one and 3-isopropylaniline: pale yellow solid; mp 180–181 °C; IR (neat) cm^{-1}: 1667 (C=O), 3192 (NH), 3311 (NH); ^{1}H NMR (500 MHz, DMSO-d_6); δ 1.17 (d, J = 6.9 Hz, 6H; CH$_3$ × 2), 2.41 (t, J = 7.4 Hz, 2H; CH$_2$), 2.74–2.83 (m, 1H; CH), 2.81 (t, J = 7.4 Hz, 2H; CH$_2$), 6.63 (d, J = 8.0 Hz, 1H; Ar), 6.75 (d, J = 8.0 Hz, 1H; Ar), 6.79 (d, J = 8.0 Hz, 1H; Ar), 6.82 (s, 1H; Ar), 6.87 (d, J = 8.0 Hz, 1H; Ar), 6.88 (s, 1H; Ar), 7.08 (t, J = 8.0 Hz, 1H; Ar), 7.83 (s, 1H; NH), 9.90 (s, 1H; NH); ^{13}C NMR (125 MHz, DMSO-d_6): δ 23.9 (2C), 25.1, 30.5, 33.5, 112.8, 113.9, 115.6, 116.8, 116.9, 117.7, 124.4, 128.9, 131.6, 137.8, 144.4, 149.3, 169.7; HRMS (FAB): calcd for $C_{18}H_{20}N_2O$ (M$^+$) 280.1576; found: 280.1569.

6-{[3-(*tert*-Butyl)phenyl]amino}-3,4-dihydroquinolin-2(1H)-one (5d). Following the general procedure for **5i**, compound **5d** (227 mg, 42% yield) was synthesized from 6-amino-3,4-dihydroquinolin-2(1H)-one and 1-bromo-3-(*tert*-butyl)benzene: white solid; mp 151–152 °C; IR (neat) cm^{-1}: 1667 (C=O), 3216 (NH), 3330 (NH); ^{1}H NMR (500 MHz, DMSO-d_6) δ 1.25 (s, 9H; *t*-Bu), 2.40 (t, J = 7.4 Hz, 2H; CH$_2$), 2.81 (t, J = 7.4 Hz, 2H; CH$_2$), 6.74 (d, J = 8.0 Hz, 1H; Ar), 6.77–6.81 (m, 2H; Ar), 6.87 (d, J = 8.0 Hz, 1H; Ar), 6.88 (s, 1H; Ar), 6.98 (s, 1H; Ar), 7.09 (t, J = 8.0 Hz, 1H; Ar), 7.84 (s, 1H; NH), 9.89 (s, 1H; NH); ^{13}C NMR (125 MHz, DMSO-d_6) δ 25.1, 30.5, 31.1 (3C), 34.3, 112.4, 113.2, 115.6, 115.9, 116.5, 117.5, 124.5, 128.7, 131.5, 138.0, 144.0, 151.5, 169.7; *Anal.* calcd for $C_{19}H_{22}N_2O$: C, 77.52; H, 7.53; N, 9.52. Found: C, 77.39; H, 7.48; N, 9.46.

6-{[3,5-Bis(trifluoromethyl)phenyl]amino}-3,4-dihydroquinolin-2(1H)-one (5e). Following the general procedure for **5i**, compound **5e** (144 mg, 58% yield) was synthesized from 6-bromo-3,4-dihydroquinolin-2(1H)-one and 3,5-bis(trifluoromethyl)-aniline: white solid; mp 180–182 °C; IR (neat) cm^{-1}: 1664 (C=O), 3229 (NH), 3314 (NH); ^{1}H NMR (500 MHz, DMSO-d_6) δ 2.44 (t, J = 7.4 Hz, 2H; CH$_2$), 2.87 (t, J = 7.4 Hz, 2H; CH$_2$), 6.87 (d, J = 8.6 Hz, 1H; Ar), 7.00 (s, 1H; Ar), 7.01 (d, J = 8.6 Hz, 1H;

Ar), 7.22 (s, 1H; Ar), 7.33 (s, 2H; Ar), 8.72 (s, 1H; NH), 10.08 (s, 1H; NH); ^{13}C NMR (125 MHz, DMSO-d_6) δ 24.9, 30.3, 109.5, 112.9 (2C), 116.0, 120.3, 121.2, 123.4 (q, 2C), 125.0, 131.2 (q, 2C), 134.4, 134.5, 147.4, 169.9; HRMS (FAB): calcd for C$_{17}$H$_{12}$F$_6$N$_2$O (M$^+$) 374.0854; found: 374.0847.

6-[(1,1'-Biphenyl)-3-ylamino]-3,4-dihydroquinolin-2(1H)-one (5f): Following the general procedure for **5i**, compound **5f** (375 mg, 86% yield) was synthesized from 6-bromo-3,4-dihydroquinolin-2(1H)-one and 3-aminobiphenyl: yellow solid; mp 143–145 °C; IR (neat) cm^{-1}: 1666 (C=O), 3218 (NH), 3316 (NH); ^{1}H NMR (500 MHz, DMSO-d_6) δ 2.42 (t, J = 7.4 Hz, 2H; CH$_2$), 2.84 (t, J = 7.4 Hz, 2H; CH$_2$), 6.79 (d, J = 8.0 Hz, 1H; Ar), 6.96–6.98 (m, 3H; Ar), 7.00 (d, J = 8.0 Hz, 1H; Ar), 7.18 (s, 1H; Ar), 7.26 (t, J = 8.0 Hz, 1H; Ar), 7.35 (t, J = 8.0 Hz, 1H; Ar), 7.45 (t, J = 8.0 Hz, 2H; Ar), 7.57 (d, J = 8.0 Hz, 2H; Ar), 8.02 (s, 1H; NH), 9.94 (s, 1H; NH); ^{13}C NMR (125 MHz, DMSO-d_6) δ 25.1, 30.5, 113.7, 114.2, 115.7, 117.2, 117.4, 118.3, 124.6, 126.5 (2C), 127.3, 128.8 (2C), 129.7, 132.0, 137.4, 140.7, 141.3, 145.1, 169.7; *Anal.* calcd for C$_{21}$H$_{18}$N$_2$O: C, 80.23; H, 5.77; N, 8.91. Found: C, 80.29; H, 5.71; N, 8.72.

6-[(3-Phenoxyphenyl)amino]-3,4-dihydroquinolin-2(1H)-one (5g): Following the general procedure for **5i**, compound **5g** (175 mg, 48% yield) was synthesized from 6-bromo-3,4-dihydroquinolin-2(1H)-one and 3-phenoxyaniline: off-white solid; mp 130–132 °C; IR (neat) cm^{-1}: 1661 (C=O), 3204 (NH), 3309 (NH); ^{1}H NMR (500 MHz, DMSO-d_6) δ 2.41 (t, J = 6.9 Hz, 2H; CH$_2$), 2.81 (t, J = 6.9 Hz, 2H; CH$_2$), 6.36 (dd, J = 8.0, 2.3 Hz, 1H; Ar), 6.54 (t, J = 2.3 Hz, 1H; Ar), 6.72 (dd, J = 8.0, 2.3 Hz, 1H; Ar), 6.77 (d, J = 8.0 Hz, 1H; Ar), 6.88 (dd, J = 8.0, 2.3 Hz, 1H; Ar), 6.92 (d, J = 2.3 Hz, 1H; Ar), 7.03 (d, J = 8.0 Hz, 2H; Ar), 7.12 (t, J = 8.0 Hz, 1H; Ar), 7.16 (t, J = 8.0 Hz, 1H; Ar), 7.38 (t, J = 8.0 Hz, 2H; Ar), 8.05 (s, 1H; NH), 9.95 (s, 1H; NH); ^{13}C NMR (125 MHz, DMSO-d_6) δ 25.1, 30.4, 104.7, 108.3, 110.0, 115.7, 117.9, 118.7, 118.8 (2C), 123.3, 124.5, 129.9 (2C), 130.4, 132.3, 136.9, 146.4, 156.5, 157.8, 169.7; HRMS (FAB): m/z calcd for C$_{21}$H$_{18}$N$_2$O$_2$ (M$^+$) 330.1368; found: 330.1374.

6-[(3-Methoxyphenyl)amino]-3,4-dihydroquinolin-2(1H)-one (5h): Following the general procedure for **5i**, compound **5h** (870 mg, 43% yield) was synthesized from 6-bromo-3,4-dihydroquinolin-2(1H)-one and 3-methoxyaniline: pale yellow solid; 160–161 °C; IR (neat) cm^{-1}: 1664 (C=O), 3214 (NH), 3325 (NH); ^{1}H NMR (500 MHz, DMSO-d_6) δ 2.41 (t, J = 7.4 Hz, 2H; CH$_2$), 2.82 (t, J = 7.4 Hz, 2H; CH$_2$), 3.69 (s, 3H; OCH$_3$), 6.32 (d, J = 8.0 Hz, 1H; Ar), 6.49 (s, 1H; Ar), 6.54 (d, J = 8.0 Hz, 1H; Ar), 6.77

(d, J = 8.0 Hz, 1H; Ar), 6.90 (d, J = 8.0 Hz, 1H; Ar), 6.92 (s, 1H; Ar), 7.07 (t, J = 8.0 Hz, 1H; Ar), 7.91 (s, 1H; NH), 9.93 (s, 1H; NH); ^{13}C NMR (125 MHz, DMSO-d_6) δ 25.1, 30.5, 54.7, 100.9, 104.0, 107.9, 115.7, 117.5, 118.4, 124.5, 129.8, 132.0, 137.4, 145.9, 160.2, 169.7; *Anal.* calcd for $C_{16}H_{16}N_2O_2$: C, 71.62; H, 6.01; N, 10.44. Found: C, 71.86; H, 5.90; N, 10.38.

6-[(3-Hydroxyphenyl)amino]-3,4-dihydroquinolin-2(1*H*)-one (5j). A suspension of 6-[(3-methoxyphenyl)amino]-3,4-dihydroquinolin-2(1*H*)-one **5h** (500 mg, 1.86 mmol) in dry CH_2Cl_2 (5 mL) was cooled to –78 °C and then BBr$_3$ (7.45 mL of 1 M solution in CH_2Cl_2, 7.45 mmol) was added. After the mixture was stirred for 30 min at -78 °C, the stirring was continued for additional 18 h at room temperature. The reaction was quenched by addition of water (12 mL), and CH_2Cl_2 was removed under reduced pressure. The aqueous solution was neutralized by addition of aqueous NaOH, and then extracted three times with EtOAc. The organic layer was washed with brine, and dried over Na_2SO_4. The organic solvent was removed under reduced pressure and the crude residue was purified by flash chromatography with *n*-hexane/EtOAc (1:3) to afford compound **5j** (232 mg, 49% yield): brown needle crystal; mp 213–214 °C; IR (neat) cm^{-1}: 1651 (C=O), 3222 (NH), 3321 (NH); ^{1}H NMR (500 MHz, DMSO-d_6) δ 2.41 (t, J = 7.4 Hz, 2H; CH$_2$), 2.81 (t, J = 7.4 Hz, 2H; CH$_2$), 6.15 (d, J = 8.0 Hz, 1H; Ar), 6.38 (d, J = 8.0 Hz, 1H; Ar), 6.39 (s, 1H; Ar), 6.74 (d, J = 8.0 Hz, 1H; Ar), 6.85 (d, J = 8.0 Hz, 1H; Ar), 6.89 (s, 1H; Ar), 6.94 (t, J = 8.0 Hz, 1H; Ar), 7.77 (s, 1H; NH), 9.07 (s, 1H; OH), 9.89 (s, 1H; NH); ^{13}C NMR (125 MHz, DMSO-d_6) δ 25.1, 30.5, 102.2, 106.0, 106.6, 115.6, 117.4, 118.2, 124.4, 129.7, 131.7, 137.7, 145.8, 158.1, 169.7; *Anal.* calcd for $C_{15}H_{14}N_2O_2$: C, 70.85; H, 5.55; N, 11.02. Found: C, 71.11; H, 5.59; N, 10.89.

6-[(3-Nitrophenyl)amino]-3,4-dihydroquinolin-2(1*H*)-one (5k). Following the general procedure for **5i**, compound **5k** (70.7 mg, 28% yield) was synthesized from 6-bromo-3,4-dihydroquinolin-2(1*H*)-one and 3-nitroaniline: red-brown solid; mp 243–244 °C; IR (neat) cm^{-1}: 1536 (NO$_2$), 1706 (C=O), 3198 (NH), 3383 (NH); ^{1}H NMR (500 MHz, DMSO-d_6) δ 2.44 (t, J = 7.4 Hz, 2H; CH$_2$), 2.86 (t, J = 7.4 Hz, 2H; CH$_2$), 6.84 (d, J = 8.0 Hz, 1H; Ar), 6.98 (d, J = 8.0 Hz, 1H; Ar), 7.00 (s, 1H; Ar), 7.30 (d, J = 8.0 Hz, 1H; Ar), 7.42 (t, J = 8.0 Hz, 1H; Ar), 7.51 (d, J = 8.0 Hz, 1H; Ar), 7.65 (s, 1H; Ar), 8.50 (s, 1H; NH), 10.03 (s, 1H; NH); ^{13}C NMR (125 MHz, DMSO-d_6) δ 24.9, 30.3, 107.7, 112.1, 115.8, 119.3, 120.1, 120.3, 124.8, 130.4, 133.6, 135.5, 146.6, 148.8, 169.8; *Anal.* calcd for $C_{15}H_{13}N_3O_3$: C, 63.60; H, 4.63; N, 14.83. Found: C, 63.44; H, 4.59; N, 14.57.

6-[(3-Aminophenyl)amino]-3,4-dihydroquinolin-2(1*H*)-one (5l). To a stirred solution of 6-[(3-nitrophenyl)amino]-3,4-dihydroquinolin-2(1*H*)-one **5k** (62.0 mg, 0.22 mmol) in AcOH (2.2 mL) at room temperature was added zinc powder (102 mg, 1.56 mmol) portionwise. After being stirred at room temperature for 1 h, the reaction mixture was filtered through a pad of Celite and concentrated under vacuum. The residue was diluted with EtOAc, and the whole was washed with saturated $NaHCO_3$, brine, and dried over Na_2SO_4. The organic solvent was removed under reduced pressure and the crude residue was purified by flash chromatography with *n*-hexane/EtOAc (1:8) to afford compound **5l** (41.6 mg, 75% yield): pale yellow solid; mp 196–198 °C; IR (neat) cm^{-1}: 1662 (C=O), 3221 (NH), 3344 (NH); ^{1}H NMR (500 MHz, DMSO-d_6) δ 2.40 (t, *J* = 7.4 Hz, 2H; CH$_2$), 2.80 (t, *J* = 7.4 Hz, 2H; CH$_2$), 4.93 (br, 2H; NH$_2$), 6.00 (d, *J* = 8.0 Hz, 1H; Ar), 6.15 (d, *J* = 8.0 Hz, 1H; Ar), 6.24 (s, 1H; Ar), 6.72 (d, *J* = 8.0 Hz, 1H; Ar), 6.80 (d, *J* = 8.0 Hz, 1H; Ar), 6.83 (d, *J* = 8.0 Hz, 1H; Ar), 6.86 (s, 1H; Ar), 7.58 (s, 1H; NH), 9.87 (s, 1H; NH); ^{13}C NMR (125 MHz, DMSO-d_6) δ 25.2, 30.5, 101.4, 104.5, 105.7, 115.5, 116.9, 117.7, 124.3, 129.3, 131.2, 138.3, 145.0, 149.2, 169.6; HRMS (FAB): calcd for $C_{15}H_{15}N_3O$ (M$^+$) 253.1215; found: 253.1213.

Methyl 3-[(2-Oxo-1,2,3,4-tetrahydroquinolin-6-yl)amino]benzoate (5m). Following the general procedure for **5i**, compound **5m** (979 mg, 50% yield) was synthesized from 6-bromo-3,4-dihydroquinolin-2(1*H*)-one and methyl 3-aminobenzoate: pale yellow solid; mp 169–171 °C; IR (neat) cm^{-1}: 1668 (C=O), 1706 (C=O), 3220 (NH), 3295 (NH); ^{1}H NMR (500 MHz, DMSO-d_6) δ 2.44 (t, *J* = 7.4 Hz, 2H; CH$_2$), 2.85 (t, *J* = 7.4 Hz, 2H; CH$_2$), 3.82 (s, 3H; CH$_3$), 6.82 (d, *J* = 8.0 Hz, 1H; Ar), 6.93 (d, *J* = 8.0 Hz, 1H; Ar), 6.94 (s, 1H; Ar), 7.19–7.21 (m, 1H; Ar), 7.28–7.31 (m, 2H; Ar), 7.54 (s, 1H; Ar), 8.17 (s, 1H; NH), 9.98 (s, 1H; NH); ^{13}C NMR (125 MHz, DMSO-d_6) δ 25.0, 30.4, 52.0, 115.2, 115.8, 118.2, 118.8, 119.1, 119.1, 124.6, 129.5, 130.5, 132.7, 136.6, 145.3, 166.4, 169.8; *Anal.* calcd for $C_{17}H_{16}N_2O_3$: C, 68.91; H, 5.44; N, 9.45. Found: C, 68.67; H, 5.39; N, 9.64.

3-[(2-Oxo-1,2,3,4-tetrahydroquinolin-6-yl)amino]benzoic acid (5n). To a solution of methyl 3-[(2-oxo-1,2,3,4-tetrahydroquinolin-6-yl)amino]benzoate **5m** (400 mg, 1.35 mmol) in 5.2 mL of MeOH/H$_2$O (3:1 v/v) was added LiOH·H$_2$O (170 mg, 4.05 mmol) at 0 °C, then the solution was warmed to 50 °C. After 1 h, the reaction mixture was acidified to below pH 2 using 1 M HCl, then EtOAc and brine were added to the mixture. The organic extracts were washed with brine and dried over Na_2SO_4. The

organic solvent was removed under reduced pressure to afford compound **5n** (366 mg, 96% yield): white solid; mp 259–261 °C; IR (neat) cm^{-1}: 1656 (C=O), 1684 (C=O), 3203 (NH), 3326 (NH); ^{1}H NMR (500 MHz, DMSO-d_6) δ 2.43 (t, J = 7.4 Hz, 2H; CH$_2$), 2.85 (t, J = 7.4 Hz, 2H; CH$_2$), 6.81 (d, J = 8.0 Hz, 1H; Ar), 6.93 (d, J = 8.0 Hz, 1H; Ar), 6.94 (s, 1H; Ar), 7.17 (d, J = 8.0 Hz, 1H; Ar), 7.27–7.31 (m, 2H; Ar), 7.53 (s, 1H; Ar), 8.12 (s, 1H; NH), 9.98 (s, 1H; NH), 12.78 (br, 1H; CO$_2$H); ^{13}C NMR (125 MHz, DMSO-d_6) δ 25.1, 30.4, 115.5, 115.8, 118.1, 118.9, 119.0, 119.2, 124.6, 129.3, 131.7, 132.6, 136.9, 145.2, 167.6, 169.8; HRMS (FAB): m/z calcd for C$_{16}$H$_{14}$N$_2$O$_3$ (M$^+$) 282.1004; found: 282.1011.

6-{[3-(Trifluoromethyl)phenyl]amino}-2H-benzo[b][1,4]oxazin-3(4H)-one **(6b).** Following the general procedure for **5i**, compound **6b** (23.1 mg, 43% yield) was synthesized from 6-bromo-2H-benzo[b][1,4]oxazin-3(4H)-one and 3-(trifluoromethyl)-aniline: pale yellow solid; mp 167–168 °C; IR (neat) cm^{-1}: 1695 (C=O), 3215 (NH), 3341 (NH); ^{1}H NMR (500 MHz, DMSO-d_6) δ 4.53 (s, 2H; CH$_2$), 6.68 (dd, J = 8.0, 2.3 Hz, 1H; Ar), 6.74 (d, J = 2.3 Hz, 1H; Ar), 6.90 (d, J = 8.0 Hz, 1H; Ar), 7.03 (d, J = 8.0 Hz, 1H; Ar), 7.16 (s, 1H; Ar), 7.19 (d, J = 8.0 Hz, 1H; Ar), 7.39 (t, J = 8.0 Hz, 1H; Ar), 8.39 (s, 1H; NH), 10.67 (s, 1H; NH); ^{13}C NMR (125 MHz, DMSO-d_6) δ 66.8, 107.0, 110.6, 113.9, 114.5, 116.8, 118.1, 124.3 (q), 128.0, 130.0 (q), 130.3, 136.6, 138.2, 145.4, 165.1; HRMS (FAB): m/z calcd for C$_{15}$H$_{11}$F$_3$N$_2$O$_2$ (M$^+$) 308.0773; found: 308.0776.

7-{[3-(Trifluoromethyl)phenyl]amino}quinolin-2(1H)-one (6c). AcOH (1.0 mL) was added to a flask containing 7-{[3-(trifluoromethyl)phenyl]amino)}-3,4-dihydroquino-lin-2(1H)-one **6a** (80.0 mg, 0.26 mmol) and Pd(OAc)$_2$ (22.4 mg, 0.10 mmol) and an oxygen balloon was connected to the reaction vessel. After stirring for 2 h at 115 °C, the reaction mixture was cooled to room temperature and concentrated *in vacuo*. The residue was purified by flash chromatography with *n*-hexane/EtOAc (1:3 to 1:5) to afford **6c** (34.1 mg, 43% yield): white solid; mp 177–179 °C; IR (neat) cm^{-1}: 1655 (C=O), 3452 (NH); ^{1}H NMR (500 MHz, DMSO-d_6) δ 6.24 (d, J = 9.2 Hz, 1H; C=CH), 6.88 (dd, J = 8.0, 2.3 Hz, 1H; Ar), 7.06 (d, J = 2.3 Hz, 1H; Ar), 7.23 (d, J = 8.0 Hz, 1H; Ar), 7.41 (s, 1H; Ar), 7.45 (d, J = 8.0 Hz, 1H; Ar), 7.50–7.53 (m, 2H; Ar), 7.75 (d, J = 9.2 Hz, 1H; C=CH), 8.99 (s, 1H; NH), 11.53 (s, 1H; NH); ^{13}C NMR (125 MHz, DMSO-d_6) δ 99.7, 112.3, 113.1, 113.5, 116.7, 117.7, 121.0, 124.1 (q), 129.0, 130.0 (q), 130.4, 139.8, 140.5, 142.9, 144.5, 162.2; HRMS (FAB): m/z calcd for C$_{16}$H$_{11}$F$_3$N$_2$O [M + H]$^+$ 305.0902; found: 305.0905.

5-{[3-(Trifluoromethyl)phenyl]amino}-3,4-dihydroquinolin-2(1*H*)-one (6d). Following the general procedure for **5i**, compound **6d** (17.1 mg, 47% yield) was synthesized from 2-oxo-1,2,3,4-tetrahydroquinolin-5-yl trifluoromethanesulfonate and 3-(trifluoromethyl)aniline: pale yellow solid; mp 182–184 °C; IR (neat) cm^{-1}: 1681 (C=O), 3214 (NH); ^{1}H NMR (500 MHz, DMSO-d_6) δ 2.40 (t, J = 7.4 Hz, 2H; CH$_2$), 2.73 (t, J = 7.4 Hz, 2H; CH$_2$), 6.64 (d, J = 8.0 Hz, 1H; Ar), 6.84 (t, J = 8.0 Hz, 1H; Ar), 7.00–7.06 (m, 3H; Ar), 7.11 (t, J = 8.0 Hz, 1H; Ar), 7.37 (t, J = 8.0 Hz, 1H; Ar), 8.05 (s, 1H; NH), 10.10 (s, 1H; NH); ^{13}C NMR (125 MHz, DMSO-d_6) δ 20.4, 29.8, 110.7, 110.8, 114.2, 115.8, 116.7, 118.3, 124.3 (q), 127.5, 129.8 (q), 130.1, 139.0, 139.7, 146.1, 170.0; HRMS (FAB): *m/z* calcd for C$_{16}$H$_{13}$F$_3$N$_2$O (M$^+$) 306.0980; found: 306.0990.

5-{[3-(Trifluoromethyl)phenyl]amino}indolin-2-one (6e). Following the general procedure for **5i**, compound **6e** (20.5 mg, 6% yield) was synthesized from 5-bromoindolin-2-one and 3-(trifluoromethyl)aniline: yellow solid; mp 147–150 °C; IR (neat) cm^{-1}: 1700 (C=O), 3209 (NH), 3330 (NH); ^{1}H NMR (500 MHz, DMSO-d_6) δ 3.47 (s, 2H; CH$_2$), 6.79 (d, J = 8.0 Hz, 1H; Ar), 6.97 (d, J = 8.0 Hz, 2H; Ar), 7.03 (s, 1H; Ar), 7.09 (s, 1H; Ar), 7.13 (d, J = 8.0 Hz, 1H; Ar), 7.35 (t, J = 8.0 Hz, 1H; Ar), 8.22 (s, 1H; NH), 10.27 (s, 1H; NH); ^{13}C NMR (125 MHz, DMSO-d_6) δ 36.1, 109.6, 110.0, 113.7, 117.2, 118.0, 120.0, 124.3 (q), 127.0, 129.9 (q), 130.1, 135.4, 138.9, 146.4, 176.1; HRMS (FAB): *m/z* calcd for C$_{15}$H$_{11}$F$_3$N$_2$O (M$^+$) 292.0823; found: 292.0822.

6-{[3-(Trifluoromethyl)phenyl]amino}benzo[*d*]oxazol-2(3*H*)-one (6f). Following the general procedure for **5i**, compound **6f** (59.3 mg, 22% yield) was synthesized from 6-bromobenzo[*d*]oxazol-2(3*H*)-one and 3-(trifluoromethyl)aniline: off-white solid; mp 162–164 °C; IR (neat) cm^{-1}: 1756 (C=O), 3258 (NH), 3350 (NH); ^{1}H NMR (500 MHz, DMSO-d_6) δ 6.93 (dd, J = 8.0, 1.7 Hz, 1H; Ar), 7.03–7.07 (m, 2H; Ar), 7.10 (d, J = 1.7 Hz, 1H; Ar), 7.17 (d, J = 1.7 Hz, 1H; Ar), 7.22 (dd, J = 8.0, 1.7 Hz, 1H; Ar), 7.40 (t, J = 8.0 Hz, 1H; Ar), 8.45 (s, 1H; NH), 11.50 (br, 1H; NH); ^{13}C NMR (125 MHz, DMSO-d_6) δ 102.3, 110.2, 110.6, 114.6, 115.5, 118.0, 124.3 (q), 125.1, 130.0 (q), 130.3, 136.6, 144.0, 145.6, 154.6; *Anal.* calcd for C$_{14}$H$_9$F$_3$N$_2$O$_2$: C, 57.15; H, 3.08; N, 9.52. Found: C, 57.22; H, 3.32; N, 9.43.

6-{[3-(Trifluoromethyl)phenyl]amino}benzo[*d*]thiazol-2(3*H*)-one (6g). Following the general procedure for **5i**, compound **6g** (9.1 mg, 5% yield) was synthesized from 6-bromobenzo[*d*]thiazol-2(3*H*)-one and 3-(trifluoromethyl)aniline: yellow solid; mp 129–130 °C; IR (neat) cm^{-1}: 1670 (C=O), 3348 (NH); ^{1}H NMR (400 MHz, DMSO-d_6) δ

7.02–7.09 (m, 3H; Ar), 7.15 (s, 1H; Ar), 7.21 (d, J = 8.2 Hz, 1H; Ar), 7.36–7.41 (m, 2H; Ar), 8.42 (s, 1H; NH), 11.73 (s, 1H; NH); ^{13}C NMR (125 MHz, DMSO-d_6) δ 110.7, 112.2, 114.0, 114.5, 117.8, 118.9, 124.3 (q), 124.4, 130.0 (q), 130.2, 131.3, 137.0, 145.6, 169.8; HRMS (FAB): m/z calcd for $C_{14}H_9F_3N_2OS$ (M$^+$) 310.0388; found: 310.0392.

7-{[((3-(Trifluoromethyl)phenyl]amino}-2*H*-benzo[*b*][1,4]oxazin-3(4*H*)-one (6h).
Following the general procedure for **5i**, compound **6h** (43.6 mg, 46% yield) was synthesized from 7-bromo-2*H*-benzo[*b*][1,4]oxazin-3(4*H*)-one and 3-(trifluoromethyl)-aniline: white solid; mp 117–118 °C; IR (neat) cm^{-1}: 1688 (C=O), 3224 (NH), 3335 (NH); ^{1}H NMR (500 MHz, DMSO-d_6) δ 4.55 (s, 2H; CH$_2$), 6.71 (d, J = 1.7 Hz, 1H; Ar), 6.75 (dd, J = 8.0, 1.7 Hz, 1H; Ar), 6.85 (d, J = 8.0 Hz, 1H; Ar), 7.04 (d, J = 8.0 Hz, 1H; Ar), 7.18 (s, 1H; Ar), 7.23 (dd, J = 8.0, 1.7 Hz, 1H; Ar), 7.40 (t, J = 8.0 Hz, 1H; Ar), 8.40 (s, 1H; NH), 10.60 (s, 1H; NH); ^{13}C NMR (125 MHz, DMSO-d_6) δ 66.8, 107.2, 110.9, 113.1, 114.7, 116.4, 118.3, 121.5, 124.3 (q), 130.0 (q), 130.3, 137.4, 143.9, 145.1, 164.2; *Anal.* calcd for $C_{15}H_{11}F_3N_2O_2$: C, 58.45; H, 3.60; N, 9.09. Found: C, 58.21; H, 3.35; N, 9.02.

7-{[3-(Trifluoromethyl)phenyl]amino}-2*H*-benzo[*b*][1,4]thiazin-3(4*H*)-one (6i).
Following the general procedure for **5i**, compound **6i** (303 mg, 65% yield) was synthesized from 7-bromo-2*H*-benzo[*b*][1,4]thiazin-3(4*H*)-one and 3-(trifluoromethyl)-aniline: pale yellow solid; mp 166–167 °C; IR (neat) cm^{-1}: 1678 (C=O), 3076 (NH), 3194 (NH); ^{1}H NMR (500 MHz, DMSO-d_6) δ 3.46 (s, 2H; CH$_2$), 6.94 (d, J = 8.6 Hz, 1H; Ar), 6.99 (dd, J = 8.6, 2.3 Hz, 1H; Ar), 7.04–7.07 (m, 2H; Ar), 7.17 (s, 1H; Ar), 7.23 (d, J = 8.6 Hz, 1H; Ar), 7.41 (t, J = 8.6 Hz, 1H; Ar), 8.43 (s, 1H; NH), 10.47 (s, 1H; NH); ^{13}C NMR (125 MHz, DMSO-d_6) δ 29.0, 111.2, 114.8, 117.5, 118.0, 118.1, 118.3, 120.2, 124.2 (q), 130.0 (q), 130.3, 131.8, 137.1, 145.0, 164.7; HRMS (FAB): m/z calcd for $C_{15}H_{11}F_3N_2OS$ (M$^+$) 324.0544; found: 324.0545.

1-Methyl-6-((3-(trifluoromethyl)phenyl)amino)-3,4-dihydroquinolin-2(1*H*)-one (6j).
Following the general procedure for **5i**, compound **6j** (205 mg, 77% yield) was synthesized from 6-bromo-1-methyl-3,4-dihydroquinolin-2(1*H*)-one and 3-(trifluoro-methyl)aniline: pale yellow solid; mp 156–158 °C; IR (neat) cm^{-1}: 1649 (C=O), 3330 (NH); ^{1}H NMR (500 MHz, DMSO-d_6) δ 2.53 (t, J = 7.4 Hz, 2H; CH$_2$), 2.84 (t, J = 7.4 Hz, 2H; CH$_2$), 3.24 (s, 3H; Me), 7.00–7.05 (m, 4H; Ar), 7.19 (s, 1H; Ar), 7.24 (d, J = 8.0 Hz, 1H; Ar), 7.39 (t, J = 8.0 Hz, 1H; Ar), 8.40 (s, 1H; NH); ^{13}C NMR (125 MHz, DMSO-d_6) δ 24.8, 29.0, 31.1, 110.8, 114.4, 115.6, 117.8, 118.0, 118.9, 124.3 (q), 127.3,

130.0 (q), 130.3, 134.9, 136.6, 145.4, 168.9; *Anal.* calcd for $C_{17}H_{15}F_3N_2O$: C, 63.75; H, 4.72; N, 8.75. Found: C, 63.56; H, 4.76; N, 8.59.

6-((3-(Trifluoromethyl)phenyl)amino)-3,4-dihydroquinoline-2(1*H*)-thione (6k). To a stirred solution of 6-{[3-(trifluoromethyl)phenyl]amino}-3,4-dihydroquinolin-2(1*H*)-one **2a** (50.0 mg, 0.16 mmol) in toluene (1.0 mL) was added Lawesson's reagent (33.0 mg, 0.08 mmol) under an argon atmosphere. After stirring for 30 min at 110 °C, the reaction mixture was cooled to room temperature and concentrated *in vacuo*. The residue was purified by flash chromatography with *n*-hexane/EtOAc (3:1) to afford **6k** (51.4 mg, 100% yield): yellow solid; mp 195–196 °C; IR (neat) cm^{-1}: 1499 (C=S), 3361 (NH); ^{1}H NMR (500 MHz, DMSO-d_6) δ 2.77 (t, J = 8.0 Hz, 2H; CH$_2$), 2.90 (t, J = 8.0 Hz, 2H; CH$_2$), 6.97 (s, 1H; Ar), 6.98 (d, J = 8.0 Hz, 1H; Ar), 7.04 (d, J = 8.0 Hz, 1H; Ar), 7.06 (d, J = 8.0 Hz, 1H; Ar), 7.20 (s, 1H; Ar), 7.27 (d, J = 8.0 Hz, 1H; Ar), 7.41 (d, J = 8.0 Hz, 1H; Ar), 8.49 (s, 1H; NH), 12.15 (s, 1H; NH); ^{13}C NMR (125 MHz, DMSO-d_6) δ 24.0, 38.9, 111.4, 114.9, 117.0, 117.3, 118.3, 118.5, 124.3 (q), 126.6, 130.0 (q), 130.3, 131.3, 138.3, 144.9, 197.3; HRMS (FAB): *m/z* calcd for $C_{16}H_{13}F_3N_2S$ (M$^+$) 322.0752; found: 322.0758.

7-{[3-(Trifluoromethyl)phenyl]amino}-1,3,4,5-tetrahydro-2*H*-benzo[*b*]azepin-2-one (6l). Following the general procedure for **5i**, compound **6l** (55.4 mg, 83% yield) was synthesized from 7-bromo-1,3,4,5-tetrahydro-2*H*-benzo[*b*]azepin-2-one and 3-(trifluoromethyl)aniline: pale yellow solid; mp 140–141 °C; IR (neat) cm^{-1}: 1657 (C=O), 3194 (NH), 3300 (NH); ^{1}H NMR (500 MHz, DMSO-d_6) δ 2.07–2.12 (m, 2H; CH$_2$), 2.16 (t, J = 6.8 Hz, 2H; CH$_2$), 2.65 (t, J = 6.8 Hz, 2H; CH$_2$), 6.91 (d, J = 8.0 Hz, 1H; Ar), 6.99–7.02 (m, 2H; Ar), 7.05 (d, J = 8.0 Hz, 1H; Ar), 7.22 (s, 1H; Ar), 7.28 (d, J = 8.0 Hz, 1H; Ar), 7.41 (t, J = 8.0 Hz, 1H; Ar), 8.44 (s, 1H; NH), 9.35 (s, 1H; NH); ^{13}C NMR (125 MHz, DMSO-d_6) δ 27.7, 30.0, 32.7, 111.2, 114.7, 117.2, 118.4, 119.8, 122.6, 124.3 (q), 130.0 (q), 130.3, 132.7, 134.9, 138.6, 145.0, 173.1; HRMS (FAB): *m/z* calcd for $C_{17}H_{15}F_3N_2O$ (M$^+$) 320.1136; found: 320.1144.

8-Fluoro-6-{[3-(trifluoromethyl)phenyl]amino}-3,4-dihydroquinolin-2(1*H*)-one (6m). Following the general procedure for **5i**, compound **6m** (275 mg, 69% yield) was synthesized from 6-bromo-8-fluoro-3,4-dihydroquinolin-2(1*H*)-one and 3-(trifluoromethyl)aniline: white solid; mp 166–167 °C; IR (neat) cm^{-1}: 1670 (C=O), 3216 (NH), 3355 (NH); ^{1}H NMR (500 MHz, DMSO-d_6) δ 2.46 (t, J = 7.4 Hz, 2H; CH$_2$), 2.90 (t, J = 7.4 Hz, 2H; CH$_2$), 6.81 (s, 1H; Ar), 6.82 (d, J = 8.0 Hz, 1H; Ar), 7.08 (d, J = 8.0 Hz,

1H; Ar), 7.20 (s, 1H; Ar), 7.28 (d, J = 8.0 Hz, 1H; Ar), 7.42 (t, J = 8.0 Hz, 1H; Ar), 8.48 (s, 1H; NH), 9.97 (s, 1H; NH); ^{13}C NMR (125 MHz, DMSO-d_6) δ 25.2, 30.5, 104.2 (d), 111.6, 113.8, 115.1, 118.6, 120.2 (d), 124.2 (q), 127.8, 130.0 (q), 130.4, 136.9 (d), 144.7, 149.7 (d), 169.5; *Anal.* calcd for $C_{16}H_{12}F_4N_2O$: C, 59.26; H, 3.73; N, 8.64. Found: C, 59.05; H, 3.64; N, 8.40.

7-Fluoro-6-{[3-(trifluoromethyl)phenyl]amino}-3,4-dihydroquinolin-2(1*H*)-one (6n). Following the general procedure for **5i**, compound **6n** (246 mg, 62% yield) was synthesized from 6-bromo-7-fluoro-3,4-dihydroquinolin-2(1*H*)-one and 3-(trifluoromethyl)aniline: white solid; mp 179–180 °C; IR (neat) cm^{-1}: 1679 (C=O), 3301 (NH); ^{1}H NMR (500 MHz, DMSO-d_6) δ 2.46 (t, J = 7.4 Hz, 2H; CH$_2$), 2.85 (t, J = 7.4 Hz, 2H; CH$_2$), 6.76 (d, J = 11.5 Hz, 1H; Ar), 6.97–7.02 (m, 3H; Ar), 7.14 (d, J = 8.6 Hz, 1H; Ar), 7.36 (t, J = 8.6 Hz, 1H; Ar), 8.11 (s, 1H; NH), 10.12 (s, 1H; NH); ^{13}C NMR (125 MHz, DMSO-d_6) δ 24.2, 30.2, 103.1 (d), 110.0, 114.0, 117.3, 120.1, 122.2 (d), 124.0, 124.3 (q), 129.8 (q), 130.0, 135.3 (d), 146.2, 154.5 (d), 169.9; *Anal.* calcd for $C_{16}H_{12}F_4N_2O$: C, 59.26; H, 3.73; N, 8.64. Found: C, 59.11; H, 3.79; N, 8.62.

6-{[6-(Trifluoromethyl)pyridin-2-yl]amino}-3,4-dihydroquinolin-2(1*H*)-one (7a). Following the general procedure for **5i**, compound **7a** (294 mg, 67% yield) was synthesized from 6-amino-3,4-dihydroquinolin-2(1*H*)-one and 2-bromo-6-(trifluoromethyl)pyridine: white solid; mp 202–204 °C; IR (neat) cm^{-1}: 1663 (C=O), 3202 (NH), 3306 (NH); ^{1}H NMR (500 MHz, DMSO-d_6) δ 2.46 (t, J = 7.4 Hz, 2H; CH$_2$), 2.86 (t, J = 7.4 Hz, 2H; CH$_2$), 6.83 (d, J = 8.0 Hz, 1H; Ar), 7.02 (d, J = 8.0 Hz, 1H; Ar), 7.11 (d, J = 8.0 Hz, 1H; Ar), 7.43 (dd, J = 8.0, 2.3 Hz, 1H; Ar), 7.50 (d, J = 2.3 Hz, 1H; Ar), 7.73 (t, J = 8.0 Hz, 1H; Ar), 9.33 (s, 1H; NH), 10.00 (s, 1H; NH); ^{13}C NMR (125 MHz, DMSO-d_6) δ 25.3, 30.5, 109.8, 113.8, 115.2, 117.8, 118.7, 121.8 (q), 123.9, 132.8, 135.1, 138.4, 144.3 (q), 156.0, 169.8; *Anal.* calcd for $C_{15}H_{12}F_3N_3O$: C, 58.63; H, 3.94; N, 13.68. Found: C, 58.81; H, 4.01; N, 13.59.

6-{[4-(Trifluoromethyl)pyridin-2-yl]amino}-3,4-dihydroquinolin-2(1*H*)-one (7b). Following the general procedure for **5i**, compound **7b** (154 mg, 54% yield) was synthesized from 6-amino-3,4-dihydroquinolin-2(1*H*)-one and 2-bromo-4-(trifluoromethyl)pyridine: white solid; mp 177–178 °C; IR (neat) cm^{-1}: 1667 (C=O), 3224 (NH); ^{1}H NMR (500 MHz, DMSO-d_6) δ 2.43 (t, J = 7.9 Hz, 2H; CH$_2$), 2.86 (t, J = 7.9 Hz, 2H; CH$_2$), 6.80 (d, J = 8.7 Hz, 1H; Ar), 6.93 (d, J = 5.5 Hz, 1H; Ar), 7.01 (s, 1H; Ar), 7.37 (dd, J = 8.7, 2.3 Hz, 1H; Ar), 7.47 (d, J = 2.3 Hz, 1H; Ar), 8.32 (d, J = 5.5 Hz, 1H; Ar),

9.27 (s, 1H; NH), 9.96 (s, 1H; NH); ^{13}C NMR (125 MHz, DMSO-d_6) δ 25.2, 30.4, 105.7, 108.1, 115.2, 118.1, 118.9, 123.1 (q), 123.9, 132.9, 135.0, 137.5 (q), 149.4, 156.5, 169.8; *Anal.* calcd for $C_{15}H_{12}F_3N_3O$: C, 58.63; H, 3.94; N, 13.68. Found: C, 58.61; H, 3.80; N, 13.45.

6-{[5-(Trifluoromethyl)pyridin-3-yl]amino}-3,4-dihydroquinolin-2(1*H*)-one   (7c).
Following the general procedure for **5i**, compound **7c** (124 mg, 29% yield) was synthesized from 6-amino-3,4-dihydroquinolin-2(1*H*)-one and 3-bromo-5-(trifluoromethyl)pyridine: white solid; mp 213–215 °C; IR (neat) cm^{-1}: 1669 (C=O), 3202 (NH), 3291 (NH); ^{1}H NMR (500 MHz, DMSO-d_6) δ 2.44 (t, J = 7.4 Hz, 2H; CH$_2$), 2.86 (t, J = 7.4 Hz, 2H; CH$_2$), 6.85 (d, J = 8.6 Hz, 1H; Ar), 6.98–7.01 (m, 2H; Ar), 7.42 (s, 1H; Ar), 8.23 (s, 1H; Ar), 8.47 (s, 1H; NH), 8.53 (s, 2H; Ar), 10.04 (s, 1H; NH); ^{13}C NMR (125 MHz, DMSO-d_6) δ 24.9, 30.3, 115.4, 115.9, 119.3, 120.1, 123.8 (q), 124.9, 125.4 (q), 133.9, 134.5, 134.8, 140.6, 141.8, 169.9; *Anal.* calcd for $C_{15}H_{12}F_3N_3O$: C, 58.63; H, 3.94; N, 13.68. Found: C, 58.58; H, 3.83; N, 13.65.

6-{[4-(Trifluoromethyl)pyrimidin-2-yl]amino}-3,4-dihydroquinolin-2(1*H*)-one (7d).
Following the general procedure for **5i**, compound **7d** (95.7 mg, 27% yield) was synthesized from 6-bromo-3,4-dihydroquinolin-2(1*H*)-one and 2-amino-4-(trifluoromethyl)pyrimidine: yellow solid; mp 230–231 °C; IR (neat) cm^{-1}: 1646 (C=O), 3390 (NH); ^{1}H NMR (500 MHz, DMSO-d_6) δ 2.44 (t, J = 7.4 Hz, 2H; CH$_2$), 2.85 (t, J = 7.4 Hz, 2H; CH$_2$), 6.81 (d, J = 8.6 Hz, 1H; Ar), 7.18 (d, J = 5.2 Hz, 1H; Ar), 7.46 (dd, J = 8.6, 1.7 Hz, 1H; Ar), 7.51 (d, J = 1.7 Hz, 1H; Ar), 8.75 (d, J = 5.2 Hz, 1H; Ar), 9.99 (s, 1H; NH), 10.03 (s, 1H; NH); ^{13}C NMR (125 MHz, DMSO-d_6) δ 25.2, 30.4, 106.6, 115.0, 118.7, 119.5, 120.6 (q), 123.7, 133.5, 133.8, 154.6 (q), 160.0, 161.6, 169.9; HRMS (FAB): *m/z* calcd for $C_{14}H_{11}F_3N_4O$ (M$^+$) 308.0885; found: 308.0880.

6-{[6-(Trifluoromethyl)pyrazin-2-yl]amino}-3,4-dihydroquinolin-2(1*H*)-one   (7e).
Following the general procedure for **5i**, compound **7e** (75.3 mg, 21% yield) was synthesized from 6-bromo-3,4-dihydroquinolin-2(1*H*)-one and 6-(trifluoromethyl)-pyrazin-2-amine: yellow solid; mp 273–275 °C; IR (neat) cm^{-1}: 1662 (C=O), 3399 (NH); ^{1}H NMR (500 MHz, DMSO-d_6) δ 2.44 (t, J = 7.4 Hz, 2H; CH$_2$), 2.86 (t, J = 7.4 Hz, 2H; CH$_2$), 6.84 (d, J = 8.6 Hz, 1H; Ar), 7.45 (dd, J = 8.6, 2.3 Hz, 1H; Ar), 7.49 (d, J = 2.3 Hz, 1H; Ar), 8.29 (s, 1H; Ar), 8.41 (s, 1H; Ar), 9.90 (s, 1H; NH), 10.05 (s, 1H; NH); ^{13}C NMR (125 MHz, DMSO-d_6) δ 25.2, 30.4, 115.3, 118.0, 118.8, 121.5 (q), 124.1, 128.4, 133.6, 133.8, 138.5 (q), 139.2, 151.5, 169.8; HRMS (FAB): *m/z* calcd for

$C_{14}H_{11}F_3N_4O$ (M$^+$) 308.0885; found: 308.0891.

7-{[4-(Trifluoromethyl)pyridin-2-yl]amino}-2H-benzo[b][1,4]thiazin-3(4H)-one (8). Following the general procedure for **5i**, compound **8** (48.5 mg, 12% yield) was synthesized from 7-bromo-2H-benzo[b][1,4]thiazin-3(4H)-one and 2-amino-4-(trifluoromethyl)pyridine: white solid; mp 217–218 °C; IR (neat) cm^{-1}: 1688 (C=O), 3194 (NH); ^{1}H NMR (500 MHz, DMSO-d_6) δ 3.45 (s, 2H; CH$_2$), 6.92 (d, J = 8.6 Hz, 1H; Ar), 6.99 (d, J = 5.2 Hz, 1H; Ar), 7.03 (s, 1H; Ar), 7.33 (dd, J = 8.6, 1.7 Hz, 1H; Ar), 7.81 (d, J = 1.7 Hz, 1H; Ar), 8.37 (d, J = 5.2 Hz, 1H; Ar), 9.43 (s, 1H; NH), 10.44 (s, 1H; NH); ^{13}C NMR (125 MHz, DMSO-d_6) δ 29.1, 106.2, 108.6, 117.1, 117.5, 117.7, 119.3, 123.0 (q), 131.7, 135.9, 137.6 (q), 149.3, 156.1, 164.8; HRMS (FAB): m/z calcd for $C_{14}H_{10}F_3N_3OS$ (M$^+$) 325.0497; found: 325.0497.

7-{[4-(Trifluoromethyl)pyridin-2-yl]amino}-1,3,4,5-tetrahydro-2H-benzo[b]azepin-2-one (9). Following the general procedure for **5i**, compound **9** (16.7 mg, 18% yield) was synthesized from 7-bromo-1,3,4,5-tetrahydro-2H-benzo[b]azepin-2-one and 2-amino-4-(trifluoromethyl)pyridine: pale yellow solid; mp 185–187 °C; IR (neat) cm^{-1}: 1688 (C=O), 2936 (NH); ^{1}H NMR (500 MHz, DMSO-d_6) δ 2.09–2.16 (m, 4H; CH$_2$ × 2), 2.67 (t, J = 6.9 Hz, 2H; CH$_2$), 6.92 (d, J = 8.0 Hz, 1H; Ar), 6.98 (d, J = 5.2 Hz, 1H; Ar), 7.07 (s, 1H; Ar), 7.53 (d, J = 8.0 Hz, 1H; Ar), 7.55 (s, 1H; Ar), 8.37 (d, J = 5.2 Hz, 1H; Ar), 9.36 (s, 1H; NH), 9.42 (s, 1H; NH); ^{13}C NMR (125 MHz, DMSO-d_6) δ 27.8, 30.1, 32.7, 106.0, 108.4, 117.4, 119.6, 121.9, 122.0, 123.0 (q), 132.7, 134.1, 137.4, 137.5 (q), 149.3, 156.3, 173.1; HRMS (FAB): m/z calcd for $C_{16}H_{14}F_3N_3O$ (M$^+$) 321.1089; found: 321.1092.

6-[3-(Trifluoromethyl)phenoxy]-3,4-dihydroquinolin-2(1H)-one (12a). To a suspension of KOt-Bu (60.5 mg, 0.54 mmol) in DMF (2.1 mL) was added 6-hydroxy-3,4-dihydroquinolin-2(1H)-one **10** (80.0 mg, 0.49 mmol) at 0 °C and the reaction mixture was stirred at this temperature for 15 min. Bis(3-trifluoromethyl-phenyl)iodonium tetrafluoroborate **11** (259 mg, 0.51 mmol) was added in one portion and the reaction mixture was stirred at 40 °C for 1 h, then quenched with H$_2$O at 0 °C and extracted into CHCl$_3$. The organic layer was washed with brine, and dried over Na$_2$SO$_4$. The organic solvent was removed under reduced pressure and the crude residue was purified by flash chromatography with n-hexane/EtOAc (1:1) to afford compound **12a** (39.9 mg, 27% yield): white solid; mp 158–159 °C; IR (neat) cm^{-1}: 1681 (C=O), 3203 (NH); ^{1}H NMR (500 MHz, DMSO-d_6) δ 2.44 (t, J = 7.4 Hz, 2H; CH$_2$), 2.87 (t, J =

7.4 Hz, 2H; CH$_2$), 6.91 (s, 2H; Ar), 6.99 (s, 1H; Ar), 7.20–7.23 (m, 2H; Ar), 7.42 (d, J = 8.0 Hz, 1H; Ar), 7.58 (t, J = 8.0 Hz, 1H; Ar), 10.12 (s, 1H; NH); ^{13}C NMR (125 MHz, DMSO-d_6) δ 24.7, 30.0, 113.6, 116.3, 118.7, 119.1, 119.5, 121.0, 123.7 (q), 125.7, 130.6 (q), 131.2, 135.3, 149.6, 158.4, 169.9; HRMS (FAB): m/z calcd for C$_{16}$H$_{12}$F$_3$NO$_2$ (M$^+$) 307.0820; found: 307.0826.

6-[(3-(Trifluoromethyl)phenyl)thio]-3,4-dihydroquinolin-2(1H)-one **(15a).** 2-Propanol (1.0 mL) was added to a flask containing 6-mercapto-3,4-dihydro-quinolin-2(1H)-one **13** (50.0 mg, 0.28 mmol), 3-trifluoromethyliodobenzene **14a** (40.4 μL, 0.28 mmol), CuI (32.0 mg, 0.17 mmol), ethylene glycol (31.2 μL, 0.56 mmol) and K$_2$CO$_3$ (96.7 mg, 0.70 mmol) under an argon atmosphere. The mixture was stirred at 80 °C for 13 h. After cooling, the reaction mixture was diluted with EtOAc, and filtered through a pad of Celite. The filtrate was concentrated *in vacuo*. Crude material was purified by flash chromatography with *n*-hexane/EtOAc (3:2) to afford compound **15a** (6.2 mg, 7% yield): white solid; mp 102–104 °C; IR (neat) cm^{-1}: 1676 (C=O), 3387 (NH); ^{1}H NMR (500 MHz, DMSO-d_6) δ 2.53 (t, J = 7.4 Hz, 2H; CH$_2$), 2.96 (t, J = 7.4 Hz, 2H; CH$_2$), 7.00 (d, J = 8.0 Hz, 1H; Ar), 7.40 (d, J = 8.0 Hz, 1H; Ar), 7.42–7.45 (m, 2H; Ar), 7.49 (s, 1H; Ar), 7.58–7.59 (m, 2H; Ar), 10.34 (s, 1H; NH); ^{13}C NMR (125 MHz, DMSO-d_6) δ 24.4, 30.0, 116.4, 122.4, 122.6, 123.0, 123.7 (q), 125.4, 129.9 (q), 130.3, 131.0, 133.5, 133.7, 139.5, 140.1, 170.1; HRMS (FAB): m/z calcd for C$_{16}$H$_{12}$F$_3$NOS (M$^+$) 323.0592; found: 323.0591.

6-[(4-(Trifluoromethyl)phenyl)thio)-3,4-dihydroquinolin-2(1H)-one (15b). Follow-ing the procedure described for **15a**, compound **15b** (10.8 mg, 15% yield) was synthesized from 6-mercapto-3,4-dihydroquinolin-2(1H)-one **13** and 1-iodo-4-(trifluoromethyl)benzene **14b**: white solid; mp 158–159 °C; IR (neat) cm^{-1}: 1646 (C=O), 3406 (NH); ^{1}H NMR (500 MHz, DMSO-d_6) δ 2.48 (t, J = 7.4 Hz, 2H; CH$_2$), 2.92 (t, J = 7.4 Hz, 2H; CH$_2$), 6.97 (d, J = 8.0 Hz, 1H; Ar), 7.25 (d, J = 8.0 Hz, 2H; Ar), 7.37 (d, J = 8.0 Hz, 1H; Ar), 7.41 (s, 1H; Ar), 7.62 (d, J = 8.0 Hz, 2H; Ar), 10.33 (s, 1H; NH); ^{13}C NMR (125 MHz, DMSO-d_6) δ 24.4, 30.0, 116.5, 121.7, 124.2 (q), 125.5, 125.8 (q), 125.9 (2C), 126.5 (2C), 134.0, 134.3, 139.8, 144.5, 170.2; HRMS (FAB): m/z calcd for C$_{16}$H$_{12}$F$_3$NOS (M$^+$) 323.0592; found: 323.0596.

KSP ATPase Assay

The microtubules-stimulated KSP ATPase assay was performed as described in Chapter 1.

Growth Inhibition Assay

A549, HCT-116 and MCF-7 cells were cultured in Dulbecco's modified Eagle's medium (DMEM; Sigma), McCoy's 5A medium (GIBCO) and EMEM medium (Wako), respectively, supplemented with 10% (v/v) fetal bovine serum at 37 °C in a 5% CO_2-incubator. Growth inhibition assays using these cells were performed in 96-well plates (BD Falcon). A549, HCT-116 and MCF-7 cells were seeded at 500, 5000 and 5000 cells/well in 50 μL of culture media, respectively, and were cultured for 6 h. Chemical compounds in DMSO were diluted 250-fold with the culture medium in advance. Following the addition of 40 μL of the fresh culture medium to the cell cultures, 30 μL of the chemical diluents were also added. The final volume of DMSO in the medium was equal to 0.1% (v/v). The cells under chemical treatment were incubated for a further 72 h. The wells in the plates were washed twice with the cultured medium without phenol-red. After 1 h incubation with 100 μL of the medium, the cell culture in each well was supplemented with 20 μL of the MTS reagent (Promega), followed by incubation for an additional 40 min. Absorbance at 490 nm of each well was measured using a Wallac 1420 ARVO SX multilabel counter (Perkin Elmer). At least three experiments were performed per condition and the averages and standard deviations of inhibition rates in each condition were evaluated to determine IC_{50} values using the GraphPad Prism software.

Steady-state KSP ATPase Assay

An enzyme-coupled system that regenerates ADP to ATP was used to measure ATP hydrolysis by KSP, with NADH absorbance at 340 nm as an indirect measurement of ATP turnover as described in Chapter 1. The observed V_{max} values were 1.10 s^{-1} in the absence of compound **2a** and 0.93 s^{-1} in the presence of **2a**.

Molecular Modeling

Docking calculations for each compound were performed to predict their binding mode. As a protein structure, the crystal structure of the KSP complex with the ligand bound in the α4/α6 allosteric site (PDB ID: 3ZCW)[9] was used. The protonation states of the amino acid residues of KSP and the direction of the hydrogen atoms involved in the hydrogen bonds were assigned using the Protonate3D algorithm[10] implemented in MOE.[11] Three binding pockets (the ATP binding pocket, the α2/α3/L5 allosteric pocket and the α4/α6 allosteric site) were chosen from the potential binding sites detected by the MOE-SiteFinder module. For each binding site, the initial docked poses (100

candidate poses for each compound) were optimized by the MMFF94x forcefield[12] and the pose with the lowest binding energy (E_{bind}) estimated by the MM/GBVI method[13] was adopted as the predicted binding mode.

Thermodynamic Solubility in Aqueous Solution

Thermodynamic solubility in an equal volume of a mixture of 1/15 M phosphate buffer (pH 7.4) and EtOH, or 1/15 M phosphate buffer (pH 7.4) was measured as described in Chapter 2, Section 1.

References

(1)   Anderson, K. W.; Tundel, R. E.; Ikawa, T.; Altman, R. A.; Buchwald, S. L. *Angew. Chem., Int. Ed*. **2006**, *45*, 6523–6527.

(2)   Bielawski, M.; Aili, D.; Olofsson, B. *J. Org. Chem*. **2008**, *73*, 4602–4607.

(3)   Jalalian, N.; Ishikawa, E. E.; Silva, L. F., Jr.; Olofsson, B. *Org. Lett*. **2011**, *13*, 1552–1555.

(4)   Kwong, F. Y.; Buchwald, S. L. *Org. Lett*. **2002**, *4*, 3517–3520.

(5)   Cava, M. P.; Levinson, M. I. *Tetrahedron* **1985**, *41*, 5061–5087.

(6)   Oishi, S.; Watanabe, T.; Sawada, J.; Asai, A.; Ohno, H.; Fujii, N. *J. Med. Chem*. **2010**, *53*, 5054–5058.

(7)   Takeuchi, T.; Oishi, S.; Watanabe, T.; Ohno, H.; Sawada, J.; Matsuno, K.; Asai, A.; Asada, N.; Kitaura, K.; Fujii, N. *J. Med. Chem*. **2011**, *54*, 4839–4846.

(8)   Garcia-Saez, I.; Yen, T.; Wade, R. H.; Kozielski, F. *J. Mol. Biol*. **2004**, *340*, 1107–1116.

(9)   Ulaganathan, V.; Talapatra, S. K.; Rath, O.; Pannifer, A.; Hackney, D. D.; Kozielski, F. *J. Am. Chem. Soc*. **2013**, *135*, 2263–2272.

(10)   Labute, P. *Proteins* **2009**, *75*, 187–205.

(11)   MOE ver 2010.10, Chemical Computing Group Inc., Montreal, Canada.

(12)   Halgren T. A.; Nachbar R. B. *J. Comput. Chem*. **1996**, *17*, 587–615.

(13)   Labute, P. *J. Comput. Chem.* **2008**, *29*, 1693–1698.

Chapter 3.　　　Conclusions

1.　　　Structure–activity relationship studies of carbazole and carboline derivatives were carried out to develop potent KSP inhibitors. Introduction of a hydrophilic group, including a urea group or lactam amide group, at the 2-position of the lead carbazole derivative improved KSP inhibitory activity and cytotoxicity. Kinetic analysis revealed that these novel KSP inhibitors showed ATP-competitive inhibition.

2.　　　The novel KSP inhibitors with diaryl amine scaffolds were designed to improve the low aqueous solubility of carbazole- and carboline-type KSP inhibitors. The diphenylamine derivative with a lactam amide group at the appropriate position exhibited potent KSP inhibitory activity and improved solubility in aqueous media. Structural analysis by using single crystal X-ray diffraction studies and free energy calculations demonstrated that fewer van der Waals interactions in the crystal packing, as well as increased solvation by the aniline nitrogen, contributed to the improved solubility.

3.　　　Optimization studies of diaryl amine-type KSP inhibitors were performed. The diaryl amine derivative with a benzoazepin-2-one and a pyridine substructure had greater aqueous solubility compared with the parent diphenylamine derivative and maintained highly potent KSP inhibitory activity. Additionally, it was demonstrated by investigation of the inhibitory mechanism and a docking simulation study of diaryl amine-type KSP inhibitors that these inhibitors bind to α4/α6 allosteric pocket of KSP in an ATP-competitive manner.

In summary, the author identified fused-indole and diaryl amine derivatives as novel classes of selective KSP inhibitors. These compounds could be promising agents for cancer chemotherapy.

Acknowledgements

List of Publications

This study was published in the following papers.

Chapter 1. Structure–Activity Relationships of Carboline and Carbazole Derivatives as a Novel Class of ATP-Competitive Kinesin Spindle Protein Inhibitors
Tomoki Takeuchi, Shinya Oishi, Toshiaki Watanabe, Hiroaki Ohno, Jun-ichi Sawada, Kenji Matsuno, Akira Asai, Naoya Asada, Kazuo Kitaura, and Nobutaka Fujii
J. Med. Chem. **2011**, *54*, 4839–4846.

Chapter 2.

Section 1. Kinesin Spindle Protein Inhibitors with Diaryl Amine Scaffolds: Crystal Packing Analysis for Improved Aqueous Solubility
Tomoki Takeuchi, Shinya Oishi, Masato Kaneda, Hiroaki Ohno, Shinya Nakamura, Isao Nakanishi, Masayoshi Yamane, Jun-ichi Sawada, Akira Asai, and Nobutaka Fujii
ACS Med. Chem. Lett. in press.

Section 2. Optimization of Diaryl Amine Derivatives as Kinesin Spindle Protein Inhibitors
Tomoki Takeuchi, Shinya Oishi, Masato Kaneda, Ryosuke Misu, Hiroaki Ohno, Jun-ichi Sawada, Akira Asai, and Nobutaka Fujii
Submitted.